How Laminar Frontal Cortex and Basal Ganglia Circuits Interact to Control Planned and Reactive Saccades

Abbreviated Title: Frontal Cortex and Basal Ganglia Saccade Control

[1]**Joshua W. Brown,** [2]**Daniel Bullock,** [3]**Stephen Grossberg**

[1]Department of Psychology
Washington University, Campus Box 1125
St. Louis, MO, 63130-4899, USA

[2,3]Department of Cognitive & Neural Systems and Center for Adaptive Systems
Boston University
677 Beacon St., Boston, MA 02215
Phone: 617-353-7858 or -7857
FAX: 617-353-7755

E-mail: jwbrown@artsci.wustl.edu, danb@cns.bu.edu, steve@cns.bu.edu

Revision of CAS/CNS Technical Report 2000-023

Submitted to *Neural Networks*
Final revision: 14 August 2003

Acknowledgements
J.B. was supported in part by Defense Advanced Research Projects Agency and the Office of Naval Research (ONR N00014-95-1-0409, ONR N00014-92-J-1309, and ONR N00014-95-1-0657). D.B. was supported in part by Defense Advanced Research Projects Agency and the Office of Naval Research (ONR N00014-95-1-0409, ONR N00014-92-J-1309) and the National Institute of Mental Health (R01 DC02852). S.G. was supported in part by Air Force Office of Scientific Research (AFOSR F49620-01-1-0397), Defense Advanced Research Projects Agency and the Office of Naval Research (ONR N00014-95-1-0409, ONR N00014-92-J-1309, ONR N00014-95-1-0657, ONR N00014-01-1-0624), and the National Science Foundation (NSF IRI-97-20333).

Abstract

How does the brain learn to balance between reactive and planned behaviors? The basal ganglia and frontal cortex together allow animals to learn planned behaviors that acquire rewards when prepotent reactive behaviors are insufficient. This paper proposes a new model, called TELOS, to explain how laminar circuitry of the frontal cortex, exemplified by the frontal eye fields, interacts with the basal ganglia, thalamus, superior colliculus, and inferotemporal and parietal cortices to learn and perform reactive and planned eye movements. The model is formulated as fourteen computational hypotheses. These specify how strategy priming and action planning (in cortical layers III, Va and VI) are dissociated from movement execution (in layer Vb), how the basal ganglia help to choose among and gate competing plans, and how a visual stimulus may serve either as a movement target or as a discriminative cue to move elsewhere. The direct, indirect and hyperdirect pathways through the basal ganglia are shown to enable complex gating functions, including deferred execution of selected plans, and switching among alternative sensory-motor mappings. Notably, the model can learn and gate the use of a What-to-Where transformation that enables spatially invariant object representations to selectively excite spatially coded movement plans. Model simulations show how dopaminergic reward and non-reward signals guide monkeys to learn and perform saccadic eye movements in the fixation, single saccade, overlap, gap, and delay (memory-guided) saccade tasks. Model cell activation dynamics quantitatively simulate seventeen established types of dynamics exhibited by corresponding real cells during performance of these tasks.

Key Words: basal ganglia, frontal cortex, cortical layer, saccade, gating, dopamine, reinforcement learning, action selection, planning, Parkinson's disease

Introduction

This article proposes detailed mechanistic solutions to several key problems in sensory-motor control: How does the brain learn to balance between reactive and planned movements? How do recognition and action representations in the brain work together to launch movements toward valued goal objects? How does the brain learn and recall the myriad movement plans it needs to switch among different tasks, when each plan may be sensitive to different combinations of scenic cues and timing constraints?

The article treats these problems by modeling the saccadic, or ballistic, eye movement system. Solving these problems requires interactions among multiple brain regions, including inferotemporal, parietal, and prefrontal cortex; basal ganglia (BG); amygdala; cerebellum; and superior colliculus (SC). In amphibians and all land vertebrates, the BG interact with a laminar structure, the optic tectum (OT), or its homolog, the SC, to control orienting actions and, in some species, prey-catching actions (Marin, Smeets & Gonzalez, 1998; Butler & Hodos, 1996). The mammalian BG also interact with distinct areas of frontal cortex – also laminar structures – to control orienting, cognitive, and manipulative behaviors (Hikosaka & Wurtz, 1989; Passingham, 1993; Strick, Dum & Picard, 1995). Lesions of the BG uniquely cause devastating disorders of the voluntary movement system, e.g., Parkinsonian akinesia, Huntington's chorea, and ballism (Albin, Young & Penney, 1989). Such observations suggest a tight link between volitional movement and BG interactions with laminar action control structures, which provide a natural basis for differentiating between plan activation and plan execution. Whereas laminar organization has been neglected in most models of BG function, the present model explains how BG interactions with laminar target structures satisfy staging and learning requirements of voluntary behavior.

The model simulates learning and performance of the saccadic tasks that are summarized in Figure 1 (cf. Hikosaka et al., 1989, p. 781). It is also used to simulate performance in two related tasks. Recording during such tasks has produced a wealth of electrophysiological data that, in concert with anatomical studies, serve as hard constraints on model development. As a set, these tasks challenge an animal's ability to plan, withhold, and generate goal-directed movements in a way that satisfies instrumental reward contingencies. Simulations (summarized in Figures 9, 10 and 11) show that the model shown in Figure 2 can learn and perform all the tasks, and can regenerate seventeen qualitatively distinct types of task-related activation dynamics exhibited by cells in the SC, BG, thalamus, and oculomotor areas of frontal and parietal cortex.

A key adaptive challenge is to balance reactive and planned movement (Hallett, 1978; Grossberg & Kuperstein, 1986). Rapid reactive movements are needed to ensure survival in response to unexpected dangers. Planned movements often take longer to elaborate. How does the brain prevent reactive movements from being triggered in situations where a more slowly occurring planned movement would be more adaptive? Movement *gates* can prevent the reactive movement from being launched until the planned movement can effectively compete with it. Then a winning movement command can open its gate and launch its movement. The proposed model shows how a cooperative set of physiological and circuit properties: prevent a reactive movement command from opening the gate before a planned movement command is ready to open it; allow the reactive and planned commands to compete for dominance; yet also allow a reactive movement command to open the gate when no planned movement command is being formed.

Conditional movements towards valued goal objects cannot be made until the goal objects are recognized and movement directions specified. Formidable memory storage problems would ensue if the brain had to learn separate object recognition codes for every retinotopic position and size of an object. To achieve efficient object recognition, the *What* cortical processing stream builds object representations that are "positionally invariant", i.e., independent of the retinotopic position or size of the object (Tanaka et al., 1991; Bar et al. 2001; Sigala & Logothetis, 2002). Given that recognition codes are independent of position, how does the brain compute how to move to the position of an object after it is recognized? After eliminating the link between an object's identity and position for purposes of object recognition, the brain needs to re-establish this link for purposes of movement. The *Where* cortical processing stream

elaborates the object positions and directions needed to compute motor commands. The model proposes how interactions across the What and Where processing streams overcome their complementary informational deficiencies to generate movements towards recognized objects.

It is not enough to recognize and move towards an object. An animal needs to know when to move towards or away from an object and when not to do so, depending on reward contingencies. Decision criteria include such stimulus properties as color, size, shape, motion and the state of the body, taken individually or in combination. In addition, when confronted with the same scene, an animal may act with respect to different objects depending on its changing needs, such as food if hungry or water if thirsty. The model explains how the brain learns and remembers many plans that involve different sets of discriminative and scheduling constraints, and how it switches among them as needed.

Figure 1 and Figure 2 about here

According to the proposed model (Figure 2), these functional problems find a mechanistic solution in BG interactions with the SC and frontal cortex. Reward-related dopaminergic signals modulate learning in the BG's striatum and the frontal cortex (Schultz, 1998; Gaspar et al., 1995). The trained BG system allows or prevents movements, according to their appropriateness (Hikosaka & Wurtz, 1983; Crosson, 1985; Bullock & Grossberg, 1991; Mink and Thach, 1993; Mink, 1996; Redgrave et al., 1999). BG outputs provide GABA-ergic inhibitory gating of their target structures. In the primate saccadic circuit, cells in the substantia nigra pars reticulata (SNr) tonically inhibit the SC but pause briefly to allow the SC to generate a saccade (Hikosaka & Wurtz, 1983; 1989). Lesions in this system can release a "visual grasp reflex" (Guitton et al., 1985), i.e., impulsive orienting to any visually salient object. Ancient vertebrate genera, such as frogs, already had a well-developed BG system (Marin et al., 1998). Though lacking a precise equivalent of the primate saccadic circuit, frogs can selectively orient while ignoring distracters, but lesions of the BG projection to the optic tectum (SC homolog) impair a frog's ability to orient selectively (Ewert et al., 1996).

Thus BG gates help create a difference between *physical* and *motivational* salience. Such gating enables an actor to acquire reward for foveating a physically weak stimulus (e.g., a dim and motionless predator) while ignoring a physically strong stimulus. In most visual scenes, many targets compete for foveation. If the saccadic gate is opened before competition among stimuli resolves, the system may foveate the most contrastive target, or may attempt to foveate multiple targets simultaneously by averaging ambiguous SC activity (Lee et al., 1988; Ottes et al., 1984). In the proposed model, feedforward striatal inhibitory interneurons (Gernert et al., 2000; Koos & Tepper, 1999; Wilson et al., 1989) keep the basal ganglia gate shut until competitive dynamics in posterior parietal cortex (PPC) and the frontal eye field (FEF) have a chance to select a unique saccade goal.

The FEF and SC are individually sufficient to generate saccades (Schiller et al., 1980; Deng et al. 1986). Yet in the normal animal, the SC is an important common pathway for saccade generation, and focal SC lesions result in transient impairment of all saccade types (Schiller et al., 1980). Imaging studies (Sweeney et al., 1996) have shown that the frontal cortex is more strongly activated in more difficult oculomotor tasks, e.g., those requiring memory-guided saccades or anti-saccades. Such tasks engage elements of the frontal oculomotor system, including the prefrontal cortex (PFC), FEF, and supplementary eye fields (SEF, an oculomotor area in dorsomedial frontal cortex, DMFC). Lesions of these frontal areas suggest that they incorporate distinct, modular contributions to oculomotor planning and control. The frontal oculomotor areas add the ability to use: head-centered or other non-motor-error coordinates (Schlag & Schlag-Rey, 1987; Schlag-Rey et al., 1997; Schiller, 1998); working memory (Goldman-Rakic, 1987; 1995; Pierrot-Deseilligny et al., 1993); conjunctions of features (Bichot & Schall, 1999); and internal sequencing (Sommer & Tehovnik, 1999). Taken together, these data suggest a hierarchy. Visual inputs to the SC dominate reactive movements by default, but plans within the frontal cortex can assume control of the SC when simple reactive eye movements are insufficient (Figure 3).

These principles, realized here as mechanisms in a saccadic control model, should also apply to adaptive control of manipulative and cognitive behaviors. The model and results were briefly reported in Brown et al. (2000).

Methods

The model realizes fourteen major computational hypotheses. These are presented verbally and diagrammatically to frame the subsequent mathematical specification. Table 1 lists abbreviations to be used in reference to neuroanatomical structures. Many of the assumptions are shared with prior verbal formulations and computational models (e.g., Hikosaka & Wurtz, 1983; 1989; Crosson, 1985; Albin et al. 1989; Bullock & Grossberg, 1991; Mink & Thach, 1993; Contreras-Vidal & Stelmach, 1995; Dominey et al., 1995; Houk & Beiser; 1995; Mink, 1996; Wichmann & DeLong, 1996; Suri et al., 1997; Wickens, 1997; Berns & Sejnowski, 1998; Graybiel, 1998; Schultz, 1998; Brown et al., 1999; Redgrave et al., 1999), although in virtually all cases the present mathematical implementation of a postulate has predictive implications that distinguish it from postulates in prior models. It is noted below where these predictive implications depart most significantly from prior models. The new model is called ***TELOS,*** which is from the ancient Greek *telos* for goal, end, or completion of a plan, but is also an acronym for **TE**lencephalic **L**aminar **O**bjective **S**elector. The BG and cerebral cortex together make up the *telencephalon*, and the BG take inputs from, and help select the outputs of, *laminar* oculomotor structures, notably the SC (superior colliculus) and the FEF (frontal eye field) in the frontal cortex. Through concerted action of these structures, the current behavioral *objective* – e.g., a desired eye movement vector or maintained eye fixation – is *selected*.

Table 1 and Figure 3 about here

1. Forebrain circuits enable competitive limited-capacity planning. The brain uses analog neuronal states to represent patterned information that is distributed across multiple cells, which have finite ranges of membrane potential, firing rates, and synaptic weights. To use these finite ranges effectively, the brain employs normalizing mechanisms, notably mutual inhibition within on-center off-surround networks whose neurons obey membrane equations. By normalizing their activities, such networks enable *relative* activity levels to represent patterned information and thereby minimize noise and saturation effects (Grossberg, 1973, 1982). The same normalizing mechanisms can also mediate competition among plans (Grossberg, 1978a; Bullock & Rhodes, 2003). Early modeling proposed how such a competitive network could create a working memory in which the relative priority (intended performance order) among the plans constituting a forthcoming sequence is represented by the relative activation levels (Boardman and Bullock, 1991; Grossberg, 1978a, 1978b) of the plan representations. There is now compelling evidence for both the normalization principle (e.g., Basso & Wurtz, 1998; Cisek & Kalaska, 2002; Pellizzer & Hodges, 2003) and the prediction that relative activation level codes relative priority in working memory (Averbeck et al. 2002). The limited number of distinct activation levels that can be simultaneously represented implies a limit on the number of simultaneously active (prioritized) plans in working memory, consistent with many experimental reports (cf. Cowan, 1999).

2. The basal ganglia contextually gate expression of reactive behaviors or plans. Parallel channels of the BG embody normally-closed gates that cooperate with the thalamus, the superior colliculus (SC) and the frontal eye fields (FEF) to withhold saccadic eye movements until a single reactive movement or saccadic plan is selected by competitive dynamics in the SC, FEF, and posterior parietal cortex (PPC). This gating hypothesis explains four data sets. (1) GABAergic inhibitory projection neurons of the two BG output nuclei, the GPi and SNr (internal or medial segment of the globus pallidus, and substantia nigra pars reticulata), exhibit tonic firing rates that are sufficiently high to suppress strong activations of recipient neurons in thalamus or SC. (2) Phasic reductions from these high resting rates, or complete pauses, release, and scale the rate of, behaviors controlled by thalamic, collicular, and other targets of GPi or SNr outputs (Hikosaka & Wurtz, 1983; 1989; Horak & Anderson, 1984; Skinner & Garcia-Rill, 1990;

Bullock & Grossberg, 1991; Turner et al., 1998; Takikawa et al. 2002). (3) Lesions in the BG pathway lead to a spectrum of disorders of voluntary movement (Young & Penney, 2001; Wichmann & DeLong, 2001), ranging from a hypokinetic extreme – bradykinesia (abnormally slow movement) and loss of ability to initiate planned movements – to a hyperkinetic extreme, including saccadic hyperdistractibility, hemi-ballism, and chorea. Thus different lesions produce too much or too little BG inhibition of plan execution. (4) Pathway tracing and physiological studies indicate an impressive degree of independence among a large number of parallel circuits that traverse the basal ganglia and return to a specific region of origin in frontal cortex (Alexander & Crutcher, 1990; Middleton & Strick, 2000). The BG thus contain a large set of parallel, programmable, gates.

3. Activation of the BG direct pathway can release plan execution. Within each parallel BG circuit, the *direct pathway*—the monosynaptic pathway from the striatum to GPi or SNr—enables transient opening of BG gates. A typical voluntary behavior is released via the direct pathway when a small set of striatal medium spiny projection neurons (SPNs) become active and inhibit a set of GABAergic projection neurons in the GPi or SNr (Figures 2 and 3B). Thus, gate opening works by inhibiting a tonically-on movement inhibitor. Although this interpretation is supported by many saccadic eye movement studies (e.g., Hikosaka & Wurtz, 1983, 1989; Handel & Glimcher, 1999, 2000), its generality remains to be established, in part because of the complexity of interactions between the direct, indirect, and hyperdirect BG pathways (e.g., Levy et al. 1997; Nambu et al. 2002).

4. Feedforward inhibition in the striatum mediates competition for plan expression. The withholding function of the normally-closed BG gates opposes tendencies to react immediately to whatever stimulus is physically most salient, and creates time for plans supported by motivational and cognitive information to activate, compete, and be selected. The striatum of the basal ganglia provides a competitive arena in which representations of alternative actions vie for execution. Competition can be mediated by surround inhibition, which could be recurrent (feedback), feedforward, or a combination of the two. Despite receiving massive numbers of excitatory fibers from cortex, the striatum is known as a "silent structure", in which only a small percentage of the dominant neuron type, SPNs, is strongly active at any one time. Prior proposals, that a striatal choice-making competition is mediated primarily by recurrent inhibitory collaterals of SPNs, cannot be logically reconciled with a "silent" striatum, because recurrent competition would require significant supra-threshold activation of many competing SPNs. Moreover, data suggest that striatal recurrent inhibition is weak (Jaeger et al., 1994). We therefore propose that cortical plan representations bid in parallel for execution via excitatory inputs to corresponding striatal SPNs, and oppose execution of other plans by exciting GABAergic striatal feedforward interneurons (GABA-SIs) that are known to strongly inhibit striatal SPNs (Wilson et al., 1989; Koos & Tepper, 1999; Gernert et al. 2000). Because the ratio of GABA-SIs to SPNs is ~1:20, such competition by feedforward surround inhibition is entirely consistent with a "silent" striatum.

5. Striatal activation requires convergent inputs from distributed plan representations. Gate opening, for any cognitive/mnemonic or motoric degree of freedom controlled by the BG system, is usually withheld until a single plan for that degree of freedom dominates alternative active plans. Examples of cases to manage are: two parietal cortex bids (Figure 3A), or one parietal and one FEF bid (Figure 3C), to move the eyes in *conflicting* directions. Expression of two conflicting plans at the same time would result in incoherent behavior. Evidence that this problem does occur when gate opening is too rapid comes from data on *saccadic averaging*: the probability of mistakenly saccading to the average position, halfway between two visual target loci, is a decreasing function of reaction time and target separation (Ottes et al., 1984). Evidence that the probability of trying to execute two plans at once can be strongly affected by BG lesions comes from studies of postural responses in PD (Parkinson's Disease) patients. Such patients exhibit non-adaptive "hybrid" responses that appear to reflect execution of two plans that are strict alternatives in healthy control subjects (Horak et al., 1989). In another BG disease syndrome, HD (Huntington's Disease), involuntary choreic movements, once thought to be random, often result from repeatable phasic coactivations of normally antagonistic muscles (J. Mink, personal communication, September 2002). Although *tonic* coactivation could arise by involuntary activation of a

single normal behavior (e.g., Humphrey & Reed, 1983), *phasic* coactivations would more likely arise from involuntary co-execution of two (or more) plans that are normally mutually exclusive.

Incoherent behavior can be avoided if broad feedforward inhibition in the striatum is complemented by a high threshold for activation of SPNs, so that they can be activated only by strong convergent excitation from cortex. Then SPNs will not activate until the several cortical representations associated with a degree of freedom, which are hypothesized to converge in the striatum, simultaneously project significant excitation to the same localized striatal region. As competition between plans resolves in favor of one winner, the cortical state becomes more *coherent*, in the sense that the remaining highly active sites are mutually compatible representations that help to specify the winning plan. Simultaneously, the signal from cortex to striatum becomes more *focused*, as diffuse signals from losing plans decline and signals from the winning plan's distributed representations grow and converge to excite the associated small region of striatum (Figure 3D). This hypothesis computationally clarifies reports that convergent cortical afferents to distinct localized regions of the striatum originate from cortical areas that are themselves strongly interconnected (Yeterian & Hoesen, 1978; Cavada & Goldman-Rakic, 1991; Flaherty & Graybiel, 1991; Gerfen & Wilson, 1996). It is also consistent with the gap junctions that may mediate broad activation of GABA-SIs (Kita et al., 1990), and SPNs' specialization to switch from OFF to ON states only if they receive strong convergent cortical excitation (Wilson, 1995a).

6. Indirect pathway activation enables deferral of a chosen plan. In "simple" (as opposed to "choice") reaction time tasks, an oft-rewarded plan can be cognitively primed for execution, yet await a permissive event that signals when it may be released. During the priming interval, excitation of SPNs in the direct pathway could inhibit the GPi or SNr and cause premature execution unless such gate opening were stopped until occurrence of the permissive event. The trainable "GO signal" function provided by the *direct* pathway is therefore complemented by a trainable "STOP signal" provided by the *indirect* BG pathway. Thus the model distinguishes two bases for non-execution of a plan. In one case, the plan may fail to satisfy the conditions for winning the direct pathway's striatal competition. In another case, an action that satisfies those conditions can be blocked by activity in the indirect pathway. Evidence that activation in the indirect pathway can be potent enough to serve this function comes from studies of PD, in which hyperactivity of the indirect pathway has been associated with inability to initiate a planned action (Wichmann & DeLong, 1996). The striatal source cells for the indirect pathway affect the GPi (or SNr) via two routes: striatum-GPe-GPi(or SNr) (Hazrati et al., 1990; Parent & Hazrati, 1995; Smith & Bolam, 1990), and striatum-GPe-STN-GPi(or SNr) (e.g., Wichmann & DeLong, 1996). Consistent with recent experimental results (Hassani et al., 1996; Levy et al., 1997), this hypothesis differs from various prior models by treating the former (shorter) route as the more potent, and thus the more important for the STOP function. Below, hypothesis 14 specifies a *distinct* function for the STN-GPi link, which is part of the so-called 'hyper-direct' pathway.

Figure 4 about here

7. Thalamo-striatal feedback guides learning of indirect pathway STOP responses. Learning necessary to generate a STOP signal occurs during trials on which premature release of a movement leads to non-reward. In the model, such experiences can lead to learned activation of the indirect channel associated with the released movement, even though striatal activation in the indirect channel is *not* a normal part of releasing the movement. How does the brain identify which indirect pathway it should recruit in order to STOP a given direct pathway? We propose that the feedback pathways (Figure 2) from the thalamus to the striatum (de las Heras et al., 1998; McFarland & Haber, 2000) help solve this credit-assignment problem by routing a specific teaching signal to the indirect channel associated with whatever direct channel has just activated. Because the thalamo-striatal pathways have been neglected in prior models of the basal ganglia, and there is little pertinent electrophysiological work, this hypothesis is currently based largely on anatomical and computational considerations.

8. Laminar maps enable gated interactions between planning and executive cells. Alternative plans are coded, in the SC and FEF, at distinct spatial positions in 2-D cellular arrays or maps. To

complement the BG's parallel gating system, "planning" cells encode preparatory activities and send bids to the BG, and associated "executive" cells generate phasic outputs if and when their BG gate opens. This hypothesis predicts a multi-layered – i.e., laminar – organization and a distinctive pattern of connectivity. Such is true of the SC, which projects to the BG (via dorsal thalamus, e.g., LP/PUL) from superficial layer maps (e.g., Hutsler & Chalupa, 1991; Hall & Lee, 1993; Butler & Hodos, 1996) and receives SNr outputs in deeper layer maps that are representationally and topographically "in-register" with superficial layers. As schematized in Figure 2, there is also abundant anatomical evidence for a similar stratification of cells and fiber systems in the frontal cortex (Jones et al., 1977; Royce & Bromley, 1984; Giuffrida et al., 1985; Berendse et al., 1992; Canteras et al., 1990; Wilson, 1995a,b; Gerfen & Wilson, 1996; Levesque et al., 1996; Yeterian & Pandya, 1994). A large portion of cortical fibers projecting to the striatum emerge from small pyramidal cells of layers II-III or III-Va (depending on species and cortical area). Although layer Vb large pyramids send some collaterals to BG (including STN and striatum; see hypothesis 14 below), such "Brainstem projecting neurons make up a very small proportion of the total population of cortico-striatal cells.... The vast majority of [cortico-striatal] neurons are more superficially situated, smaller pyramidal neurons (Wilson, 1995a, p. 38)", which also have cortico-cortical connections. There is accumulating physiological evidence (Iwabuchi & Kubota, 1998; Sawaguchi, 2001; Segraves & Goldberg, 1987; Bruce et al., 1985; Turner & DeLong, 2000) that the cortico-striatal cells in layers III-Va have different task-related properties than the large pyramidal cells that are clustered in layer Vb and send outputs to the brainstem and effectors. For the part of FEF (area 8) that they examined, Iwabuchi & Kubota (1998) found that neurons with early onsets coupled to a GO cue (signaling whether to release a response) were numerous in layer III, whereas neurons whose onsets were late and movement-coupled were more numerous in layer V. Thus there was a normal sequence involving activation of layer III neurons *before* layer V output neurons. These data support the hypothesis of at least distinct, if not completely segregated (Sommer & Wurtz, 2000; Wurtz et al., 2001) laminar distributions of "planning" and "executive" cells within areas of frontal cortex. Some models assume or imply that such a functional differentiation is achieved across cortical areas, rather than by layers within areas. However, moving across areas typically implies a change in cortical representation. Columnar laminar neocortex can efficiently implement the planning/execution distinction across layers.

Although the concept of planning has some connotations that go beyond the competence of the current model, the current usage of "plan cell" is consistent with prior usage (e.g., Bullock & Grossberg, 1991). A neural representation qualifies as a plan if it helps specify a possible forthcoming response, and if the circuit controlling the effects of the representation's activation provides a basis for withholding the active representation's access to the effector apparatus until a decision has been reached to execute the plan. To this the current analysis adds another condition: that the putative plan representations must send bids to the telencephalic decision centers that gate their access to effectors. Thus the response representations that exist in ungated reflex systems do not qualify as plans; nor do gatable output stages that send no projections to telencephalic decision centers. Finally, although the plan cells in the current model can remain active across significant delays after stimulus offset (hypothesis 12 and Figure 9F, 9G, below) this may not be true of all cells properly so-called.

9. Small BG gating channels control large topographic zones in laminar target structures. How broad a region of frontal cortex (or SC) is affected by opening of a particular BG gate? On gross anatomical grounds, the cortico-striatal-GPi/SNr projection has been described as a "funnel", and indeed there is an order of magnitude reduction in numbers of cells from the pool of cortico-striatal cells to the pool of striatal SPNs (Zheng & Wilson, 2002), and another order of magnitude reduction from the pool of SPNs to the pool of GPi/SNr projection neurons (Oorschot, 1996; Wickens, 1997). The "funnel" usage has waned because it was interpreted to imply *mixing* rather than the (now well-established) *segregation* of channels, but the radical reduction in cell counts implied by "funnel" remains a key constraint on models. In frontal cortex, *many* more cells are reached by the projection from PNR-THAL (pallidum or nigra receiving thalamus) than there are cells in PNR-THAL, or in the GPi/SNr. We thus hypothesize a one-to-many relationship between cells in GPi/SNr and gatable cells in frontal cortex. It is probable that, similar to SNr-SC interactions (Hikosaka & Wurtz, 1983, 1989; Handel & Glimcher, 1999, 2000),

pausing by each small cluster of cells in the GPi/SNr directly affects (via PNR-THAL) a much larger set of cells that are distributed across a moderate-sized zone of a given frontal cortical area. Further cells will then be affected by secondary, e.g., cortico-cortical, interactions.

Thus action-selection theories of the BG cannot plausibly assume a one-to-one relationship between plan representations and BG channels. Models must explain how the effect of gating can be highly selective and accurate even though the number of cellular degrees of freedom in the GPi/SNr is relatively small. In many cases, two or more cortical plans will have similarly high activation levels, and the gating signal needs to select the cortical plan that has won the striatal competition rather than any highly active alternatives. The current model hypothesizes that loops through the BG circuit respect fronto-cortical topography: each frontal zone receives thalamo-cortical fibers from a zone of PNR-THAL that receives fibers from a zone of GPi/SNr that receives fibers from the striatal zone targeted by the frontal zone of origin. This principle has been established for the large-scale topographic organization of frontal cortex. For example, there are separate motor (area 4), premotor (area 6), oculomotor (FEF) and prefrontal circuits (Alexander & Crutcher, 1990; Middleton and Strick, 2000). To explain how the system achieves sufficient selectivity, the model proposes that such circuits also respect finer-grained topographic organization. In particular, selectivity can be achieved even if the cortical activation levels of two plans are indistinguishable, so long as the plans exist in different **gateable cortical zones** (GCZs). For simplicity, the model (see Figure 5) defines three BG channels and three associated GCZs in FEF, but these discrete elements could be replaced by an overlapping continuum in a straightforward way in a population model. The main computational requirement is that the cortical activity foci representing two competing plans be sufficiently separated that one receives a reliably stronger GO signal from the PNR-THAL.

Hypotheses 4,5 and 9 imply a kind of complementarity in the macrocircuit's management of competitive plan execution. Any two cells that represent different plans in the same GCZ are likely to compete via strong mutual intra-cortical inhibition, so that when the competition resolves and the gate opens for the entire GCZ, only the winning plan will execute. If two plan cells pertinent to a given degree of freedom do not reside in the same GCZ, then they are less likely to compete via such strong mutual intra-cortical inhibition, so a large activation of one may not imply a small activation of the other. However, in this case, striatal competition can ensure that only one of the GCZs receives a strong GO signal. In either case, a non-viable "hybrid" response is generally avoided.

10. Selective gating of premotor zones enables fast sensory-motor remapping. A gating system can control which of several alternative sensory-motor or cognitive-motor pathways are used to generate behavior. This ability is fundamental because a visual stimulus may serve either as a movement target or as a discriminative cue to move elsewhere. Sensory/cognitive and motor information is often represented in different coordinate sytems. The model shows how learned associations can form between such different coordinate representations, notably from spatially invariant sensory/cognitive representations to spatially coded motor representations. For example, in the SC map, plan representations cluster on the basis of eye movement direction and amplitude (a vector code), not on the basis of the stimulus modality (vision, audition, or touch) that may excite them. In contrast, premotor frontal cortex embodies superimposed gradients, across the cortical map, based on modality and source of cortico-cortical input. This creates a multiplexed patchiness in receptive field structure and the sensitivity of local cortical zones to perceptual, categorical, and mnemonic inputs. Within each patch, many movement vectors are also represented, so such movement features are not the basis of map structure. In particular, in premotor cortex (area 6), there is a well-established medio-lateral gradient of sensitivity to proprioceptive vs. exteroceptive inputs (Mushiake, Inase & Tanji, 1991; Passingham, 1993). In FEF, which spans major parts of areas 8 and 45, there is a medio-lateral gradient for saccadic amplitude, from large-to-small saccades, in the rostral bank of the arcuate sulcus (Bruce et al. 1985). Moreover, this medio-lateral gradient for amplitude reflects differences in the nature of the afferents arriving in subareas of the FEF (Barbas & Mesulam, 1981; Barbas, 1988; Schall et al., 1995a, 1995b; Bullier et al. 1996). The medial, "large-saccade", part of FEF receives afferents from dorsal stream visual and auditory areas that process information about stimuli in, or even beyond, the visual periphery. This medial FEF area appears to lack

significant inputs from ventral stream areas TEO/V4 (ITp) and TE (ITa), both of which preferentially represent stimuli in the foveal and parafoveal regions of the visual field. In the lateral FEF, a strong projection from ITp terminates in FEF zone 45A and a strong projection from ITa terminates in FEF zone 45B (Bullier et al., 1996). Thus FEF zones receive functionally distinct types of inputs.

The model's GCZs (gateable cortical zones) in FEF reflect these input differences. Specifically, the model incorporates the fact that cells in ITp are sensitive to simple features falling within particular retinotopic loci (Tanaka et al., 1991; Komatsu & Ideura, 1993; Kobatake & Tanaka, 1994), whereas "position invariant" cells in ITa are sensitive to feature complexes ("objects") regardless of specific retinotopic locus (Gross et al. 1985; Tanaka et al. 1991). These systematic differences in the types of cues to which the FEF sub-areas are sensitive are consistent with the more general pattern observed for motor and premotor areas of frontal cortex (Passingham, 1993). The model proposes that sensitivity to distinct classes of inputs covaries with the GCZs. Thus, unlike BG gating of SC, BG gating of cortex operates on plan clusters defined by cue type and modality. The emphasis on cue sensitivity differences in FEF may seem surprising, because it was established long ago that FEF neurons *may* show no selectivity for stimulus properties such as shape or color (e.g., Mohler et al., 1973). However, evidence on the anatomical projections from feature sensitive areas such as ITp, when combined with physiological evidence on the emergence of feature selectivity in FEF neurons when features are consistently rewarded (Bichot et al., 1996), support the present hypothesis, as well as hypothesis 12 (below) regarding reward-guided learning mediated by weight changes on the IT to FEF pathways.

Figure 5 about here

Figure 5A illustrates this hypothesis. Maps of retinotopic inputs and motor error outputs at cortical and collicular levels are modeled by 3x3 cell grids. Each square within a grid represents a model cell with a receptive or movement field corresponding to its grid position, so each grid represents fixation (the null direction) plus eight saccade directions (each with unit amplitude). Figure 5B shows that each of the three FEF zones has input, plan, and output layers.

Overall, the model has twelve gateable zones, three cortical zones of 9-cells each, and nine collicular zones of 1-cell each. The model approximates the SNr-SC system with a map-like array of 9 SNr cells, each with output restricted to a corresponding region of the 9-cell SC map. Each SNr output to the SC is specific for a zone coding similar saccadic directions and amplitudes (Hikosaka & Wurtz, 1989; Bayer et al., 1999). Thus, there is *not* a single non-specific release of the entire SC when a BG gate opens. Although gating is specific to a subset of the SC map, it is coarse relative to the direction-specifying signals that are received by the SC from other structures, such as the PPC, FEF, and the retina (which is not modeled). Thus, saccadic accuracy depends mostly on non-nigral inputs to the SC, but saccadic occurrence, and to a lesser extent, velocity, depend on the degree of release of nigral inhibition (Takikawa et al. 2002). Greater realism could be achieved by scaling up the resolution of the SC map relative to the SNr map, but this was unnecessary for present purposes.

For the model FEF, there are three BG gates and corresponding PNR-THAL cells, each used to excite the entire grid within one of the three model GCZs. These GCZs correspond to patches of FEF that differ in whether they receive inputs from ITa or ITp, and, for the two GCZs with inputs from ITp, whether they respond more strongly to one discriminative visual feature or another. Thus each FEF GCZ controls a full range of saccadic directions, but its cells have a similar sensitivity to one or another visual feature, e.g., "red" or "T-shaped". In the following exposition, one of these GCZs is called the **GCZf** (GCZ, fixation feature) because cells in its ITp receptive field respond selectively to salient features of the fixation stimulus that distinguish it from the target stimuli to which the monkey will saccade after fixation light offset (Figure 1). The second GCZ is called the **GCZt** (GCZ, target feature) because its ITp receptive field is selective for salient features of target stimuli that distinguish them from the fixation stimulus. The model's third FEF gateable zone (Figure 5B) is called the **GCZo** because it corresponds to the part of area 45 that receives inputs from ITa (area TE) cells that show selectivity for feature complexes ("objects") regardless of where these complexes fall on the retina. Although the GCZo does not receive a retinotopic

projection from ITp, it does have other inputs, from the SC and LIP (not shown in Figure 5), that endow it with retinotopically organized planning and output layers. These two properties allows the GCZo to learn to associate a spatially invariant object category with a saccade direction, thus mapping a What stream sensory cue to a Where stream saccade plan. These GCZo cells thus mediate a learned What-to-Where transformation between different coordinate systems. Although cells in the GCZf and GCZt are in the What stream, in a sense they mediate a Where-to-Where transformation because their feature-specific filtering also reflects retinotopic organization within ITp.

With these three GCZs, the model is able to open one gate in the presence of two or more competing visual stimulus representations, and release movement only toward the stimulus that matches the feature or object class associated with the open gate. Thus, the correct movement will occur provided that the plan cell sitting in the correct GCZ becomes able (via reinforcement learning, see below) to win the striatal competition to open its gate. In a larger scale implementation, these fully discrete channels would be replaced by overlapping populations.

11. Sustained plan cell activity is a local cortical circuit property modulated by layer VI. Cortical cells whose activity correlates with plans often show task-dependent sustained firing that outlasts the stimulus presentations that cue the initial activation of these cells. In the model, sustained activation results from local, intra-cortical, recurrent excitation whenever the plan cell resides in a GCZ that has been aroused or primed. Such activation occurs when input from prefrontal cortex reaches plan cells via a cellular link in cortical layer VI; see Figure 2. These same layer VI cells are a source of excitation to the PNR-THAL cells whose disinhibition allows plans to execute. Differential priming via layer VI allows the frontal cortex to bias the pool of candidate plans to favor those that fall under the particular input-output relation enabled by the primed GCZ (Asaad et al., 2000; Hoshi et al., 1998). In contrast, some models have proposed that the basis of sustained frontal activations is a cortico-thalamo-cortical loop that starts with a cortical plan cell, traverses a thalamic stage subject to inhibition by the GPi or SNr, and returns to the plan cell of origin. In such a model, a BG gate *must* open to enable sustained activity of each plan cell. The latter seems unnecessarily restrictive for brief maintenance of candidate plans in FEF before one plan is selected and released, and may not even be necessary for prolonged storage in PFC (cf. Durstewitz et al., 2000). Moreover, anatomical studies (cited in Table 2) show that the thalamo-cortical projection (to layers III and V) from PNR-THAL may not even reach, and is certainly not restricted to, the layer VI cells of origin of the cortico-thalamic projection. Thus, there seems to be no anatomical basis for restricting modeled thalamo-cortical input so that it excites only plan cells, and therefore no basis for preventing this input from activating output cells in layer Vb. If so, it cannot serve the priming function proposed in alternative models.

12. Reinforcement signals guide learning of cortico-cortical and cortico-striatal links. Reinforcement learning can modify links from representations of arbitrary contexts and cues to plan representations. It can also affect interactions among candidate plans. Phasic, non-specific, dopaminergic signals emerging from the VTA/SNc in response to unpredicted rewarding events (Schultz, 1998) reach both frontal cortex and the striatum, where they modulate synaptic plasticity (Berger et al. 1988; Law-Tho et al., 1995; Wickens et al., 1996; Charpier & Deniau, 1997; Calabresi et al., 2000; Gurden et al., 2000; Bao et al., 2001; Reynolds et al., 2001; Cohen et al., 2002; Eyny & Horvitz, 2003). In the model, arbitrary cueing of plan activation is learned through reinforcement-guided modification of cortico-cortical links terminating in frontal cortex; see Figure 2. Then these cue-activated plan representations compete while exciting GABA-SIs and SPNs in the striatum. Learned weights on the cortico-striatal projections to SPNs can affect the competition for plan execution and thereby facilitate appropriate queuing of plans that are rewarded if performed in the proper context/sequence, but not otherwise. Consistent with recent data (Zheng & Wilson, 2002), this proposal departs from views of the striatum as a general adaptive pattern recognizer capable of representing arbitrary combinations of cortical states (Graybiel, 1998; Amos, 2000). In our model's BG direct and indirect channels (see Figure 4), phasic dopaminergic bursts and dips (Schultz, 1998; Brown et al., 1999) have opposite learning effects (Eyny and Horvitz, 2003), mediated by the differential expression of D1 and D2 dopamine receptors in striatal SPNs of the two channels. In particular, DA bursts cause increments of weights on recently active pathways to D1, substance P (SP)

and dynorphin (DYN) expressing SPNs of the direct channel, whereas DA dips cause increments of weights on recently active pathways to D2 and enkephalin (ENK) expressing SPNs of the indirect channel. This is consistent with observations (review in Steiner & Gerfen, 1998) that D1 and D2 receptor activations normally exert opposite effects on IEG (immediate-early gene) expression in SPNs. D1 activation induces IEG expression in D1 SPNs, but D2 activation does not induce IEG expression in D2 SPNs. Instead, given cortical input or NMDA receptor activation, D2 blockade induces IEG expression in D2 SPNs. Note that the D2 blockade may be equivalent to what occurs naturally when DA input dips due to pausing of SNc cell activity (Schultz, 1998). Overall, we emphasize cortico-cortical learning for control of the direct channel and cortico-striatal learning for control of the indirect channel. The latter is supported by recent data of Berretta et al. (1997). Unlike some (e.g., Young & Penney, 2001), we do not interpret the Berretta et al. (1997) data to imply a scarcity of adaptive mono-synaptic cortico-striatal links to the direct pathway. Many other data, e.g. the nature of cortical and SNc axon synapses with spines on virtually all SPNs, and the IEG and plasticity studies cited above, argue otherwise.

The model predicts that dopaminergic (DA-ergic) reinforcement signals interact with *traces* of stimulus and plan activations, not with plan activations, or responses, as such. When a delayed reinforcement signal signifies a positive outcome, it can strengthen an input's ability to activate the plan representation causally responsible for the rewarded act at a time when the plan representation has already been de-activated by response feedback. In the model, the time between termination of plan cell activation and the reinforcement signal is assumed to be bridged by an intracellular second messenger, which provides a short-term "trace" of the earlier plan activation. Such traces are predicted to be of brief duration, consistent with data showing that reinforcement learning falls off steeply when reward occurs more than a few seconds after the response. The time scale of these traces is shorter than that of working memory traces in dorsolateral PFC, which is not needed for reinforcement-guided learning or performance of externally cued behavior (Goldman-Rakic, 1987).

13. Feedback from superior colliculus to FEF serves learning and performance functions. Whenever any collicular zone becomes active enough to exceed a threshold, it excites FEF plan layer cells tuned to the same direction and grid position, across the 3 GCZs. This excitation of FEF plan cells by SC (via thalamus; Sommer & Wurtz, 1998) serves as a teaching signal that enables GCZs not initially responsible for SC activation to learn to take over responsibility for activating a specific SC map region on future occasions. This teaching signal is specific, and therefore more like the specific thalamo-striatal teaching signal proposed in hypothesis 7 than the non-specific DA teaching signal proposed in hypothesis 12. When the collicular activation becomes large enough to initiate a saccade, the SC to FEF excitation also activates FEF inhibitory interneurons that can selectively "reset" FEF plan cells tuned to the same direction as the activated SC cells. The model interprets the post-saccadic cells (see Figure 9E) found in FEF (Bruce et al., 1985) to be inhibitory reset neurons (Figure 2) that terminate specific plan representations once plan execution has initiated.

14. Cortico-subthalamic signals enhance lockout of competing plans during plan execution. Once a degree of freedom has been allocated to execute a plan, it should be protected from further plan bids and from interfering reactive movements (cf., Mink, 1996) while that plan is executing. The basis for such protection in the model is distributed, and includes the persistence of plan cell activity into the movement interval. One anatomical basis for locking out disruptive bids during execution is excitation of the BG's "hyperdirect" pathway (cortex-STN-GPi) by collaterals of the executive pathways. This hypothesis explains observations that collaterals of frontal cortical layer Vb projection neurons excite the STN (Canteras et al., 1990; Gerfen & Wilson, 1996), which in turn excites the GPe and GPi or SNr. It also explains why the GPi/SNr receives focused inhibition from striatum but broad excitation from STN (Parent & Hazrati, 1995). Further components of lockout protection may be supplied by specialized membrane properties (Wilson, 1995a) and recurrent GABAergic collaterals of SPNs, but these have not yet been incorporated in the model. Although hypothesis 14 differs from the recent proposal regarding the 'hyperdirect' pathway made by Nambu et al. (2002), their proposal was based on electrical stimulation studies that did not take account of either the laminar differences between (most) cortico-striatal and

cortico-STN cells or the physiological differences between such cells, as suggested by the results of Iwabuchi & Kubota (1998) and explicitly probed by Turner & DeLong (2000).

The macrocircuit implied by these fourteen hypotheses is schematized in Figure 2, which also serves as a key to most of the important variable names in the mathematical specification of the model. Table 2 tabulates anatomical studies supportive of the connectivity shown in Figure 2.

Table 2 about here

Mathematical model

Mathematical specification of the TELOS model's hypotheses required a system of differential equations, whose exposition follows. The Results section may be read before studying these equations. Figures 6a and 6b depict every model cell type, together with labeled inputs. These labels refer to variables in the equations. Each cell type obeys a nonlinear membrane (or "shunting") equation (Hodgkin, 1964; Grossberg, 1973), in which excitatory and inhibitory inputs affect separate conductances and thus do not act as additive injected currents that directly affect activation/potential. Often, a second and third equation further define the membrane equation by computing the cell's net excitatory and inhibitory inputs, symbolized by superscripts $^{(E)}$ and $^{(I)}$. In addition to explaining the form of the equations, this section cites additional data that support model details.

Figure 6 about here

Visual inputs to the cortical cell types.

External visual stimuli I^{*}_{xyj} were convolved with a Gaussian kernel to approximate visual cortical receptive field properties, in order to generate the pre-processed internal signal I_{xyj} (Figure 2). Specifically,

$$I_{xyj} = \sum_{(p,q)\in\Psi} I^{*}_{pqj} e^{\frac{-(p-x)^2-(q-y)^2}{(0.7)^2}}, \qquad (1)$$

where Ψ is the set of eight nearest neighbors in the Cartesian input space.

In the position-sensitive GCZs of the FEF, the signal I_{xyj} then generated two further signals, namely $I^{(p)}_{xy}$ and $I^{(d)}_{xyj}$ (Figure 2). The **positional FEF input** $I^{(p)}_{xy}$ is a transient, rapid-onset, input to FEF:

$$I^{(p)}_{xy} = \begin{cases} \sum_j I_{xyj} \ \textit{if}\ 50\,ms \le t - t^{(on)}_{xyj} \le 80\,ms \\ 0 \quad \textit{otherwise} \end{cases} \qquad (2)$$

This models the property that FEF input cells respond quickly (with about 50 ms. latency) to stimuli in their retinotopic receptive fields, regardless of stimulus features. The symbol $t^{(on)}_{xyj}$ is the time at which the convolved stimulus signal I_{xyj} rises above 0.3, an arbitrary threshold chosen to register activity but ignore spurious noise, and t is the current simulation time. Equation (2) specifies that input $I^{(p)}_{xy}$ to FEF spans the interval of 50 to 80 msec after I_{xyj} rises above threshold. The interval was set to accord with data on FEF cell onset and offset; see first burst in Figure 9A. By default, $I^{(p)}_{xy}$ = 0 outside that interval, or if no inputs are active. The quantity $t^{(on)}_{xyj}$ is not reset unless I_{xyj} first falls below the threshold 0.3. If the features possessed by the external stimulus are preferred by an FEF cell, then it fires a second burst at around 100 ms. This is modeled with the **stimulus-discriminating FEF input signal**, $I^{(d)}_{xyj}$, assumed to arrive from visual area V4 and ITp:

$$I^{(d)}_{xyj} = \begin{cases} I_{xyj} \ \textit{if}\ 100\,ms \le t - t^{(on)}_{xyj} \le 130\,ms \\ 0 \quad \textit{otherwise} \end{cases} . \qquad (3)$$

The interval 100-130 msec. was based on timing of the onset of the second burst in the data; see second burst in Figure 9A.

Input $I_{xy}^{(pc)}$ to the PPC is similar to the positional $I_{xy}^{(p)}$ input to FEF, except that there is no upper time limit, because PPC activity is sustained as long as the visual input remains on (Figure 10C). Thus,

$$I_{xy}^{(pc)} = \begin{cases} \sum_j I_{xyj} \ \textit{if } t - t_{xyj}^{(on)} > 50\,ms \\ 0 \quad \textit{otherwise} \end{cases}. \tag{4}$$

The 50 msec onset delay reflects the time required for light impinging on the retina to activate PPC, as seen in Figure 11C.

In addition to these positionally-sensitive visual signals, the model also invokes signals to the gated cortical zones that respond to objects independent of their positions. Thus inputs T_j from ITa cells (Figures 2 and 6a) respond to visual features of type j regardless of their spatial position (hence the absence of a subscript xy). The dynamics of **space-invariant anterior IT cells** T_j were modeled by:

$$\frac{d}{dt}T_j = 150(1-T_j)I_j^{(IT)} - 30T_j, \tag{5}$$

Thus T_j can be excited by model input $I_j^{(IT)}$ to a maximum value of 1, and can also spontaneously decay.

Reactive and attentive processing: PPC, SC, and SNr gating signal

The model supposes that developmental processes have enabled the FEF representations of oculomotor plans to be in register with the SC and PPC representations; see Gancarz & Grossberg (1999) for a consistent model that proposes how this happens.

PPC cell activities P_{xy} (Figures 2 and 6a) represent responses in the lateral bank of the intraparietal cortex (LIP), which code visual stimuli in motor error coordinates (Gnadt & Andersen, 1988). These activities were modeled by:

$$\frac{d}{dt}P_{xy} = 25\left[\left(1-P_{xy}\right)P_{xy}^{(E)} - P_{xy}P_{xy}^{(I)}\right]. \tag{6}$$

Equation (6) says that P_{xy} can be excited by net input $P_{xy}^{(E)}$ to a maximum value of 1, and inhibited by net input $P_{xy}^{(I)}$ to a minimum value of zero. The **excitatory input $P_{xy}^{(E)}$ to PPC cells** was defined by

$$P_{xy}^{(E)} = 5(I_{xy}^{(PC)} + \sum_i f^{(O)}(F_{xyi}^{(O)})) + 2([F_{xyi}^{(P)}]^+)^4, \tag{7}$$

which includes excitation from visual signals ($I_{xy}^{(PC)}$; defined below in (8)), FEF output layer cells ($F_{xyi}^{(O)}$; defined in (21)), and FEF plan layer cells ($F_{xyi}^{(P)}$; defined in (14)). Here the summation index i ranges from 1 to 3 to represent different FEF zones, as in Figure 5. The notation $[w]^+ = \max(w,0)$ means that the argument w is thresholded at zero. The visual signals to PPC can drive reactive saccades. However, the potent input from FEF can override the visual signals and reprogram the PPC to reflect the spatial goal of a previously rewarded saccadic plan.

For reactive saccades, the strengths of competing visual signals must be unequal for a decision to be made. Both cortical magnification and motivational signals play a role in the competition that determines PPC attentional focusing (Platt & Glimcher, 1999). Here cortical magnification sufficed, and the **visual inputs $I_{xy}^{(PC)}$** to the model PPC cells were defined by:

$$I_{xy}^{(PC)} = I_{xy}^{(pc)} + 0.01(1.1|x-1| + |y-1|). \tag{8}$$

This ensures that given multiple inputs of equal strength, peripheral inputs are more likely to evoke a saccade than foveal inputs, and objects left or right of the fovea are more likely to attract the eye than objects above or below. Nonetheless, this peripheral bias is not sufficient to maladaptively break fixation of a visible stimulus.

The **inhibitory input** $P_{xy}^{(I)}$ to PPC cells in (6) was defined by

$$P_{xy}^{(I)} = 1 + 10P_{xy}^{(R)} + 200 \sum_{(p,q)\neq(x,y)} ([P_{pq}]^+)^4 . \quad (9)$$

Term $P_{xy}^{(R)}$ specifies recurrent self-inhibition, which ensures phasic PPC activity, as seen in Figure 11C. Dynamics for the interneuron mediating self-inhibition were defined by

$$\frac{d}{dt} P_{xy}^{(R)} = 2[(1 - P_{xy}^{(R)})P_{xy} - P_{xy}^{(R)}] . \quad (10)$$

The summation term in (9) describes quickly-acting lateral inhibition.

Activities S_{xy} of **SC cells** (Figures 2 and 6b) were excited by signals from PPC (P_{xy}) and the FEF output layer ($F_{xyi}^{(O)}$), and inhibited by the topographic and potent SNr output, $G_{xy}^{(SNr)}$, and a tonic signal set to a value of 10:

$$\frac{d}{dt} S_{xy} = (1 - S_{xy})(60P_{xy} + 5\sum\nolimits_i f^{(O)}(F_{xyi}^{(O)})) - S_{xy}(800[G_{xy}^{(SNr)} - 0.3]^+ + 10) \quad (11)$$

The inhibitory input $G_{xy}^{(SNr)}$ from SNr (defined in (32)) tends towards 1 when the BG gate is shut, and towards zero when open. In the former case, Equation (11) implies that SC activity will be low even in the presence of strong excitatory inputs. When the gate opens as $G_{xy}^{(SNr)}$ is driven near zero, S_{xy} can become highly active in response to inputs from PPC or FEF. In the simulations, the SNr output signal $G_{xy}^{(SNr)}$ had the same indices and spatial resolution as the model SC map. Although the *in vivo* SC map has much higher resolution than the SNr output, this higher resolution was not needed for the data simulated. Also, the simple SC model used here has SC burst cells but omits SC buildup cells (Munoz & Wurtz, 1995). A consistent but more detailed SC model, with buildup cells as well as burst cells, was described in Grossberg et al. (1997), but the added detail was not needed for the data modeled in this article. Because of its simplified SC treatment, the present model does not include connections from FEF plan cells to the SC, a projection that is consistent with the computational hypotheses of the model and that appears to be justified by physiological observations (e.g., Sommer & Wurtz, 2000).

Planning in the frontal eye fields

The activity $F_{xyi}^{(I)}$ of an **FEF input cell** (Figures 2 and 6a) was defined by:

$$\frac{d}{dt} F_{xyi}^{(I)} = 60(1 - F_{xyi}^{(I)})[I_{xyj}^{(d)} + I_{xy}^{(p)}] - F_{xyi}^{(I)} \left[100 + 30 \sum_{(r,s)\neq(x,y)} (I_{rs}^{(p)} + I_{rsj}^{(d)}) \right] . \quad (12)$$

Here the index *i* in the subscript of $F_{xyi}^{(I)}$ ranges from 1 to 3 and denotes FEF GCZ, as in Figure 5. These model FEF "visual cells" (Schall et al., 1995a) respond to excitation from areas including V4 and ITp, and are predicted to reside in granular or supragranular layers. The excitatory inputs $I_{xyj}^{(d)}$ (where *j* denotes stimulus feature) and $I_{xy}^{(p)}$ were defined in (2) and (3). Feedforward lateral inhibition (the term Σ in (12)) among FEF visual cells (Schall et al., 1995b) helps to normalize the overall activity and allows a stronger response to a unique, isolated stimulus than to multiple stimuli, consistent with the "oddball discrimination" effect observed in the FEF (Thompson et al., 1997).

The model **FEF layer VI** cells arouse a zone of cells in the columns above (see Figures 2 and 6a). Model layer VI activity $F_i^{(G)}$ was defined by

$$\frac{d}{dt} F_i^{(G)} = (1 - F_i^{(G)})(80T_j + 2000 \sum_j W_{ji}^{(CG)} [C_j - 0.35]^+) - 160F_i^{(G)} \quad . \quad (13)$$

Input T_j from ITa provides a training signal that enables positionally-invariant inputs C_j, from prefrontal working memory cells to learn to select a zone of FEF cells, constituting a premotor zone *i*, by activating

module *i*'s layer VI cells. The adaptive weight $W_{ji}^{(CG)}$, on the path from PFC site *j* to FEF module *i*, denotes a synaptic strength that can be modified by reinforcement learning; see equation (55).

Model **FEF plan layer cells** correspond anatomically to layer III/Va cells from which the cortico-striatal projection arises (Figures 2 and 6a), and physiologically to FEF "visuo-movement cells". As shown in Figure 5, they may be fixation- or saccade-related, and they may perform a "What-Where" or a "Where-Where" transformation via distinct cortical zones. The combination of these attributes leads to four kinds of plan layer cells with distinct connectivity patterns. Within a cortical zone, cells generally compete, but there is no general between-zone competition. However, learned selectivity of zone activation was found to develop more quickly if the *same* saccade vector (including the special case of fixation) does not have simultaneous strongly active representations in different zones. This rate effect occurs because weight change is a function of activation level. Although not necessary for learning as such, the learning speed advantage warrants the hypothesis that competition exists between like vectors in different zones. Moreover, a basis exists in the model for self-organization of such vector-specific competition based on a "fire-together, wire-together" principle: As shown in equations (15) and (18) below, all plan cells coding for vector (x,y) receive a common excitatory input $k^{sfp}[S_{xy} - 0.25]^+$ from SC zone (x,y) and a common inhibitory input $F_{xy}^{(X)}$ from FEF post-saccadic cells excited by SC zone (x,y). For these reasons, the model presented here includes between-zone competition between cells coding for the same vector. However, *different* saccade vector plans may simultaneously be highly active in different zones, to provide alternative plans from which to choose.

Activity $F_{xyi}^{(P)}$ of **FEF plan layer** cell *xyi* was defined by

$$\frac{d}{dt}F_{xyi}^{(P)} = 500[(1-F_{xyi}^{(P)})F_{xyi}^{(PE)} - (F_{xyi}^{(P)} + 0.4)F_{xyi}^{(PI)}] \tag{14}$$

where $F_{xyi}^{(PE)}$ is the total excitatory input to a plan layer cell, and $F_{xyi}^{(PI)}$ is the total inhibitory input. The **excitatory input** $F_{xyi}^{(PE)}$ of (14) was defined by

$$\begin{aligned} F_{xyi}^{(PE)} &= F_{xyi}^{(I)} + 0.025q(F_i^{(G)}, 0.15) + k^{fpr} f^{(P)}(F_{xyi}^{(P)}) \\ &\quad + 0.1\sum\nolimits_j W_{jxyi}^{(TP)} T_j + k^{sfp}[S_{xy} - 0.25]^+. \end{aligned} \tag{15}$$

Input $F_{xyi}^{(I)}$ from the FEF input layer was defined in (12). Term $F_i^{(G)}$ is input from layer VI, defined by (13). The **threshold signal function** *q(x,a)* that transforms $F_i^{(G)}$ was defined by

$$q(x,a) = \begin{cases} 0 & if \quad x < a \\ x & if \quad x \geq a \end{cases}. \tag{16}$$

It allows background noise to be filtered out while even small suprathreshold signals can generate robust activity. Parameter k^{fpr} of (15) scales the FEF plan layer recurrent excitation, $f^{(P)}(F_{xyi}^{(P)})$, which is restricted to the cell of origin. The **sigmoid signal function** $f^{(P)}$ in (15) was defined by

$$f^{(P)}(x) = \frac{\left([x]^+\right)^8}{(0.5)^8 + \left([x]^+\right)^8}. \tag{17}$$

With $F_{xyi}^{(P)}$ as its argument, the steep sigmoid specified by (17) ensures that recurrent excitation within the plan layer can result in self-sustaining activity when a plan layer cell's activity exceeds 0.5 due to inputs from layer VI, ITa, and/or SC.

Term T_j in (15) is input from ITa that is defined by (5). It is multiplied by the adaptive synaptic weight $W_{jxyi}^{(TP)}$ that is defined by (56). This weight is non-zero only for projections to FEF What-Where (not Where-Where) GCZs. This link allows a category representation in ITa to learn to activate a saccadic plan. The term S_{xy} (defined by (11)) is from the SC (Lynch et al., 1994). The rectified signal $[S_{xy} - 0.25]^+$ grows linearly with S_{xy} above the signal threshold 0.25 but is zero for all S_{xy} below 0.25. Parameter k^{sfp} is the SC-to-FEF plan layer synaptic strength.

Fixation-related plan cells are those cells with Cartesian coordinates (x,y) = (1,1). There were three such cells, one in each FEF zone. For saccade-related cells, $k^{fpr} = 0.18$, $k^{sfp} = 8$; for fixation-related cells, $k^{fpr} = 0.0$, $k^{sfp} = 0.0$. Thus saccade-related, but not fixation-related, cells can receive movement-related corollary discharges from the SC and exhibit self-sustaining recurrent excitation.

The **inhibitory inputs** $F_{xyi}^{(PI)}$ of (14) were defined by:

$$F_{xyi}^{(PI)} = 0.06 + 5F_{xy}^{(X)} + k^{fpri}\left(\sum_{m\neq i} f^{(P)}(F_{xym}^{(P)})\right) + k^{fpi}\left(f_j^{(W)}(F_{xyi}^{(P)}) - f^{(P)}(F_{xyi}^{(P)})\right) + k^{fop}\left(\sum_k \sum_{(p,q)\neq(1,1)} [F_{pqk}^{(O)} - 0.6]^+ + 5\sum_{m\neq i} f^{(P)}(F_{11m}^{(P)})\right) \quad (18)$$

Here $F_{xy}^{(X)}$ is inhibition from FEF postsaccadic cells, defined below by (26). The parameter k^{fpri} scales FEF plan layer recurrent inhibition from same-direction saccade-related cells in other zones. Recurrent inhibition prevents multiple representations of the same saccade vector from being active, to prevent interference between different GCZs while strategies are learned. For plan cells in the fixation and target feature zones, which can mediate Where-Where transformations, $k^{fpri} = 0.1$. However, $k^{fpri} = 0.0$ for cells in the What-Where zone, GCZo: Since this zone lacks the positional inputs of the Where-Where zones, interference during learning will not occur. Of the final two terms in equation (18), only one is non-zero for any single cell, because the model's saccade- and fixation-related plan cells have different patterns of inhibitory afferents. The parameter k^{fpi} scales recurrent inhibition from saccade-related cells to saccade-related cells tuned to different directions, indexed by the coordinates (x,y). The parameter k^{fop} scales the FEF output layer and plan layer inhibition to fixation-related plan cells. Thus, for saccade-related cells, $k^{fpi} = 0.1$, but $k^{fop} = 0.0$. For fixation-related cells, $k^{fpi} = 0.0$, but $k^{fop} = 1.0$. The summation index k denotes the zone (k=1,2,3) of cells representing motor error vectors (p,q).

In the fourth term of (18), the **lateral inhibitory signal,** $f_j^{(W)}(F_{xyi}^{(P)})$, takes a different form for Where-Where (indexed by j=1) and What-Where (indexed by j =2) cells. Although Where-Where plans encoding the same saccade vector inhibit each other across zones, Where-Where plan cells do not inhibit What-Where plan cells. Lateral inhibition from saccade-related plan cells to saccade-related plan cells in either Where-Where zone, was defined by

$$f_1^{(W)}(F_{xyi}^{(P)}) = \sum_{k\in\Omega} \sum_{(p,q)\neq(1,1)} f^{(P)}(F_{pqk}^{(P)}), \quad (19)$$

where Ω is the set of all plan layer cells in the Where-Where zones, for which index k = 0 and 1. (More generally, the indices i and k refer to zones in the cortex and basal ganglia, respectively. Use of separate indices allows computation of the interaction among zones, e.g., in equation (52).)

In (18), the subtraction of $f^{(P)}(F_{xyi}^{(P)})$ from $f_1^{(W)}(F_{xyi}^{(P)})$ excludes self-inhibition. Excitatory term $k^{fpr} f^{(P)}(F_{xyi}^{(P)})$ of (15) and inhibitory term $k^{fpi}\left(f_1^{(W)}(F_{xyi}^{(P)}) - f^{(P)}(F_{xyi}^{(P)})\right)$ of (18) together define a recurrent on-center, off-surround network, which acts to normalize and contrast-enhance network activity (Grossberg, 1973) .

For cells in the What-Where zone, $k^{fpri} = 0.0$ in (18), and the lateral inhibitory signal $f_2^{(W)}(F_{xyi}^{(P)})$ was

$$f_2^{(W)}(F_{xyi}^{(P)}) = \sum_{(p,q)\neq(1,1)} f^{(P)}(F_{pqi}^{(P)}). \quad (20)$$

Lateral inhibition came only from saccade-related cells of the same zone.

Model FEF output cells correspond to FEF movement or presaccadic cells, and are predicted to reside in layer Vb; see Figures 2 and 6a. They are divided into fixation- and saccade-related categories. Their activity $F_{xyi}^{(O)}$ was defined by:

$$\frac{d}{dt}F_{xyi}^{(O)} = 125[(1-F_{xyi}^{(O)})F_{xyi}^{(OE)}F_i^{(G)} - (F_{xyi}^{(O)} + 0.6)F_{xyi}^{(OI)}], \quad (21)$$

where $F_{xyi}^{(OE)}$ excites the output cells and $F_{xyi}^{(OI)}$ inhibits them. The arousal signal $F_i^{(G)}$ from layer VI, defined by (13), multiplies $F_{xyi}^{(OE)}$, which was defined by:

$$F_{xyi}^{(OE)} = 1.5[V_k - 0.5]^+ + 0.4q(F_{xyi}^{(P)}, 0.2) + k^{sfo}[S_{xy} - 0.4]^+. \quad (22)$$

In (22), $1.5[V_k - 0.5]^+$ is the thalamocortical input; see (38). It conveys a GO signal from the BG if thalamic activity V_k exceeds 0.5. Subscript *k* of V_k has the same range (1-3) as *i* of $F_{xyi}^{(OE)}$ because there is a one-to-one relationship between FEF zones and associated thalamic sites controlled by distinct BG channels. Signal function *q(x,a)* was defined in (16). Input $F_{xyi}^{(P)}$ is from the plan layer and S_{xy} is from the SC. The product of $F_{xyi}^{(OE)}$ and $F_i^{(G)}$ in (21) makes output contingent on a conjunction of arousal with plan layer, thalamocortical, and SC inputs. In particular, corollary discharges from the SC cannot activate output layer cells whose corresponding zone is not active. Parameter k^{sfo} in (22) is the strength of the SC's projection to the FEF output layer. For saccade-related cells, k^{sfo}=10; for fixation-related cells, k^{sfo}=0. Therefore, a corollary discharge from the SC can excite saccade-related but not fixation-related cells.

The inhibitory input $F_{xyi}^{(OI)}$ in (21) differs for fixation-related and saccade-related output cells. The latter are inhibited by both postsaccadic cells and output layer cells that are tuned to other saccadic vectors. The **inhibitory signals $F_{xyi}^{(OI)}$ to saccade-related FEF output cells**, for which (x,y) ≠ (1,1), were defined by:

$$F_{xyi}^{(OI)} = 0.3 + 6F_{xy}^{(X)} + \sum_k \sum_{(p,q)\neq(1,1)} f^{(O)}(F_{pqk}^{(O)}) - f^{(O)}(F_{xyi}^{(O)}), \quad (23)$$

where $F_{xy}^{(X)}$ is input from postsaccadic cells defined by (26), the summation index *k* denotes zone, and the **output layer signal function** $f^{(O)}$ was a sigmoid:

$$f^{(O)}(x) = \frac{([x]^+)^{10}}{([x]^+)^{10} + 0.4^{10}}. \quad (24)$$

Because of the steep shape of the sigmoid in (24), output layer cell activity must exceed 0.4 to inhibit other output layer cells. The high threshold for competition among FEF output cells creates an interval – before any cells exceed this threshold on the basis of dual inputs from the plan layer and the thalamus – during which FEF output cells can be transiently activated by visually driven signals arriving via the plan layer. Such a transient visual response is seen in the presaccadic movement cell shown in Figure 9D.

The **inhibitory signal to fixation-related FEF output cells** was defined by

$$F_{11i}^{(OI)} = 0.3 + 6F_{xy}^{(X)} + \sum_k \sum_{(p,q)=(1,1)} f^{(O)}(F_{pqk}^{(O)}) - f^{(O)}(F_{11i}^{(O)}) + 10\sum_k \sum_{(p,q)\neq(1,1)} [F_{pqk}^{(O)} - 0.6]^+. \quad (25)$$

Again, summation index *k* denotes zone. The final term in (25) allows saccade-related FEF output cells to inhibit fixation-related output cells via inhibitory interneurons. Fixation-related plan and output cell activities, specified in equations (14-18) and (21,22, 25), respectively, begin to shut off immediately prior to a saccade due to the inhibition from saccade-related FEF plan and output cells.

FEF postsaccadic cell activities $F_{xy}^{(X)}$ were defined by:

$$\frac{d}{dt}F_{xy}^{(X)} = 500\left(1 - F_{xy}^{(X)}\right)[S_{xy} - 0.6]^{+} - 10F_{xy}^{(X)}. \tag{26}$$

Postsaccadic cells delete executed plans; see (18). They are excited by the corresponding SC cell activities S_{xy}; see (11). The SC signal was modeled by thresholding the SC activity. The 0.6 threshold for exciting them is also the threshold of saccade initiation in the SC.

Model BG and PNR-THAL cells

Cortical afferents to the striatum of the BG include projections from inferotemporal cortex (Hoesen et al., 1981; Steele and Weller, 1993), parietal cortex (Cavada and Goldman-Rakic, 1991), and frontal cortex (Parthasarathy et al., 1992; Strick et al., 1995). All three classes of afferents project to the BG model. Basal ganglia components that ultimately project to the SC are denoted by the symbol *G*, and those that ultimately return to frontal cortex via the PNR-THAL are denoted by the symbol *B.* The model coordinate systems are also distinct because the thalamus-projecting population codes a zone's choice, while the colliculus-projecting population codes motor error.

The SC-projecting **striatal SPN direct pathway activity** $G_{xy}^{(SD)}$ (Figures 2 and 6b) was defined by:

$$\frac{d}{dt}G_{xy}^{(SD)} = 30\left[\left(1 - G_{xy}^{(SD)}\right)G_{xy}^{(SDE)} - \left(G_{xy}^{(SD)} + 0.58\right)G_{xy}^{(SDI)}\right], \tag{27}$$

where the excitatory input is $G_{xy}^{(SDE)}$, and the inhibitory input is $G_{xy}^{(SDI)}$. The excitatory signal was defined by:

$$G_{xy}^{(SDE)} = N + 75\left[P_{xy} - 0.25\right]^{+} + 100\sum\nolimits_{i} f^{(O)}\left(F_{xyi}^{(O)}\right), \tag{28}$$

where *N* refers to a dopamine burst (Ljungberg et al., 1992), which can activate the striatum and modulate corticostriatal reinforcement learning (Wickens et al., 1996). Signals from parietal cortex $[P_{xy} - 0.25]^{+}$, and FEF output cells, $f^{(o)}(F_{xyi}^{(O)})$, promote opening of the BG-to-SC gate to allow execution of the plans that they represent. The model assumes that the excitatory inputs are strong but specific: they are pooled only across parietal and FEF sites that represent the same motor vector. In contrast, the inhibitory inputs are convergent: they are pooled across parietal and FEF sites regardless of the motor error vector represented. The **inhibitory input** $G_{xy}^{(SDI)}$ was defined by:

$$G_{xy}^{(SDI)} = 1 + 20\left(\sum_{pq}\left[P_{pq} - 0.25\right]^{+} + \sum_{pqi} f^{(O)}\left(F_{pqi}^{(O)}\right)\right), \tag{29}$$

which models fast-acting feedforward striatal inhibitory interneurons (Wilson et al., 1989; Koos & Tepper, 1999) that are excited by convergent parietal cortex and FEF outputs from all positions (p,q) and zones *i*. Because of the relative strengths of the inputs in (28) and (29), a plan-representing saccade vector (*x*,*y*) can always activate the striatum if the main source of inhibition in the summations of (29) comes from cells at grid coordinate (*x*,*y*). This condition will be met when the cortical competition resolves in favor of one winning plan. Otherwise, inhibition can overwhelm excitation; see Figure 3. Also noteworthy is that equation (29) does not include feedback inhibition from SPNs. This is consistent with electrophysiological data of Jaeger et al. (1994) indicating that such inhibition is weak. The theory does not, however, preclude a role for feedback inhibition; see equation (41).

Colliculus-controlling **striatal SPN activity** $G_{xy}^{(SI)}$ (Figures 2 and 6b) was defined by:

$$\frac{d}{dt}G_{xy}^{(SI)} = 30\left[\left(1 - G_{xy}^{(SI)}\right)10\overline{N}S_{xy} - \left(G_{xy}^{(SI)} + 0.58\right)\right], \tag{30}$$

where $\overline{N}$ corresponds to a transient depression in the dopamine signal (a dopamine dip), as described by Ljungberg et al. (1992). The excitatory action of $\overline{N}$ is attributable to reduced binding of inhibitory D2 receptors on indirect path SPNs. Excitatory input, S_{xy}, from the SC informs the indirect channel that the

SC region that is gated by the corresponding direct channel is being activated. As noted for the analogous case of thalamo-striatal feedback in hypothesis 7, such an input to the indirect channel can serve as a training signal for other excitatory afferents to SPNs; see equation (34). However, no such afferents were needed to SPNs represented by equation (30) in the present simulations. The constant term (0.58) of equation (30) specifies tonic inhibition.

Colliculus-controlling **GPe activity** $G_{xy}^{(GPe)}$ (Figures 2 and 6b) was defined by:

$$\frac{d}{dt}G_{xy}^{(GPe)} = 30\left[0.5\left(1-G_{xy}^{(GPe)}\right)-\left(G_{xy}^{(GPe)}+1\right)\left(0.2+0.8\left[G_{xy}^{(SI)}\right]^{+}\right)\right]. \tag{31}$$

The first term of (31) represents a combination of intrinsic excitation and tonic excitation from the STN. Input $G_{xy}^{(SI)}$ from the striatal indirect pathway SPN provides inhibition.

SNr activity $G_{xy}^{(SNr)}$ (Figures 2 and 6b) was defined by:

$$\frac{d}{dt}G_{xy}^{(SNr)} = 100\left(1-G_{xy}^{(SNr)}\right)-\left(G_{xy}^{(SNr)}+1\right)\left(54\left[G_{xy}^{(SD)}\right]^{+}+80\left[G_{xy}^{(GPe)}\right]^{+}\right). \tag{32}$$

The first term of (32) represents a combination of intrinsic excitation and tonic excitation from the STN. Both the striatal direct pathway SPN ($G_{xy}^{(SD)}$) and the GPe ($G_{xy}^{(GPe)}$) provide inhibition.

The **thalamus-projecting BG system** differs from the SC-projecting system in having adaptive cortico-striatal pathways. The thalamus-projecting **striatal SPN direct pathway activity** $B_k^{(SD)}$ (Figures 2 and 6b) was defined by:

$$\frac{d}{dt}B_k^{(SD)} = 50\left[\left(1-B_k^{(SD)}\right)\left(70\sum\nolimits_{xyi}\left[F_{xyi}^{(P)}-0.33\right]^{+}W_{xyik}^{(PSD)}+8\sum\nolimits_j T_j W_{jk}^{(TSD)}+N+2\left[V_k\right]^{+}\right)\right.$$
$$\left.-\left(B_k^{(SD)}+0.58\right)\left(1+1.17\left(\sum\nolimits_{xyi}F_{xyi}^{(P)}+2\sum\nolimits_i V_i\right)\right)\right]. \tag{33}$$

Subscript *k* ranges from 1-3 to denote the three thalamus-controlling BG channels associated with the three FEF zones. The FEF plan layer activities $F_{xyi}^{(P)}$, defined in (14), and the anterior IT activities T_j, defined in (5), provide learned excitation to striatal direct pathway SPNs. The adaptive weight $W_{xyik}^{(PSD)}$ is defined by (53), and the adaptive weight $W_{jk}^{(TSD)}$ is defined by (54). A dopamine burst *N* provides a dopamine-mediated enhancement of striatal activity via D1 receptors. Thalamic inputs V_k provide excitatory feedback that can help train FEF and ITa inputs to activate the striatal direct pathway. Activity in the FEF plan layer and thalamus also use feedforward striatal inhibitory interneurons (the last two terms in (33)) to inhibit striatal direct pathway activity, as in (27) and (29).

Striatal indirect pathway SPN activity $B_k^{(SI)}$ (Figures 2 and 6b) was defined by:

$$\frac{d}{dt}B_k^{(SI)} = 30\left[\left(1-B_k^{(SI)}\right)\left(70\sum\nolimits_{xyi}W_{xyik}^{(PSI)}\left[F_{xyi}^{(P)}-0.33\right]^{+}+10\overline{N}\left[V_k\right]^{+}\right)\right.$$
$$\left.-\left(B_k^{(SI)}+0.58\right)\left(1+.17\sum\nolimits_{xyi}\left[F_{xyi}^{(P)}\right]^{+}\right)\right]. \tag{34}$$

Learned excitatory inputs from the FEF plan layer $F_{xyi}^{(P)}$ are adaptively weighted by the $W_{xyik}^{(PSI)}$ and add with excitatory input V_k from the thalamus that is enhanced when a dip ($\overline{N}>0$) occurs in the dopaminergic input, which acts on D2 receptors. Indirect pathway SPNs are also suppressed by feedforward inhibitory interneurons, which are driven by FEF plan layer inputs $F_{xyi}^{(P)}$. The adaptive

weights $W_{xyik}^{(PSI)}$ in (34) are defined by (52).

The SNr/GPi receives input from the STN, the striatal direct pathway projections, and the GPe. The **SNr/GPi activity** $B_k^{(GPi)}$ (Figures 2 and 6b) was defined by:

$$\frac{d}{dt}B_k^{(GPi)} = 100\left[\left(1-B_k^{(GPi)}\right)\left(0.77+2\left[B^{(STN)}\right]^+\right) - \left(B_k^{(GPi)}+1\right)\left(0.54\left[B_k^{(SD)}\right]^+ + 0.8\left[B_k^{(GPe)}\right]^+\right)\right]. \quad (35)$$

By (35), the GPi receives tonic excitation and glutamatergic excitation $B^{(STN)}$ from the STN, and is inhibited by striatal direct pathway SPN outputs $B_k^{(SD)}$ and GPe outputs $B_k^{(GPe)}$. In the case of the oculomotor system, the SNr rather than GPi projects to the PNR-THAL, which projects to FEF. These SNr projections are distinct from SNr-to-SC projections modeled by $G_{xy}^{(SNr)}$ in equation (32) above (Kemel et al., 1988).

The **GPe activity** $B_k^{(GPe)}$ (Figures 2 and 6b) is excited by the STN output $B^{(STN)}$ and inhibited by the striatal indirect path SPN outputs $B_k^{(SI)}$:

$$\frac{d}{dt}B_k^{(GPe)} = 30\left[\left(1-B_k^{(GPe)}\right)\left(0.46+0.25B^{(STN)}\right)-\left(B_k^{(GPe)}+1\right)\left(0.2+0.8\left[B_k^{(SI)}\right]^+\right)\right]. \quad (36)$$

The **STN activity** $B^{(STN)}$ (Figures 2 and 6b) is excited by afferents from layer Vb (the output layer, $F^{(O)}$) of the FEF and inhibited by the GPe outputs $B_k^{(GPe)}$:

$$\frac{d}{dt}B^{(STN)} = 25\left[\left(1-B^{(STN)}\right)\left(0.016+10\sum_i\sum_{(p,q)\neq(1,1)}\left[F_{pqi}^{(O)}-0.5\right]^+\right) - 0.1B^{(STN)}\sum_k\left[B_k^{(GPe)}\right]^+\right]. \quad (37)$$

With $(p,q) \neq (1,1)$, the summation index spans inputs from saccade-related, but not fixation-related, cells.

STN hyperactivity in Parkinson's disease has, in the past (Wichmann & DeLong, 1996), been attributed to GPe hypoactivity and the subsequent loss of GPe-STN inhibition. This argument has supported the prevailing model of basal ganglia function in which the GPe-STN projection is an essential link in the indirect pathway. However, Levy et al. (1997) reviewed evidence that GPe activity is not significantly reduced in Parkinsonism, suggesting that loss of GPe-STN inhibition may not be sufficient to account for STN hyperactivity in Parkinson's disease. Moreover, dopaminergic lesions directly in the STN, which contains D1 and D2 receptors (Brown et al., 1979; Martres et al., 1985), result in five times the STN hyperactivity induced by GPe lesions alone (Hassani et al. 1996), although the precise mechanism for this is not clear. Therefore we have modeled the GPe-STN projection as weak relative to the GPe-GPi/SNr projection (Parent & Hazrati, 1995; Smith & Bolam, 1990).

Activities V_k in the PNR-THAL, e.g., VA and Vlo, are excited by afferents from cortical layer VI (the category layer, $F_k^{(G)}$) and inhibited by the GPi ($B_k^{(GPi)}$). **Thalamic activity** V_k (Figures 2 and 6b) was defined by:

$$\frac{d}{dt}V_k = 400\left[\left(1-V_k\right)\left(0.5\left[F_k^{(G)}-0.47\right]^+ + f^{(V)}\left(V_k\right)+v^{(tonic)}\right) - \left(V_k+0.1\right)\left(0.2+3.4\left[B_k^{(GPi)}-0.2\right]^+ + \sum_{i\neq k} f^{(V)}\left(V_i\right)V_i^{(X)}\right)\right], \quad (38)$$

where the **feedback signal function** $f^{(V)}$ was defined by

$$f^{(V)} = \left([x]^+ \right)^2 . \tag{39}$$

The term $v^{(tonic)}$ is 0.0 if the thalamic cell projects to a Where-Where FEF zone (i.e., $k < 2$) and 0.1 if the thalamic cell projects to a What-Where FEF zone (i.e., $k = 2$). This small tonic level biases the system to use What-Where FEF plans initially during learning. For example, in learning the delay task, the model first attempts a saccade to the target that was learned in the gap task. This target is recalled via a learned What-Where transformation. Subsequent punishment trains the model to suppress the response learned in the gap task.

Thalamic recurrent inhibition, which is well established in the visual thalamus (Lo and Sherman, 1994), mediates a local winner-take-all competition that allows only the thalamocortical projection of one FEF zone at a time to generate output. Since lateral inhibition within a zone in the plan layer allows only one plan to be active per zone, this helps ensure that multiple conflicting plans are not simultaneously executed. In the thalamus, newly formed plans can shut off a prior plan and instate themselves as current winner if the ability of the prior winner to maintain itself wanes through time. This will occur if self-excitation and/or recurrent surround inhibition use habituative signals. The current implementation uses only the latter. Thus, a transmitter level, symbolized $V_k^{(X)}$ in (38) and defined in (40), is assumed to mediate GABA-ergic lateral inhibition and to habituate (inactivate, or depress) with continued firing. As a result, a new plan can be instated and can effectively inhibit a previously active plan whose inhibitory signals have habituated. **Thalamic habituative transmitter** $V_k^{(X)}$ was defined (cf., Grossberg, 1982) by:

$$\frac{d}{dt} V_k^{(X)} = 0.25\left(1 - V_k^{(X)}\right) - 12.5 V_k^{(X)} \left[V_k - 0.4\right]^+ , \tag{40}$$

where $V_k^{(X)}$ habituates via term $V_k^{(X)} \left[V_k - 0.4\right]^+$ if activity $V_k > 0.4$, but accumulates to a baseline of 1.0 via term $(1\text{-}V_k^{(X)})$ when the thalamic signal V_k is inactive. In vivo, this habituative dynamic may be attributable to short-term depression of excitatory synapses on inhibitory interneurons of the thalamus.

Second messenger traces and working memory equations

Reward signals subserving reinforcement learning arise after an action has been generated, with a delay of hundreds of milliseconds or even seconds. However, movement-related cell discharges shut off rapidly after a movement is initiated (Figures 9C, 9F). Thus, reinforcement learning signals must modify synapses for which the pre- and post-synaptic cells were previously, but are no longer, active. In order for credit or blame to be properly assigned to synapses on non-discharging cells that previously helped activate a movement, a record or trace of recent cell activity persists after spiking ceases (Sutton & Barto, 1981; Klopf, 1982; Grossberg & Schmajuk, 1987; Grossberg & Merrill, 1992; Dominey et al., 1995; Houk et al. 1995; Fiala et al., 1996). Such traces can take the form of intracellular second messengers, which are critical for some aspects of learning in many plastic brain areas (Hemart et al. 1995; Otani et al., 1999; Sung et al. 2001; Vezina & Kim, 1999). Other options, such as working memory representations of previous movements, occur in situations where the cell activation can itself be sustained over the interstimulus interval.

Trace variables that embody these proposed second messenger effects were introduced in the BG as follows. To support reinforcement learning for awhile after direct pathway activity ceases, a trace, or transient record, of recent striatal direct pathway activity was carried by **second messenger activity** $\overline{B}_k^{(SD)}$ (Figure 6b):

$$\frac{d}{dt} \overline{B}_k^{(SD)} = 750\left(1 - \overline{B}_k^{(SD)}\right)\left[B_k^{(SD)} - 0.4\right]^+ - \overline{B}_k^{(SD)} \left(0.75 + 75 \sum\nolimits_{k \neq i} f^{(B)}\left(B_i^{(SD)}\right)\right). \tag{41}$$

The threshold 0.4 ensures that the trace forms only if $B_k^{(SD)}$ is sufficiently large. The trace $\overline{B}_k^{(SD)}$ influences learning of the weights $W_{xyik}^{(PSD)}$ in (33); see (53). The final term in (41) formalizes the assumption that GABA-ergic recurrent collaterals of striatal direct pathway projection neurons suppress second messenger-based records of activity within neighboring striatal projection neurons. This

hypothesis may explain why collaterals of striatal SPNs exist despite their apparent failure to produce potent lateral inhibition (Jaeger et al., 1994). The **inhibitory feedback signal function** $f^{(B)}$ in (41) was defined by:

$$f^{(B)} = \left([x]^+ \right)^2. \tag{42}$$

Learning by the adaptive weights $W_{xyik}^{(PSI)}$ in (34) that impinge on indirect pathway cells suppress a negatively reinforced response. **Second messenger activity** $\overline{B}_k^{(SIL)}$ serves as a trace of thalamic input V_k to striatal indirect channel SPNs, and determines whether the weights $W_{xyik}^{(PSI)}$ from the FEF plan layer to these SPNs are eligible to learn, should negative reinforcement occur; see (52):

$$\frac{d}{dt}\overline{B}_k^{(SIL)} = 750\left(1 - \overline{B}_k^{(SIL)}\right)[V_k - 0.5]^+ - \overline{B}_k^{(SIL)}\left(0.75 + 75\sum\nolimits_{i \neq k} f^{(V)}(V_i) V_i^{(X)}\right). \tag{43}$$

Here V_k is thalamic activity defined by (38), and $V_i^{(X)}$ is transmitter that habituates with continued firing, as defined in (40). The signal function $f^{(V)}$ was defined by

$$f^{(V)} = \left([x]^+ \right)^2. \tag{44}$$

The second term in (43) models the hypothesis that the trace is suppressed in neighboring cells via habituative feedforward inhibition from striatal interneurons (Kawaguchi et al., 1995; Kawaguchi, 1997) that are excited by thalamic signals V_k. Simulations showed that this striatal habituation to V_k could be identical to the thalamic habituation to V_k, which was already modeled in (38) and (40). For convenience, the same variable, $V_i^{(X)}$, was therefore used in both (38) and (43).

A **trace of FEF plan layer activity** $\overline{F}_{xyi}^{(P)}$ (Figure 6a) was specified by:

$$\frac{d}{dt}\overline{F}_{xyi}^{(P)} = 15(1 - \overline{F}_{xyi}^{(P)})[F_{xyi}^{(P)} - \Gamma^{pt}]^+ - 0.75\overline{F}_{xyi}^{(P)}. \tag{45}$$

Equation (45) compactly describes the dynamics of two physically distinct traces of FEF plan cell activity. One of these traces modulates learning in anterior IT projections to the plan layer (see (56)). It is naturally interpreted as a process localized in the ITa-recipient dendrites of FEF cortico-striatal cells. The second trace (whose dynamics are also described by (45)) modulates learning (Berretta et al., 1997) in the plan layer projection to the striatal direct pathway (see (53)). It is naturally interpreted as a process in the axon terminals of projections from FEF plan layer cells to striatal direct pathway SPNs. For Where-Where cells, Γ^{pt} = .4; for What-Where cells, Γ^{pt} = 0.15 to compensate for weaker What-Where plan cell activity by reducing the threshold for trace activation.

A plan layer cell is prevented from learning to activate those striatal indirect-pathway SPNs that can prevent the same plan from being executed. Otherwise, when a dopamine dip occurred, a plan could learn to prevent itself from ever being executed (a kind of learned helplessness). However, plans can block each other's execution via learned FEF-to-indirect pathway links. The model accomplishes these goals using traces within plan layer cells that gate plan-layer to indirect-pathway learning. These traces create eligibility only for *recently active but unexecuted* plans because plan execution generates feedback, via model GABA-ergic FEF postsaccadic cells, that resets activities and traces only within plan and output cells responsible for execution of the current response. This **trace of plan layer activity,** $\overline{F}_{xyi}^{(PA)}$, (Figure 6a) was defined by:

$$\frac{d}{dt}\overline{F}_{xyi}^{(PA)} = 15(1 - \overline{F}_{xyi}^{(PA)})[F_{xyi}^{(P)} - \Gamma^{pt}]^+ - \overline{F}_{xyi}^{(PA)}[0.75 + 75F_{xy}^{(X)}]. \tag{46}$$

Like the trace in (45), this trace is activated only if FEF plan layer activity $F_{xyi}^{(P)}$, which is defined in (14), satisfies $F_{xyi}^{(P)} > \Gamma^{pt}$. However, unlike other trace variables in the model, which decay slowly once their source cell's activity falls below Γ^{pt}, this trace collapses quickly when its source cell is shut off, notably

when an FEF post-saccadic cell generates an inhibitory signal $F_{xy}^{(X)}$, defined in (26). For convenience, the dependence on this inhibitory event is shown directly in the final term of equation (46), where a function that became large when $F_{xyi}^{(P)}$ nears zero would also work. This captures the hypothesis that a small activity in the source cell is necessary to prevent rapid collapse of this type of trace. This trace is interpreted as a process in cortico-striatal axon terminals that abut dendrites of indirect pathway SPNs. Consistent with this proposal, Berretta et al. (1997) showed that applying a GABA agonist in motor cortex prevents learning-related gene expression in projections to the striatal indirect, but not direct, pathways. The model captures this functional difference by introducing the dependence on cortical inhibition in (46) but not in (45).

A **trace of layer VI activity** $\overline{F}_i^{(G)}$ (Figure 6a) was used to support reinforcement learning, after movement completion, of adaptive weights between PFC context representations and FEF zones that can be primed by PFC inputs to layer VI. This trace variable was defined by:

$$\frac{d}{dt}\overline{F}_i^{(G)} = 750(1-\overline{F}_i^{(G)})[F_i^{(G)} - 0.5]^+ - \overline{F}_i^{(G)}(0.75 + 75\sum_{k\neq i} f^{(G)}(F_k^{(G)})). \tag{47}$$

The inhibitory summation term in (47) represents lateral inhibition among layer VI cells. The inhibitory **signal function** $f^{(G)}$ in (47) was defined by

$$f^{(G)} = ([x]^+)^4. \tag{48}$$

Equations (47) and (48) ensure that a synapse between a PFC fiber and a layer VI cell will remain eligible to learn until the trace either passively decays or is actively shut off by competitive activity in a neighboring layer VI cell.

A **trace of ITa activity** $\overline{T}_j$ (Figure 6a) was defined by

$$\frac{d}{dt}\overline{T}_j = 750(1-\overline{T}_j)[T_j - 0.4]^+ - 0.75\overline{T}_j \tag{49}$$

and may be realized by second messenger activity within terminals of anterior IT cell synapses with FEF plan cells. Although the What pathway trace in (49) facilitates *learning*, it does not control *performance*. Working memory areas in the PFC provide a basis for persistent activation of contextual representations that is useful for controlling performance, specifically which premotor zones are set in an active or primed state. As noted in (47), model PFC What representations learn to activate layer VI cells via long-range cortico-cortical projections. **PFC What working memory activities** C_j (Figure 2 and 6a) were defined by:

$$\begin{aligned}\frac{d}{dt}C_j = 30[&(1-C_j)(1.5I^{(M)} + T_j + 4f^{(C)}(C_j)) \\ &-(C_j + 0.3)(1 + 0.35\sum_{k\neq j} f^{(C)}(C_k))]\end{aligned}. \tag{50}$$

Motivational input $I^{(M)}$ is either 0 or 1. Model PFC representations require such an input $I^{(M)}$, assumed to be from limbic areas, in order to become aroused. Then a specific ITa signal T_j can activate a working memory representation as follows. Positive feedback $4f^{(C)}(C_j)$ via the **sigmoidal signal function** $f^{(C)}$,

$$f^{(C)} = \frac{x^8}{x^8 + 0.6^8}, \tag{51}$$

is balanced by recurrent inhibition $0.35\sum_{k\neq j} f^{(C)}(C_k)$ from other cells. By (51), C_j activity must exceed approximately 0.6 for recurrent excitation to engage and maintain C_j in a self-sustaining regime. Input T_j from ITa cannot activate working memory alone, because it cannot drive activity C_j above 0.6. However, when motivational input $I^{(M)}$ is active, the sum of the non-specific $I^{(M)}$ and the specific input T_j can drive one or multiple prefrontal cells C_j above 0.6 and into the self-sustaining regime; cf., Grossberg (1971,

1982b). Once self-sustaining, C_j persists only as long as at least one of $I^{(M)}$ and T_j is active. In a more complete model, sustained activity in PFC might also depend on reciprocal excitation between frontal and parietal cortices (Chafee & Goldman-Rakic, 2000).

Adaptive weight equations

Five similar learning equations describe the functional dependence of adaptive weight changes on the intracellular traces of recent activity defined above. Learning of the **plan-to-indirect pathway weights** $W_{xyik}^{(PSI)}$ (Figure 6b) in (34) was defined by

$$\frac{d}{dt}W_{xyik}^{(PSI)} = \overline{N}\left[500q\left(\overline{B}_k^{(SIL)}, 0.35\right)\left[q\left(\overline{F}_{xyi}^{(PA)}, 0.5\right) - W_{xyik}^{(PSI)}\right]^+ - W_{xyik}^{(PSI)}\right]. \tag{52}$$

A negative reinforcement signal $\overline{N}$, generated by the omission of primary reward at the expected time during training (Brown et al., 1999), allows recently active *but unexecuted* plans, which are marked by plan layer traces $\overline{F}_{xyi}^{(PA)}$ of (46), to learn to suppress the previously selected zone with synaptic efficacy $W_{xyik}^{(PSI)}$. The zone is suppressed via activity in striatal indirect pathway SPNs, whose signals $\overline{B}_k^{(SIL)}$, defined in (43), are still on when signal $\overline{N}$ arrives. The signal function *q* of equation (16) in learning rules mimics the voltage-dependent effect of NMDA channel blocking with magnesium (Mayer et al., 1984). Noise below the threshold is filtered out, while even a small activity above the threshold causes a robust learning response.

Learning of the **plan-to-direct pathway weights** $W_{xyik}^{(PSD)}$ (Figure 6b) in (33) was defined by:

$$\frac{d}{dt}W_{xyik}^{(PSD)} = \left(N\left[\overline{F}_{xyi}^{(P)} - W_{xyik}^{(PSD)}\right]^+ - 0.1\left(N + \overline{N}\right)W_{xyik}^{(PSD)}\right)q\left(\overline{B}_k^{(SD)}, 0.5\right). \tag{53}$$

Expansion yields two products on the right hand side. The first product specifies a process of LTP: weights increase toward $\overline{F}^{(P)}$ when a dopamine burst *N* coincides with recent presynaptic activity $\overline{F}^{(P)}$ from the plan layer and recent postsynaptic activity $\overline{B}_k^{(SD)}$. The second product specifies a process of LTD: weights decrease slowly when a dopamine burst or dip (*N* or $\overline{N}$, respectively) coincides with recent postsynaptic activity $\overline{B}_k^{(SD)}$ that occurs in the absence of recent presynaptic activity. Thus localized FEF planning activities become potent exciters of the striatal direct pathway if they predict striatal activations leading to forthcoming rewards, but they can lose this potency if they predict striatal activations leading to punishment, or if reward is forthcoming in their absence.

The **anterior IT-to-striatal direct pathway weights** $W_{jk}^{(TSD)}$ (Figure 6b) in (33) were defined by:

$$\frac{d}{dt}W_{jk}^{(TSD)} = \left(N\left[\overline{T}_j - W_{jk}^{(TSD)}\right]^+ - 0.1\left(N + \overline{N}\right)W_{jk}^{(TSD)}\right)q\left(\overline{B}_k^{(SD)}, 0.5\right). \tag{54}$$

Here positive reinforcement *N* allows the traces $\overline{T}_j$ of ITa representations in (49), in conjunction with striatal direct pathway SPN trace activity $\overline{B}_k^{(SD)}$, to drive learning in the adaptive weights $W_{jk}^{(TSD)}$. Both positive *(N*) and negative ($\overline{N}$) reinforcement allow weight decay in response to irrelevant stimuli, whose ITa representations are inactive when the direct pathway and reinforcement are active. By selectively augmenting only recently active and positively reinforced inputs, the learning rules in equations (53) and (54) prevent irrelevant stimuli and plans from learning to open the basal ganglia gate.

The **PFC-to-FEF layer VI weights** $W_{ki}^{(CG)}$ (Figure 6a) in (13) were governed by

$$\frac{d}{dt}W_{ji}^{(CG)} = (500N[q(C_j, 0.5) - W_{ji}^{(CG)}]^+ - 0.1(N + \overline{N})W_{ji}^{(CG)})q(\overline{F}_i^{(G)}, 0.5). \tag{55}$$

By (13), this weight can enable the PFC working memory to learn to activate the appropriate zone in layer VI, and by (55) the weight grows when the working memory activity C_j and layer VI trace $\overline{F}_i^{(G)}$ are both active while a reinforcement learning signal N is active. The weight declines when $\overline{F}_i^{(G)}$ is active without C_j, or if C_j predicts punishment.

The **anterior IT-to-FEF plan layer (What-Where) weights** $W_{jxyi}^{(TP)}$ (Figure 6a) in (15) were defined by:

$$\frac{d}{dt}W_{jxyi}^{(TP)} = (500N[\overline{F}_{xyi}^{(P)} - W_{jxyi}^{(TP)}]^+ - 0.1(N + \overline{N})W_{jxyi}^{(TP)})q(\overline{T}_j, 0.5). \quad (56)$$

Here active ITa traces $\overline{T}_j$, and active plan layer traces $\overline{F}_{xyi}^{(P)}$ together drive learning of adaptive weights $W_{jxyi}^{(TP)}$ when reinforcement N occurs. The ITa projection reaches only What-to-Where zone cells in the FEF plan layer, in keeping with the topographical distribution of ventral and dorsal stream afferents to FEF (Schall et al., 1995a). In other words, $W_{jxyi}^{(TP)} = 0$ if i corresponds to a Where-to-Where plan layer cell. Equations (55) and (56) explicate hypothesis 12, that DA-ergic signals influence cortical reinforcement learning and plasticity in a manner similar to the way they influence reinforcement learning in the BG.

Simulations. Details regarding simulated inputs, of visual stimuli and reward signals, are provided in the Results section. The simulations were implemented with a C++ program that used the fourth order Runge-Kutta method for integrating the system of differential equations.

Parameters. In many cases, parameters were found for a given equation by specifying several equilibrium values of the governed variable and specific corresponding inputs to the governing equation. For example, the GPi is required to have low activity (0.2) when the striatal direct pathway afferents are active and the GPe is tonically active. This provides one constraint. Second, it is required to have higher activity (0.5) when the striatal direct pathway projection is inactive and the GPe is tonically active. This provides a second constraint. Finally it must have high activity (0.8) when the striatal direct pathway is inactive and the indirect pathway is active, resulting in a loss of GPe-GPi inhibition. This provides a third constraint. Together, these three constraints can be used to simultaneously fit as many parameters. The constrained inputs here refer to all variables that are not parameters, such as afferent signals from other parts of the model. For a given governing equation, each desired equilibrium value and input condition pair constitute a constraint on the parameters. This equilibrium-fitting approach required much less computational power than fitting spike histograms to the model output curves. The governing differential equation can be set to zero (equilibrium), and each constraint then yields an algebraic equation in the unknown parameters. In principle, if the number of constraints equals the number of unknown parameters in a given equation, the resulting system of equations can be solved exactly.

In practice, two gradient descent methods were used to solve the equations. In the first method, the objective function is the sum of the squared time derivatives (which we refer to as STID) of the governing equation for each constraint. The objective function is minimized if the time derivatives are zero, indicating that equilibrium is achieved for all constraints. In the second method, the objective function is the sum of the squared equilibrium errors (which we refer to as SEE) between the desired equilibrium value and the actual equilibrium value for the constraint, given the parameter choice. The two methods are not equivalent, because the time derivative and equilibrium error are not linearly related, due to the nonlinearity of the equations themselves. For example, doubling the equilibrium error does not necessarily double the time derivative. Although the SEE method was more accurate in some cases, it was the slower of the two because it required solving each constraint for its equilibrium value at each iteration, given the parameters. The STID method simply calculated the time derivative directly from the governing equation. For this reason, STID was run to get an initial parameter estimate, and then SEE was used to refine the estimate. In cases where the constraints were not especially complex, parameters were adjusted manually. The equilibrium-fitting technique could not specify the overall time constant for a given governing equation; these were also adjusted manually. In cases where each term in the governing

equation contained a parameter to be fitted, the solver tended to find the trivial solution, corresponding to a zero constant multiplier for each term in the equation. This was prevented by constraining the sum of parameters to be normalized to a constant value *n* equal to the number of parameters to be fit. For all model variables, the parameters found were not particularly sensitive, and they could be rounded up to only a few significant digits. For example, the plan-to-output layer weight scale factor in equation (22) was rounded from 0.377 to 0.4, and the anterior IT to striatal scale factor in equation (33) was rounded from 7.858 to 8. Even when all of the model parameters were rounded to one or two significant digits *simultaneously,* there was no significant difference in model learning or performance after vs. before parameter rounding, indicating a relative insensitivity to parameter choice.

Figure 7 about here

Results

Model simulations of oculomotor tasks. Learning and performance of seven oculomotor tasks were simulated: the five tasks shown in Figure 1, and two additional ones described below. With the exception of the fixation task, all the tasks required generation of a saccade, and Figure 7 summarizes the activation dynamics implied by hypotheses 1-14 (and the system of equations) for a typical plan-execute episode. However, the cortical paths via which the BG gate was opened, the need to use the indirect BG pathway to STOP unrewarding gate opening, and the time required to open the BG gate following fixation point offset, varied across tasks.

The TELOS model was trained on the five tasks that required learning in a single order: saccade, fixation, overlap, gap, and delay. (The tasks could be learned in other orders, but no others were simulated.) The model was required to correctly perform one task trial before proceeding to learn a subsequent task. Trials were given at five second intervals, which provided sufficient time for the model activity to subside and equilibrate between trials. Time *t* was reinitialized to be zero at the beginning of each trial. At time $t = 0$, a motivational signal, $I^{(M)}$ was always set to 1.0 and input to the model dorsolateral PFC (the "What" working memory activity C_j in Figure 2; also see Figure 6a), which in turn excited model FEF layer VI cells. These cells excited overlying model FEF plan cells (layers II/III/Va), thereby enabling subsequent inputs from IT and PPC to induce reverberating activations in these plan cells. Input $I^{(M)}$ remained on until reward or punishment signals (N or $\overline{N}$, respectively) terminated at the end of the trial. Input to the model of a visible external stimulus, I^{*}_{xyj}, always set to 1.0 the internal input, $I^{(IT)}_{j}$, which excited the ITa (TE) stage activity T_j, shown on the upper left of Figure 2. (The superscript asterisk marks the associated variable as external to the brain.) Subscript (x,y) indexes the input's visual field (grid) location, $j=1$ or 2 indexes its distinctive feature value (to distinguish Fixation points from other, Target, inputs), and its ITa-coded (feature-based and position independent) classification. When a saccade was performed, visual inputs shifted position 30 ms after saccade initiation to bring the saccade's goal into the grid's "fovea" at locus $(x,y) = (1,1)$. Featural information from the shifted scene began updating the FEF representations after a 50 ms., consistent with the empirical delay (see Figure 9).

The model output was determined by the state of the superior colliculus (SC), which was modeled (Figure 5) as a map of "motor errors" (Grossberg & Kuperstein, 1986; Lee, Rohrer & Sparks, 1988), i.e., of eye movement vectors which, if performed, would zero the difference, or error between current and desired eye position (x,y). The SC map was excited by the model's PPC stage, FEF output layer, or both (Figures 2 and 6b). Whenever an SC cell's activity rose above 0.25, it began to excite FEF plan cells tuned to the same direction. If the SC cell's activity reached a threshold of 0.60, it was deemed to have initiated a saccade (Hanes & Schall, 1996) corresponding to the cell's motor error vector representation. Such initiation resulted in excitation of FEF inhibitory interneurons capable of suppressing FEF plan cell firing (Burman & Bruce, 1997). After a 100 ms delay following saccade initiation, a reward signal (N =1.0) was given if the saccade was correct, and a punishment signal ($\overline{N}$ = 1.0) was given if the response was incorrect. The reinforcement learning signals N and $\overline{N}$ could not be simultaneously active. They

correspond to dopamine bursts and dips, respectively, and they lasted 100 ms (Ljungberg et al., 1992; Brown et al., 1999).

Application of the model to the **saccade task** (Figure 1) is summarized by the canonical plan-execute sequence of Figure 7, in which there is no STOP signal generation in the indirect pathway. At time $t = 0$, the fixation light was presented in the fovea: I^*_{xyj} was set to 1.0 for $(x,y,j) = (1,1,1)$; i.e., location (1,1) where $j = 1$ indicates that the input possessed the distinctive feature of a Fixation point. The input $I^{(IT)}_j$ to ITa was set to 1.0 for $j = 1$, to activate a spatially-invariant, feature-based representation of the fixation light. At $t = 200$ ms, the fixation light shut off, and the target I^*_{xyj} appeared to the right, at $(x,y) = (2,1)$, with $j = 2$ to signify that the input possessed the distinctive feature of a Target. This target input activates ITp and then the corresponding target feature GCZ in FEF. Via the Target cortical zone GCZt, the model initiated a saccade at $t = 279$ ms, so the reaction time (RT) between fixation light offset and saccade onset was just 79 ms (Figure 9). At $t = 309$ ms, which is 30 ms after saccade onset, the target moved to the fovea as a result of the saccade, meaning that I^*_{xyj} shifted from $(x,y) = (2,1)$ to $(x,y) = (1,1)$, where $j = 2$. At $t = 379$ ms, which was 100 ms after saccade initiation, reward was given by setting N to 1.0 for 100 ms. At $t = 479$ ms, the trial ended and all inputs were shut off, including $I^{(M)}$, I^*_{xyj}, $I^{(IT)}_j$, and N. Thus, on the first trial, the GCZt mediated correct performance of the saccade task, which involves visually-guided saccades with no STOP requirements. In addition, SC activation provided a teaching signal that caused like-tuned planning cells in the object cortical zone GCZo to be briefly excited. Because of the predictive relationship between fixation light onset, plan cell excitation in the GCZo, and generation of a positive reinforcement signal 100 ms after performance of a rightward saccade, an ITa-FEF link began to be learned between fixation light identity and the plan for a rightward saccade in the What-Where module – even though that module had not generated the reinforced saccade. (This link would have enabled anticipatory excitation of an FEF plan for a rightward saccade in the saccade task if training of the saccade task had continued; see below).

The **fixation** task (Figure 1) was presented next. At $t = 0$, the fixation light appeared in the fovea. It activated the link learned (as a consequence of the last rewarded trial in the saccade task) from the ITa representation of the fixation light to GCZo plan cell for a rightward saccade. The GCZo then generated an anticipatory saccade, even before the target light could excite a saccade through GCZt. This erroneous response led to a punishment signal, $\overline{N}$, which triggered a weight increment on the pathway from the FEF fixation plan cell to the BG indirect pathway associated with GCZo; see Figure 2. The punishment signal also caused a decrement in the ITa to FEF link that had caused the anticipatory saccade. Consequently, on the next trial, the anticipatory activation of the GCZo plan cell by fixation light onset was no longer able to open the BG gate. At $t = 200$ ms, the distracting target appeared to the right at $(x,y) = (2,1)$ while the fixation light remained visible. Distracter onset excited the rightward saccade plan cell in GCZt, which was able to open its BG gate. The model thus erroneously initiated a saccade to the distracter target, at 361 ms, which led to activation of the punishment signal. This caused a large increment in the weight on the link from the FEF fixation plan cell to the BG indirect pathway associated with the GCZt. On the next trial, neither GCZt nor GCZo were able to open their BG gates in response to the fixation light. Consequently, the model was able to avoid looking at the distracter, and to maintain fixation, on this trial. The model was rewarded beginning at $t = 500$ ms. Because the fixation light was still on and activating the learned pathway to GCZo, this reward further strengthened the link (from .3 to .9) between the fixation stimulus representation in ITa and the rightward saccade plan in GCZo. However, the rightward saccade plan is not executed while the fixation cue is present, because the fixation plan has also learned to activate the indirect pathway, which STOPs saccades driven by GCZo as long as the fixation cue is present.

The **overlap** task (Figure 1) was presented next and the model performed correctly on the first trial. It did not saccade immediately upon target onset, because the model had previously learned to withhold a planned saccade despite distracters while the fixation light remained on. It did saccade at fixation light

offset because then the fixation plan vanished as a source of a STOP signal. The fixation light appeared in the fovea at $t = 0$. At $t = 200$ ms, the target appeared to the right at $(x,y) = (2,1)$. Fixation light offset at $t = 500$ ms removed the source of excitation of the indirect pathway, and thereby released, at $t = 559$ ms, a correct saccade to the target. Because of the weights acquired during the two prior tasks, both the GCZt and GCZo helped generate this saccade. Both weights were helpful because the response required in the overlap task was the same as that required in both prior tasks. Following the correct saccade, a reward was given, but only modest further change occurred in model adaptive weights.

The **gap** task (Figure 1) was presented with a 500 ms delay between fixation light offset and target onset. At fixation light offset, an anticipatory saccade was performed correctly on the first trial. This was because the fixation light feature activated a saccade plan of the appropriate direction, mediated by the ITa-FEF pathway, which had been learned in the saccade task and not unlearned in the intervening tasks. Indeed, it had been strengthened in the fixation task. The anticipatory saccade was generated only once the fixation light shut off, because then the fixation light was no longer able to drive the indirect pathway to suppress the anticipatory saccade. The fixation light appeared in the fovea at $t = 0$ and shut off at $t = 200$ ms. A saccade to the anticipated target location at $(x,y) = (2,1)$ was generated via GCZo at $t = 340$ ms. Reward was given and the trial ended prior to $t = 700$ ms (at which point the target would have appeared had the anticipatory saccade not been generated). Had the anticipatory saccade not occurred, the appearance of the target would have driven a visually-guided saccade to foveate it. This version of the gap task differs from that often used, e.g. in studies of express saccades (Fischer & Weber, 1993). In that version, reward is withheld if the saccade is anticipatory. Although this is intended to force the animal to wait until the target stimulus appears, animals and humans nevertheless generate *some* anticipatory saccades, and our simulations indicate that the model is also capable of learning to generate anticipatory saccades.

The **delay** (or memory) task (Figure 1) was next presented. The fixation light was visible in the fovea from $t = 0$ until $t = 800$ ms. The target appeared in the upper right at $(x,y) = (2,2)$ and was visible from $t = 200$ until $t = 500$ ms. When the fixation light shut off, two saccade plans had formed in the plan layer: one was maintained by recurrent excitation in GCZt to represent the remembered target location; the other, in GCZo, represented the fixation light activated, ITa-FEF mediated, anticipated location of the target that had been used in prior tasks. At $t = 987$ ms, an "anticipatory" saccade to the previously rewarded locus was erroneously initiated by GCZo, and punishment was given. This caused a large weight increment in the STOP pathway between the GCZt plan cell and the indirect pathway controlling GCZo. On the next trial, this new link stopped the previously learned tendency to initiate an anticipatory saccade via GCZo, and thus a saccade was correctly initiated after the delay by GCZt. The model's saccade to the remembered target location at $t = 969$ ms was rewarded. The brief 300 ms delay between target offset and fixation light offset was chosen for convenience, and could have been much longer for a wide set of parameters. Because the model is noiseless, there is no limit on how long it can maintain a plan cell activation representing the target locus, provided that recurrent excitation is strong enough and that no other salient visual inputs are presented during the memory interval.

Since the model had now learned to perform each of the tasks correctly, the training ended, and the next trials marked a final testing phase of the simulation. The state of the simulation was saved at the beginning of the next trial and served as the initial condition for testing each of the tasks. The tasks were presented as during training and were all performed correctly. Reaction times (measured from fixation light offset to saccade onset) from this final test are listed in Table 3. They are similar to those measured on the first correct trial during initial training of each task.

Subsequent to training, a **visual discrimination** task was performed to assess choice between simultaneously presented peripheral stimuli, one possessing the fixation light feature, and one the target light feature. The usual fixation light was first presented in the fovea at $t = 0$. At $t = 200$ ms, a stimulus that also possessed the fixation light feature appeared in the upper left at $(x,y) = (0,2)$, and a stimulus possessing the target feature simultaneously appeared in the upper right at $(x,y) = (2,2)$. GCZf activity quickly began to reflect both the foveal and the peripheral fixation feature input. Competition between these two GCZf activities resolved in favor of the peripheral activity. Since GCZf received a permissive

signal from the PNR-THAL, at t = 402 ms, with the foveal fixation light still on, the model initiated a saccade to the upper left; i.e., to the peripheral stimulus that possessed the fixation light feature. This response was "correct" given past training, because the model had never been punished for saccading to such a stimulus, but had been punished for saccading to stimuli possessing the target feature whenever the fixation light remained on. At t = 432 ms, the stimulus at the upper left moved to the fovea, and all other stimuli were extinguished. The reaction time appears under "choice" in Table 3.

Also, subsequent to training, the model was tested on a **countermanding** saccade task (Hanes et al., 1998; Logan & Cowan, 1984). This was essentially a saccade task, except that on a fraction of trials, the fixation light reappeared after a brief time off. The reappearance constituted an imperative STOP signal. It instructed the system to cancel the planned saccade and instead maintain fixation. Provided that the STOP signal was not presented too late, the model was able to cancel the saccade by using a fixation light activated STOP signal mediated by the BG indirect pathway. The last two tests illustrate that the model can perform some tasks on which it was not trained.

Adaptive weights were adjusted as described above, in accord with learning equations detailed in the *Mathematical Model* section. An algorithm (see *Mathematical Model*) had previously adjusted other model parameters to minimize the difference between model cell dynamics and the observed cell dynamics of a large number of electrophysiological cell types identified in published experimental studies of the modeled areas. Table 4 lists electrophysiological reports that were used to guide parameter adjustment. Activation traces from many of these experimental reports are reprinted below (in Figures 9, 10 and 11) alongside simulated activation traces of corresponding model cells. Clearly, the model learned faster than real monkeys. This was largely due to simulation parameters, in particular, a lack of any uncontrolled distracting stimuli, no noise, unflagging motivational input signals, maximal between-task compatibility, and a conveniently high learning (weight adjustment) rate. Less favorable parameters would amplify the number of trials to criterion.

Tables 3 and 4 about here
Figure 8 about here

Illustration of model cell dynamics in one task. Panels A-U of Figure 8 depict the dynamics of 22 model cells during the overlap task; see Figure 1. Panel A shows activations of two model FEF input-layer cells whose dynamics differ because only one cell's receptive field is such that it (dotted line) receives both an early input based on the target's retinotopic locus and a delayed input, from ITp, based on a conjunction of the target's position *and* feature. The other cell (solid line) shares the initial input but lacks the second because it is tuned to a different position-feature conjunction in ITp. All other panels show only one cell. Panels M and N respectively show a winning and a losing FEF plan-layer cell. The Figure 8 caption gives the number of the equation (see *Mathematical Model*) that mediated each dynamic.

Reinforcement learning of plan activations. The trial-by-trial progress of successful learning and performance of the task series was described above. The dotted lines in Figure 8L-N depict the second messenger traces ($\overline{F}$) induced by recent plan cell activations. These intracellular trace variables allowed the model to bridge the time delays between plan cell offset and the later arrival at planning cells of signals indicating rewarding or non-rewarding response outcomes. Consequently, reinforcement learning in model cortico-cortical synapses was able to bring plan cell activation under control of inputs to FEF. The simulations exemplify computational hypothesis 12, that reinforcement learning establishes stimulus control over plans, not responses, even though plan cell activation is suppressed by feedback inhibition from post-saccadic cells well before reward or non-reward signals have been generated. More generally, the model illustrates how learning and performance processes evolve in parallel and in real-time, with no need for "off-line" learning.

Comparisons of model with real cell dynamics. Figures 9-11 show side-by-side comparisons of 17 model cell activations with neurophysiological data (citations in Table 4). These comparisons illustrate the ability of the model to match data across the range of tasks simulated. In particular, Figure 9A data

and simulation are from the delay task, 9B from the discrimination task, and 9C-9G from the overlap task. Figure 10 data and simulation are from the delay task, and Figure 11 from the overlap task.

Figures 9 about here

Figure 9 shows plots of model cell behavior alongside reprinted plots of electrophysiological data for various real FEF cells with distinctive types of task-related dynamics. Figure 9A shows FEF *visual cells* (Schall et al., 1995a). These cells fire weakly at 50 ms after stimulus onset (time t=0) in the receptive field. If the stimulus is a preferred feature for the cell, a second burst occurs at 100 ms due to input from ITp. In the model (see Figures 2 and 6a), these are FEF input layer cells ($F_{xyi}^{(I)}$ in equation (12)). Figure 9B shows traces from two FEF *discriminating visuomovement* cells (Schall & Bichot, 1998). Such cells initially respond to either a preferred or non-preferred stimulus, but begin to discriminate with a bifurcation around 100-120 ms after stimulus onset. In the model, these are plan layer cells ($F_{xyi}^{(P)}$ in equation (14)), and their bifurcation is due to both recurrent, competitive dynamics and the selectiveness of their inputs (shown in Figure 9A). Either factor may explain the the slightly faster decline of actvity in the "losing" model cell than in the corresponding real cell. Figure 9C exemplifies *transient sensory-movement cells* (Schall, 1991), which fire both in response to the stimulus and around the time of the saccade. In the model, these are plan layer cells ($F_{xyi}^{(P)}$, equation (14)) that lose the competition for sustained activity, due to recurrent inhibition in (18). A corollary discharge from the SC (term S_{xy} in (15)) drives the burst just before movement onset. That the 9C real cell has some sustained activity whereas the 9C model cell has none is not significant because both data and model indicate a continuum from none to the robust sustained activity shown in 9F.

Figure 9D shows *presaccadic cells* (Schall, 1991), which peak at the time of saccade onset, when activity is sufficient to initiate a saccade but inhibition from postsaccadic cells ($F_{xy}^{(X)}$, equation (26)) has not yet taken effect. In the model, these are layer Vb output cells ($F_{xyi}^{(O)}$, equation (21)) that mediate execution of the saccade. Some movement-related layer Vb cells that projected to SC also showed visual rather than movement activity when the stimulus in the receptive field was not to be foveated, and others showed weak but sustained, working memory-like activity. These were epiphenomenal in the model and emerged due to the complex constraints on parameters governing movement gating in layer V. However, these unexpected findings agree with and functionally interpret otherwise puzzling observations of non-motor responses in SC-projecting cells in layer V of FEF (Sommer & Wurtz, 2000). Figure 9E shows *postsaccadic cells* (Schall, 1991), which begin firing at the point of saccade initiation. In the model, these cells ($F_{xy}^{(X)}$, equation (26)), which are driven by a corollary discharge of movement initiation from SC burst cells, serve to shut off the successfully executed saccadic plan. Figure 9F shows *sustained sensory-movement cells* (Hanes et al., 1998), which are active from stimulus onset until just after saccade initiation. These contrast with preparatory set or fixation cells, which cease activity before, rather than after, saccade initiation. In the model, the sustained sensory-movement cells (equation (14)) exist in the plan layer (II/III/Va) and represent planned but not yet executed saccades. Their sustained activity is initiated by afferents from the input layer ($F^{(I)}$ in (12)), maintained by recurrent self-excitation, and shut off by inhibition from postsaccadic cells ($F^{(X)}$ in (26)). Figure 9G shows FEF *preparatory set cells* (Schall et al., 1995b). The vertical line on the right denotes saccade onset. Set cells remain active during fixation, and shut off prior to saccade initiation. In the model FEF, such cells exist in both the plan ($F_{xyi}^{(P)}$, equation (14)) and the output layers ($F_{xyi}^{(O)}$, equation (21)) to maintain fixation. They are driven by foveal activity and are shut off by inhibition from saccade-related output cells $F_{xyi}^{(O)}$, subject to parameter k^{fop} in (18) and the last term in (25), when saccade initiation is imminent.

Figure 10 about here

Figure 10 shows neurophysiological data collected from BG and PNR-THAL cell types (see Figure 2) and the dynamics of corresponding simulated cells. Figure 10A (left side) shows data from GPe and GPi from the reaching study of Turner & Anderson (1997). GPe cells ($B_k^{(GPe)}$, equation (36)) increase their firing rate prior to movement onset, whereas GPi cells ($B_k^{(GPi)}$, equation (35)) show a pause prior to movement onset. Similar pausing data have been reported by Hikosaka & Wurtz (1983) for SNr in a saccade task, as shown in Figure 11. In the simulation (Figure 10A, right), the GPi pause is due to increased inhibition from both the GPe ($B_k^{(GPe)}$, equation (36)) and the striatum ($B_k^{(SD)}$, equation (33)), and the pause disinhibits the PNR-THAL, thereby allowing the movement to be executed. STN activity ($B^{(STN)}$, equation (37)) that begins at movement initiation transiently increases both the GPi and GPe activities. Figure 10B shows PNR-THAL cells (Schlag-Rey & Schlag, 1984; equation (38)) that show a transient burst just prior to movement initiation. In the model, this reflects excitation from FEF layer VI ($F_i^{(G)}$) and transient disinhibition (gating) in the GPi-thalamic projection. Figure 10C shows STN cells (Wichmann et al., 1994) that exhibit a transient increase in activity immediately following movement onset. In the model, this reflects a transient corollary discharge from FEF output layer cells ($F_{xyi}^{(O)}$, equation (21)) to the STN ($B^{(STN)}$, equation (37)).

Figure 11 about here

Figure 11 shows the dynamics of PPC, SC, and SC-related BG cells. Figure 11A shows an SNr cell pausing prior to saccade initiation. In the simulation ($G_{xy}^{(SNr)}$, equation (32)), the similar pause is caused by inhibitory action of the model direct path from the striatum ($G_{xy}^{(SD)}$, equation (27)). Indeed, the mirror image of the SNr off-response, also shown in Figure 8F, can be seen in the striatal on-response shown in Figure 8E, consistent with data reviewed in Hikosaka & Wurtz (1989). Figure 11B shows SC burst cell activity (Munoz & Wurtz, 1995) during the overlap task. In the simulation (S_{xy}, equation (11)), the excitatory inputs that energize the burst come from both PPC cells (P_{xy}) and FEF output cells ($F_{xyi}^{(O)}$). Although the former excite the SC throughout the overlap interval, the SC shows a burst response only after the removal of inhibition from the model SNr ($G_{xy}^{(SNr)}$). Figure 11C shows PPC activity (Kalaska & Crammond, 1995) during a GO-NOGO task on a GO trial similar to an overlap task trial. The real and simulated PPC activities show sustained activity during the delay interval followed by a pre-movement burst response. However, note that the model lacks the tonic baseline activity seen in the real cell. The model (P_{xy}, equation (6)) attributes the sustained delay-interval activity to inputs from visual cortex ($I_{xy}^{(P)}$) and the FEF planning layer III/Va ($F_{xyi}^{(P)}$), and the burst response to input from the FEF output layer Vb ($F_{xyi}^{(O)}$). Figure 11D shows fixation-related activity in the SC (Munoz & Wurtz, 1993). Such SC fixation cells pause briefly during a saccade. In the simulation (S_{xy}, equation (11)), the pause results from both the collapse of excitatory input from FEF fixation-related output cells ($F_{11i}^{(O)}$) and the onset of inhibition from the fixation-related component of the SNr ($G_{11}^{(SNr)}$).

Discussion

General issues. The theory developed in this paper proposes how the basal ganglia interact with laminar circuits in the frontal cortex and SC to help satisfy the staging requirements of conditional voluntary behavior. Fourteen functional hypotheses were elaborated to clarify the roles played by components of the

known circuitry treated by the theory. The mathematical model based on this theory is able to account for a wide range of anatomical, neurophysiological, and psychophysical data about planned and reactive saccadic eye movements. During performance, the model regenerated seventeen distinct types of activation dynamics exhibited by electrophysiologically-recorded cell types, while also predicting the behavior of several additional cell types. By virtue of learning guided by reinforcement signals, and selective cue sensitivities of premotor mapping zones, the model system was able to learn five, and to perform seven, oculomotor tasks, without forgetting previously learned tasks, and with a single set of parameters. As such, the TELOS model goes some distance toward explaining both procedural learning of arbitrary condition-action rules (Wise and Murray, 2000) and the ability to switch at will among the large number of rules that may eventually be learned and simultaneously preserved in memory.

Comparison with other models. The model introduces new concepts while also incorporating and extending concepts from previous models. The concept of *zones* consisting of cortex and basal ganglia channels has been discussed previously (Houk & Wise, 1995; Beiser & Houk, 1998; Redgrave et al., 1999) in terms of cortico-basal ganglia modules. Consistent with data on distinct sensitivities of frontal premotor areas (review in Passingham, 1993), we have extended the module concept to denote groups of cells organized into gatable cortical zones (GCZs) that each mediate a distinctive sensorimotor strategy or mapping. The resultant GCZ concept shares features with the "mixture of experts" model (Jacobs et al., 1991), which has been discussed with references to basal ganglia function (Graybiel et al., 1994; Graybiel, 1998). However, whereas previously the striatum has been suggested as the location of the "experts" (Graybiel, 1998), in the present model of primate action control, the "experts" are cortical, indeed frontal, and the basal ganglia function as a GCZ selector.

Basal ganglia control of cortico-thalamo-cortical projections. Previous models have assumed reciprocal excitation between the cortex and thalamus (Houk & Wise, 1995; Arbib & Dominey, 1995; Beiser & Houk, 1998; Taylor & Taylor, 2000; Frank et al., 2001), which was proposed as a basis for sustained, working memory-like activity enabled by basal ganglia disinhibition of the thalamus. The working memory in turn biases, rather than determines, movement selection (Houk & Wise, 1995). Studies of the laminar anatomy of frontal cortex show thalamocortical projections terminating on cells in layers III and V, but not layer VI (Iriki et al., 1991; Zin-Ka-Ieu et al., 1998). Since layer VI is the main source of corticothalamic projections, its apparent omission as a recipient of thalamocortical afferents challenges the cortico-thalamo-cortical loop theory of working memory storage. A reciprocal thalamocortical excitation remains possible if layer III cells excite layer VI, or if thalamocortical fibers terminate on dendrites of layer VI neurons that extend into overlying laminae, but the known thalamic excitation of layer V will cause outputs that would – on the loop theory – make it impossible for a single cortical area to function both to reverberate a plan during a delay interval and then to also execute that plan at the end of the delay. In our theory, both functions are realized by a single cortical area. Given the anatomical constraints and the ease with which basic working memory functionality can be achieved by local circuits, or even by intracellular mechanisms, our theory treats plan maintenance during delays as a local circuit property and treats BG-mediated disinhibition of thalamus as a mechanism for gating excitation of layer V and, thereby, execution of action plans. Finally, it is worth noting that nothing in our interpretation precludes a role for the basal ganglia in selective activation of prefrontal areas supporting working memory.

Lateral vs. feedforward inhibition within the striatum. Recurrent competition between striatal SPNs (spiny projection neurons), mediated by potent lateral inhibition among SPNs, has been assumed by previous models (Arbib & Dominey, 1995; Beiser & Houk, 1998; Contreras-Vidal & Schultz, 1999). However, other data (Jaeger et al., 1994) challenge the potency assumption. Also, it is difficult to reconcile the idea of many actively competing SPNs with observations of a relatively silent striatum. The present model resolves the dilemma by emphasizing the competitive role of the GABA-SIs (GABA-ergic striatal interneurons), which, though outnumbered by SPNs 20 to 1, mediate potent feedforward inhibition (Koos & Tepper, 1999; Wilson et al., 1989). In our model, such cells prevent disparate plans from gaining simultaneous control of the same executive degrees of freedom. Although the model GABA-SIs mediate striatum-level competition between vying plans, choice-making cannot be wholly localized to the

striatum. The present model broadly distributes plan-selective dynamics across competitive inhibitory mechanisms in the thalamus, SC, and both supragranular and infragranular cortical layers. Finally, the existence of striatal recurrent inhibition is compatible with the present model. Although not needed to make the selection, recurrent inhibition would be useful in vivo to help *sustain* the striatal choice in the face of noise and modest input fluctuations (which were not present in our deterministic simulations).

Basal ganglia direct and indirect pathways. The few BG computational models that treat the indirect pathway have ascribed to it roles other than a STOP function. In some models, the indirect pathway generally opposes the direct pathway effect, without explicit justification for why this is needed (Contreras-Vidal & Stelmach, 1995; Suri et al., 1997; Suri et al., 2001). Gurney et al. (2001a, 2001b) suggested that the components of the indirect pathway may be thought of as forming a "control" pathway, which modulates the tonic arousal of the GPi in proportion to the overall level of dopamine and excitation of the striatum. Berns & Sejnowski (1998) assumed that reciprocal activity between the STN and GPe mediated a kind of working memory which subserved sequence production. Contreras-Vidal & Stelmach (1995) modeled the GPe's possible role in enhancing the effects of dopamine loss in Parkinson's disease. Our model reconceptualizes the indirect pathway and suggests a specific rationale for why it is needed in addition to the direct pathway, namely to actively STOP inappropriate action plans from execution until such time as they become appropriate.

Dominey and Arbib model. Dominey et al. (1995) and Arbib and Dominey (1995) reported a model of the FEF, BG, and related oculomotor areas, with which our model shares several features. Their model also used retinotopic and motor error map representations throughout. Their FEF model contained visual, memory, fixation, and saccade "layers", which although not identified with cortical laminae, resemble the cortical layers of the present model. Their visual layer was similar to our visual or input layer, except that our visual cells do not drive FEF output (output) cells directly. Their FEF memory layer corresponds to saccade-related cells in our plan layer, and their "fixation ON" layer corresponds to fixation-related cells in our plan layer (both here predicted to reside in cortical layers II/III/Va). Their FEF output layer corresponds to our output layer (here predicted to reside in layer Vb), in that both drive the SC, although their output layer does not receive corticothalamic projections, which enable gating of movement execution in our model. Their model also had distinct FEF- and SC-controlling BG channels and assumed a motor error map representation in nigro-SC projections, as does ours. The two models address a large and overlapping body of data.

Additional important features distinguish the two models. Our explicit treatment of the laminar anatomy of frontal cortex led us to model the basal ganglia as a system for gating plan execution rather than for reverberation of working memories. Our model relies on neither striatal lateral inhibition nor reciprocal thalamocortical excitation. Whereas the Dominey et al. (1995) model simulates sequence learning, our model simulates multiple task learning and, during performance of the multiple tasks, simulates the dynamics of seventeen electrophysiologically-identified cell types spread across all the brain regions treated. Their model predicts that cortico*striatal* projections mediate conditional motor learning, whereas our model predicts that cortico*cortical* projections from anterior or posterior IT to the FEF plan layers (II/III/Va) mediate conditional motor learning, including "What-to-Where" transformations. Our model also implicates the indirect channel in the conditioned STOP function neglected in prior models. Their model predicts that working memory activity is shut off by a nonspecific, inhibitory corollary discharge from the SC to the thalamus. Ours proposes that the SC drives postsaccadic cells in cortex to shut off specific, already-executed, movement plans.

Future extensions. The TELOS model may be extended in several ways. Its treatment of the ability of the frontal cortex to replace a parietal target representation excited by a transient visual input with a remembered target plan, and to generate an internally guided saccade following resolution of the parietal competition, applies with minor changes to how primates perform the anti-saccade task (Hallett, 1978; Amador et al. 1998; Everling et al. 1998; Funahashi et al. 1993). One of these changes would be the addition of the supplementary eye fields (SEF) to expand the representational scope (Chen & Wise, 1995a, 1995b) of the model's premotor GCZs. More generally, although we have focused primarily on the FEF, BG, and SC, the anatomical principles used to structure the model govern many other parts of

the frontal cortex (e.g., Middleton & Strick, 2000). Therefore the model should generalize to other frontal cortical areas. For another example, the prefrontal cortex (PFC, e.g., areas 9 and 46) is represented in the model as a single layer working memory (Figure 2) which could itself be expanded into a multi-layered system similar to the present FEF model. The output layer (or even plan layer) of such an expanded prefrontal model could provide the control signals to the FEF layer VI. This would constitute a kind of hierarchical decision-making scheme, in which the PFC decides, based on current working memory activity, what strategies will be primed in lower areas such as FEF. These lower areas then determine the specifics of a planned movement.

Another fruitful direction for extensions is the explanation of serial behavior. In the existing model, if a "losing" plan remains, after the winning plan is executed and has its activity deleted by postsaccadic cell activity, then the losing plan may be executed subsequently. This means that the model can serve as part of what has been called a *competitive queuing* system, in which several to-be-performed plans are simultaneously active before movement begins. Then through iterative choice making (and deletion of plans as they are executed), the corresponding actions are executed in a sequence determined by the initial gradient of activation levels, namely from most to least active. Evidence for such gradient representations of winning versus losing plans, and of planned sequences, have recently been reported in prefrontal and dorsal premotor cortices (Averbeck, Chafee, Crowe & Georgopoulos, 2002; Cisek & Kalaska, 2002). This mechanism can be used to help learn and perform movement sequences (Grossberg, 1982; Grossberg & Kuperstein, 1986; Boardman & Bullock, 1991; Hartley & Houghton, 1996; Bullock & Rhodes, 2003), for which the basal ganglia system has been implicated (e.g., Kermadi et al., 1993; Martin et al., 1994; Weiss et al., 1997; Aldridge & Berridge, 1998).

References

Albin, R.L., Young, A.B. & Penney, J.B. (1989). The functional anatomy of basal ganglia disorders. *Trends in Neurosciences, 12,* 366-374.

Aldridge, J.W. & Berridge, K.C. (1998). Coding of serial order by neostriatal neurons: A "natural action" approach to movement sequence. *Journal of Neuroscience, 18,* 2777-2787.

Alexander, G. & Crutcher, M. (1990). Functional architecture of basal ganglia circuits: neural substrates of parallel processing. *Trends in Neurosciences, 13,* 266-271.

Amador, N., Schlag-Rey, M. & Schlag, J. (1998). Primate antisaccades. I. Behavioral characteristics. *Journal of Neurophysiology, 80,* 1775-86.

Amos, A. (2000). A computational model of information processing in the frontal cortex and basal ganglia. *Journal of Cognitive Neuroscience, 12,* 505-519.

Arbib, M.A. & Dominey, P.F. (1995). Modeling the roles of basal ganglia in timing and sequencing saccadic eye movements. In J. Houk, J. Davis and D. Beiser (Eds.), *Models of information processing in the basal ganglia* (pp. 149-162). Cambridge: MIT Press.

Asaad, W.F., Rainer, G. & Miller, E.K. (2000). Task-specific neural activity in the primate prefrontal cortex. *Journal of Neurophysiology, 84,* 451-459.

Averbeck, B.B., Chafee, M.V., Crowe, D.A. & Georgopoulos, A.P. (2002). Parallel processing of serial movements in prefrontal cortex. *Proceedings of the National Academy of Science, 99,* 13172–13177.

Bao, S., Chan, V.T. & Merzenich, M.M. (2001). Cortical remodelling induced by activity of ventral tegmental dopamine neurons. *Nature. 412,* 79-83.

Bar, M., Tootell, R.B.H., Schacter, D.L., Greve, D.N., Fischl, B., Mendola, J.D., Rosen, B.R. & Dale, A.M. (2001). Cortical mechanisms specific to explicit object recognition. *Neuron, 29,* 529-535.

Barbas, H. (1988). Anatomic organization of basoventral and mediodorsal visual recipient prefrontal regions in the rhesus monkey. *Journal of Comparative Neurology, 276,* 313-342.

Barbas, H. & Mesulam, M.M. (1981). Organization of afferent input to subdivisions of area 8 in the rhesus monkey. *Journal of Comparative Neurology, 200,* 407-431.

Bayer, H.M., Handel, A. & Glimcher, P.W. (1999). Do the saccade-related neurons of the substantia nigra pars reticulata (SNr) carry information about saccadic amplitude or endpoint? *Society for*

Neuroscience Abstracts, 25, 1921.

Beiser, D.G. & Houk, J.C. (1998). Model of cortical-basal ganglionic processing: Encoding the serial order of sensory events. *Journal of Neurophysiology, 79*, 3168-3188.

Berendse, H.W., de Galis, G.Y., & Groenewegen, H.J. (1992). Topographical organization and relationship with ventral striatal compartments of prefrontal corticostriatal projections in the rat. *Journal of Comparative Neurology, 316*, 314-347.

Berger, B., Trottier, S., Verney, C., Gaspar, P., & Alvarez, C. (1988). Regional and laminar distribution of the dopamine and serotonin innervation in the macaque cerebral cortex: a radioautographic study. *Journal of Comparative Neurology, 273*, 99-119.

Berns, G. & Sejnowski, T. (1998). A computational model of how the basal ganglia produce sequences. *Journal of Cognitive Neuroscience, 10*, 108-121.

Berretta, S., Parthasarathy, H.B. & Graybiel, A.M. (1997). Local release of GABAergic inhibition in the motor cortex induces immediate-early gene expression in indirect pathway neurons of the striatum. *Journal of Neuroscience, 17*, 4752-4763.

Bichot, N.P., Schall, J.D. & Thompson, K.G. (1996). Visual feature selectivity in frontal eye fields induced by experience in mature macaques. *Nature, 381*, 697-699.

Bichot, N.P., Schall, J.D. (1999). Effects of similarity and history on neural mechanisms of visual selection. *Nature Neuroscience, 2*, 549-554.

Boardman, I. & Bullock, D. (1991). A neural network model of serial order recall from short-term memory. *Proceedings of the International Joint Conference on Neural Networks, II*, 879-884.

Brown, J., Bullock, D. & Grossberg, S. (1999). How the basal ganglia use parallel excitatory and inhibitory learning pathways to selectively respond to unexpected rewarding cues. *Journal of Neuroscience, 19*, 10502-10511.

Brown, J., Bullock, D., Grossberg, S. (2000). How laminar frontal cortex and basal ganglia circuits interact to control planned and reactive saccades. *Society for Neuroscience Abstracts*, 26.

Brown, L.L., Makman, M.H., Wolfson, L.I., Dvorkin, B., Warner, C., & Katzman, R. (1979). A direct role of dopamine in the rat subthalamic nucleus and an adjacent intrapeduncular area. *Science, 206*, 1416-1418.

Bruce, C.J., Goldberg, M.E., Bushnell, M.C., & Stanton, G.B. (1985). Primate frontal eye fields. II. Physiological and anatomical correlates of electrically-evoked eye movements. *Journal of Neurophysiology, 54*, 714-734.

Bullier, J., Schall, J.D. & Morel, A. (1996). Functional streams in occipito-frontal connections in the monkey. *Behavioral Brain Research, 76*, 89-97.

Bullock, D. & Grossberg, S. (1991). Adaptive neural networks for control of movement trajectories invariant under speed and force rescaling. *Human Movement Science, 10*, 3-53.

Bullock, D., Rhodes, B. (2003). Competitive queuing for serial planning and performance. In M. Arbib (Ed.), *Handbook of brain theory and neural networks, 2ed* (pp. 241-244). Cambridge, MA: MIT Press.

Burman, D.D. & Bruce, C.J. (1997). Suppression of task-related saccades by electrical stimulation in the primate's frontal eye field. *Journal of Neurophysiology, 77*, 2252-2267.

Butler, A.B. & Hodos, W. (1996). *Comparative vertebrate neuroanatomy.* New York: Wiley-Liss.

Calabresi, P., Gubellini, P., Centonze, D., Picconi, B., Bernardi, G., Chergui, K., Svenningsson, P., Fienberg, A.A. & Greengard P (2000). Dopamine and cAMP-regulated phosphoprotein 32 kDa controls both striatal long-term depression and long-term potentiation, opposing forms of synaptic plasticity. *Journal of Neuroscience, 20*, 8443-8451.

Canteras, N.S., Shammah-Lagnado, S.J., Silva, B.A., & Ricardo, J.A. (1990). Afferent connections of the subthalamic nucleus: a combined retrograde and anterograde horseradish peroxidase study in the rat. *Brain Research, 513*, 43-59.

Cavada, C. & Goldman-Rakic, P.S. (1991). Topographic segregation of corticostriatal projections from posterior parietal subdivisions in the macaque monkey. *Neuroscience, 42*, 683-696.

Chafee, M.V. & Goldman-Rakic, P.S. (2000). Inactivation of parietal and prefrontal cortex reveals inter-

dependence of neural activity during memory-guided saccades. *Journal of Neurophysiology, 83,* 1550-1566.

Charpier, S., Deniau, J.M. (1997). In vivo activity-dependent plasticity at cortico-striatal connections: evidence for physiological long-term potentiation. *Proceedings of the National Academy of Science, 94,* 7036-7040.

Chen, L.L. & Wise, S.P. (1995a). Neuronal activity in the supplementary eye field during acquisition of conditional oculomotor associations. *Journal of Neurophysiology, 73,* 1101-1121.

Chen, L.L. & Wise, S.P. (1995b). Supplementary eye field contrasted with the frontal eye field during acquisition of conditional oculomotor associations. *Journal of Neurophysiology, 73,* 1122-1134.

Cisek, P. & Kalaska, J.F. (2002). Simultaneous encoding of multiple potential reach directions in dorsal premotor cortex. *Journal of Neurophysiology, 87,* 1149-1154.

Cohen, J.D., Braver, T.S., & Brown J.W. (2002). Computational perspectives on dopamine function in prefrontal cortex. *Current Opinion in Neurobiology, 12,* 223-229.

Contreras-Vidal, J. & Schultz, W. (1999). A predictive reinforcement model of dopamine neurons for learning approach behavior. *Journal of Computational Neuroscience, 6,* 191-214.

Contreras-Vidal, J. & Stelmach, G.E. (1995). A neural model of basal ganglia-thalamocortical relations in normal and parkinsonian movement. *Biological Cybernetics, 73,* 467-476.

Crosson, B. (1985). Subcortical functions in language: a working model. *Brain and Language, 25,* 257-292.

De Las Heras, S., Mengual, E., Velayos, J.L., & Gimenez-Amaya, J.M. (1998). Re-examination of topographic distribution of thalamic neurons projecting to the caudate nucleus. A retrograde labeling study in the cat. *Neuroscience Research, 31,* 283-293.

Deng, S.Y., Goldberg, M.E., Segraves, M.A., Ungerleider, L.G., & Mishkin, M. (1986). The effect of unilateral ablation of the frontal eye fields on saccadic performance in the monkey. In E. Keller and D. Zee (Eds.), *Advances in the Biosciences, Vol. 57: Adaptive processes in visual and oculomotor systems*. New York: Pergamon.

Dominey, P., Arbib, M., & Joseph, J. (1995). A model of corticostriatal plasticity for learning oculomotor associations and sequences. *Journal of Cognitive Neuroscience, 7,* 311-336.

Durstewitz, D., Seamans, J.K., and Sejnowski, T.J. (2000). Dopamine-mediated stabilization of delay-period activity in a network model of prefrontal cortex. *Journal of Neurophysiology, 83,* 1733-1750.

Everling, S., Spantekow, A., Krappmann, P., & Flohr, H. (1998). Event-related potentials associated with correct and incorrect responses in a cued antisaccade task. *Experimental Brain Research, 118,* 27-34.

Ewert, J.P., Schurg-Pfeiffer, E., & Schwippert, W.W. (1996). Influence of pretectal lesions on tectal responses to visual stimulation in anurans: field potential, single neuron and behavior analyses. *Acta Biologica Hungarica, 47,* 89-111.

Eyny, Y.S. & Horvitz, J.C. (2003). Opposing roles of D_1 and D_2 receptors in appetitive conditioning. *Journal of Neuroscience, 23,* 1584-1587.

Fiala, J., Grossberg, S., & Bullock, D. (1996). Metabotropic glutamate receptor activation in cerebellar Purkinje cells as substrate for adaptive timing of the classically conditioned eye-blink response. *Journal of Neuroscience, 16,* 3760-3774.

Fischer, B. & Weber, H. (1993). Express saccades and visual attention. *Behavioral and Brain Sciences, 16,* 553-610.

Flaherty, A.W. & Graybiel, A.M. (1991). Corticostriatal transformations in the primate somatosensory system. Projections from physiologically mapped body-part representations. *Journal of Neurophysiology, 66,* 1249-1263.

Frank, M.J., Loughry, B., & O'Reilly, R.C. (2001). Interactions between the frontal cortex and basal ganglia in working memory: A computational model. *Cognitive, Affective, and Behavioral Neuroscience, 1,* 137-160.

Funahashi, S., Chafee, M.V., & Goldman-Rakic, P.S. (1993). Prefrontal neuronal activity in rhesus monkeys performing a delayed anti-saccade task. *Nature, 365,* 753-756.

Gancarz, G. & Grossberg, S. (1999), A neural model of saccadic eye movement control explains task-

specific adaptation. *Vision Research, 39,* 3123-3143.

Gaspar, P., Bloch, B., & Le Moine, C. (1995). D1 and D2 receptor gene expression in the rat frontal cortex: cellular localization in different classes of efferent neurons. *European Journal of Neuroscience, 7,* 1050-1063.

Gerfen, C. & Wilson, C. (1996). The basal ganglia. In L.W. Swanson, A. Bjorklund, and T. Hokfelt, (Eds.) *Handbook of chemical neuroanatomy, Vol 12, Integrated systems of the CNS, Part III,* pp. 371-468. Holland: Elsevier Science B.V.

Gernert, M., Hamann, M., Bennay, M., Loscher, W., & Richter, A. (2000). Deficit of striatal parvalbumin-reactive GABAergic interneurons and decreased basal ganglia output in a genetic rodent model of idiopathic paroxymal dystonia. *Journal of Neuroscience, 20,* 7052-7058.

Giuffrida, R., Volsi, G.L., Maugeri, G., and Perciavalle, V. (1985). Influences of the pyramidal tract on the subthalamic nucleus in the cat. *Neuroscience Letters, 54,* 231-235.

Goldman-Rakic, P.S. (1987). Circuitry of primate prefrontal cortex and regulation of behavior by representational memory. In V.B. Mountcastle, F. Plum, and S.R. Geiger (Eds.) *Handbook of physiology, Vol I* (pp. 373-417). New York: Oxford University Press.

Goldman-Rakic, P.S. (1995). Toward a circuit model of working memory and the guidance of voluntary motor action. In J. Houk, J. Davis and D. Beiser (Eds.), *Models of information processing in the basal ganglia* (pp. 131-148). Cambridge: MIT Press.

Gnadt, J.W. & Andersen, R.A. (1988). Memory related motor planning activity in posterior parietal cortex of macaque. *Experimental Brain Research, 70,* 216-20.

Graybiel, A.M., Aosaki, T., Flaherty, A., & Kimura, M. (1994). The basal ganglia and adaptive motor control. *Science, 265,* 1826-1831.

Graybiel, A.M. (1998). The basal ganglia and chunking of action repertoires. *Neurobiology of Learning and Memory, 70,* 119-136.

Gross, C.G., Desimone, R., Albright, T.D., & Schwartz, EL (1985). Inferior temporal cortex and pattern recognition. *Experimental Brain Research, Supplement 11,* 179-201.

Grossberg, S. (1971). On the dynamics of operant conditioning. *Journal of Theoretical Biology, 33,* 225-55.

Grossberg, S. (1973). Contour enhancement, short term memory, and constancies in reverberating neural networks. *Studies in Applied Mathematics, 52,* 213-257.

Grossberg, S. (1982). Processing of expected and unexpected events during conditioning and attention: a psychophysiological theory. *Psychological Review, 89,* 529-572.

Grossberg, S. (1982). *Studies of mind and brain*. Boston: Kluwer/Reidel Press.

Grossberg, S. & Kuperstein, M. (1986). *Neural dynamics of adaptive sensory-motor control: Ballistic eye movements*. Holland: Elsevier.

Grossberg, S., Merrill, J. (1992). A neural network model of adaptively timed reinforcement learning and hippocampal dynamics. *Cognitive Brain Research, 1,* 3-38.

Grossberg, S., Roberts, K., Aguilar, M., & Bullock, D. (1997). A neural model of multimodal adaptive saccadic eye movement control by superior colliculus. *Journal of Neuroscience, 17,* 9706-9725.

Grossberg, S. & Schmajuk, N.A. (1987). Neural dynamics of attentionally modulated Pavlovian conditioning: Conditioned reinforcement, inhibition and opponent processing. *Psychobiology, 15,* 195-249.

Guitton, D., Buchtel, H.A., & Douglas, R.M. (1985). Frontal lobe lesions in man cause difficulties in suppressing reflexive glances and in generating goal-directed saccades. *Experimental Brain Research, 58,* 455-472.

Gurden, H., Takita, M., & Jay, T.M. (2000). Essential role of D1 but not D2 receptors in the NMDA receptor-dependent long-term potentiation at hippocampal-prefrontal cortex synapses in vivo. *Journal of Neuroscience, 20,* RC106

Gurney, K., Prescott, T.J., & Redgrave, P. (2001a). A computational model of action selection in the basal ganglia: A new functional anatomy. *Biological Cybernetics, 84,* 401-410.

Gurney, K., Prescott, T.J., & Redgrave, P. (2001b). A computational model of action selection in the

basal ganglia: Analysis and simulation of behavior. *Biological Cybernetics, 84,* 411-423.
Hall, W.C., Lee, P. (1993). Interlaminar connections of the superior colliculus in the tree shrew. I. The superficial gray layer. *Journal of Comparative Neurology, 332,* 213-223.
Hallett, P.E. (1978). Primary and secondary saccades to goals defined by instructions. *Vision Research, 18,* 1279-1296.
Handel, A. & Glimcher, P.W. (2000). Contextual modulation of substantia nigra pars reticulata neurons. *Journal of Neurophysiology, 83,* 3042-3048.
Handel, A., Glimcher, P.W. (1999). Quantitative analysis of substantia nigra pars reticulata activity during a visually guided saccade task. *Journal of Neurophysiology, 82,* 3458-3475.
Hanes, D.P. & Schall, J.D. (1996). Neural control of voluntary movement initiation. *Science, 274,* 427-430.
Hanes, D.P., Patterson, W.F. II, & Schall, J.D. (1998). Role of frontal eye fields in countermanding saccades: Visual, movement, and fixation activity. *Journal of Neurophysiology, 79,* 817-834.
Hartley, T.A. & Houghton, G. (1996). A linguistically constrained model of short-term memory for nonwords. *Journal of Memory and Language, 35,* 1-31.
Hassani, O.K., Moroux, M., & Feger, J. (1996). Increased subthalamic neuronal activity after nigral dopaminergic lesion independent of disinhibition via the globus pallidus. *Neuroscience, 72,* 105-115.
Hazrati, L.N., Parent, A., Mitchell, S., & Haber, S.N. (1990). Evidence for interconnections between the two segments of the globus pallidus in primates: a PHA-L anterograde tracing study. *Brain Research, 533,* 171-175.
Hemart, N., Daniel, H., Jaillard, D., & Crepel, F. (1995). Receptors and second messengers involved in long-term depression in rat cerebellar slices *in vitro*: a reappraisal. *European Journal of Neuroscience, 7,* 45-53.
Hikosaka, O., Wurtz, R.H. (1983). Visual and oculomotor functions of monkey substantia nigra pars reticulata. IV. Relation of substantia nigra to superior colliculus. *Journal of Neurophysiology, 49,* 1285-1301.
Hikosaka, O., Sakamoto, M., & Usui, S. (1989). Functional properties of monkey caudate neurons I. Activities related to saccadic eye movements. *Journal of Neurophysiology, 61,* 780-798.
Hikosaka, O. & Wurtz, R.H. (1989) The basal ganglia. In R.Wurtz and M. Goldberg (Eds.), *The neurobiology of sacccadic eye movements,* pp. 257-281. Amsterdam: Elsevier.
Hodgkin, A.L. (1964) *The conduction of the nervous impulse.* Thomas: Springfield, IL.
Hoesen, G.W.V., Yeterian, E.H., & Lavizzo-Mourey, R. (1981). Widespread corticostriate projections from temporal cortex of the rhesus monkey. *Journal of Comparative Neurology, 199,* 205-219.
Horak, F.B. & Anderson, M.E. (1984). Influence of globus pallidus on arm movements in monkeys, II. Effects of stimulation. *Journal of Neurophysiology, 52,* 305-322.
Horak, F.B., Shupert, C.L., & Mirka, A. (1989). Components of postural dyscontrol in the elderly: A review. *Neurobiology of Aging, 10,* 727-738.
Hoshi, E., Shima, K., & Tanji, J. (1998). Task-dependent selectivity of movement-related neuronal activity in the primate prefrontal cortex. *Journal of Neurophysiology, 80,* 3392-3397.
Houk, J., Adams, J., & Barto, A. (1995). A model of how the basal ganglia generate and use neural signals that predict reinforcement. In J. Houk, J. Davis and D. Beiser (Eds.), *Models of information processing in the basal ganglia* (pp 249-270). Cambridge, MA: MIT Press.
Houk, J.C. & Wise, S.P. (1995). Distributed modular architectures linking basal ganglia, cerebellum, and cerebral cortex: Their role in planning and controlling action. *Cerebral Cortex, 2,* 95-110.
Hutsler, J.J. & Chalupa, L.M. (1991). Substance P immunoreactivity identifies a projection from the cat's superior colliculus to the principal tectorecipient zone of the lateral posterior nucleus. *Journal of Comparative Neurology, 312,* 379-390.
Iriki, A., Pavlides, C., Keller, A., & Asanuma, H. (1991). Long-term potentiation of thalamic input to the motor cortex induced by coactivation of thalamocortical and corticocortical afferents. *Journal of Neurophysiology, 65,* 1435-1441.
Iwabuchi, A., Kubota, K. (1998). Laminar organization of neuronal activities in area 8 of rhesus monkeys

during a symmetrically reinforced visual go/no-go task. *International Journal of Neuroscience, 94,* 1-25.

Jacobs, R.A., Jordan, M.I., Nowland, S.J., & Hinton, G.E. (1991). Adaptive mixtures of local experts. *Neural Computation, 3,* 79-87.

Jaeger, D., Kita, H., & Wilson, C.J. (1994). Surround inhibition among projection neurons is weak or nonexistent in the rat neostriatum. *Journal of Neurophysiology, 72,* 2555-2558.

Jones, E.G., Coulter, J.D., Burton, H., & Porter, R. (1977). Cells of origin and terminal distribution of corticostriatal fibers arising in the sensory-motor cortex of monkeys. *Journal of Comparative Neurology, 173,* 53-80.

Kalaska, J.F. & Crammond, D.J. (1995). Deciding not to GO: neuronal correlates of response selection in a GO/NOGO task in primate premotor and parietal cortex. *Cerebral Cortex, 5,* 410-428.

Kang, Y. & Kayano, F. (1994). Electrophysiological and morphological characteristics of layer VI pyramidal cells in the cat motor cortex. *Journal of Neurophysiology, 72,* 578-591.

Kawaguchi, Y., Wilson, C.J., Augood, S.J., & Emson, P.C. (1995). Striatal interneurones: chemical, physiological and morphological characterization. *Trends in Neurosciences, 18,* 527-535.

Kawaguchi, Y. (1997). Neostriatal cell subtypes and their functional roles. *Neuroscience Research, 27,* 1-8.

Kemel, M.L., Desban, M., Gauchy, C., Glowinski, J., & Besson, M.J. (1988). Topographical organization of efferent projections from the cat substantia nigra pars reticulata. *Brain Research, 455,* 307-323.

Kermadi, I., Jurquet, Y., Arzi, M., & Joseph, J.P. (1993). Neural activity in the caudate nucleus of monkeys during spatial sequencing. *Experimental Brain Research, 94,* 352-356.

Kimura, A., Caria, M.A., Melis, F., & Asanuma, H. (1994). Long-term potentiation within the cat motor cortex. *Neuroreport, 5,* 2372-2376.

Kita, H., Kosaka, T., & Heizmann, C.W. (1990). Parvalbumin-immunoreactive neurons in the rat neostriatum: A light and electron microscope study. *Brain Research, 536,* 1-15.

Klopf, A.H. (1982). *The hedonistic neuron: a theory of memory, learning, and intelligence.* Washington D.C.: Hemisphere.

Kobatake, E. & Tanaka, K. (1994). Neuronal selectivities to complex object features in the ventral visual pathway of the macaque cerebral cortex. *Journal of Neurophysiology, 71,* 856-867.

Komatsu, H. & Ideura, Y. (1993). Relationships between color, shape, and pattern selectivities of neurons in the inferior temporal cortex of the monkey. *Journal of Neurophysiology, 70,* 677-694.

Koos, T. & Tepper, J.M. (1999). Inhibitory control of neostriatal projection neurons by GABAergic interneurons. *Nature Neuroscience, 2,* 467-472.

Law-Tho, D., Desce, J.M., & Crepel, F. (1995). Dopamine favours the emergence of long-term depression versus long-term potentiation in slices of rat prefrontal cortex. *Neuroscience Letters, 188,* 125-128.

Lee, C., Rohrer, W.H., & Sparks, D.L. (1988). Population coding of saccadic eye movements by neurons in the superior colliculus. *Nature, 332,* 357-360.

Levesque, M., Charara, A., Gagnon, S., Parent, A., & Deschenes, M. (1996). Corticostriatal projections from layer V cells in rat are collaterals of long-range corticofugal axons. *Brain Research, 709,* 311-315.

Levy, R., Hazrati, L.-N., Herrero, M.-T., Vila, M., Hassani, O.-K., Mouroux, M., Ruberg, M., Asensi, H., Agid, Y., Feger, J., Obeso, J., Parent, A., & Hirsch, E. C. (1997). Re-evaluation of the functional anatomy of the basal ganglia in normal and parkinsonian states. *Neuroscience, 76,* 335-343.

Ljungberg, T., Apicella, P., & Schultz, W. (1992). Responses of monkey dopamine neurons during learning of behavioral reactions. *Journal of Neurophysiology, 67,* 145-163.

Lo, F.-S. & Sherman, S.M. (1994). Feedback inhibition in the cat's lateral geniculate nucleus. *Experimental Brain Research, 100,* 365-368.

Logan, G.D. & Cowan, W.B. (1984). On the ability to inhibit thought and action: A theory of an act of control. *Psychologial Review, 91,* 295-327.

Lynch, J.C., Hoover, J.E., Strick, P.L. (1994). Input to the primate frontal eye field from the substantia

nigra, superior colliculus, and dentate nucleus demonstrated by transneuronal transport. *Experimental Brain Research, 100,* 181-186.

Marin, O., Sweets, W.J., & Gonzalez, A. (1998). Evolution of the basal ganglia in tetrapods: A new perspective based on recent studies in amphibians. *Trends in Neurosciences, 21,* 487-494.

Martin, K.E., Phillips, J.G., & Iansek, R. (1994). Inaccuracy and instability of sequential movements in Parkinson's disease. *Experimental Brain Research, 102,* 131-140.

Martres, M.P., Bouthenet, M.L., Sales, N., Sokoloff, P., & Schwartz, J.C. (1985). Widespread distribution of brain dopamine receptors evidenced with [^{125}I] iodosulpride, a highly selective ligand. *Science, 228,* 752-755.

Mayer, M.L., Westbrook, G.L., & Guthrie, P.B. (1984). Voltage-dependent block by Mg2+ of NMDA responses in spinal cord neurones. *Nature, 309,* 261-263.

McFarland, N.R., Haber, S.N. (2000). Convergent inputs from thalamic motor nuclei and frontal cortical areas to the dorsal striatum in the primate. *Journal of Neuroscience, 20,* 3798-813.

Middleton, F.A. & Strick, P.L. (2000). Basal ganglia and cerebellar loops: motor and cognitive circuits. *Brain Research Reviews, 31,* 236-250.

Mink, J.W. (1996). The basal ganglia: focused selection and inhibition of competing motor programs. *Progress in Neurobiology, 50,* 381-425.

Mink, J.W. & Thach, W.T. (1993). Basal ganglia intrinsic circuits and their role in behavior. *Current Opinion in Neurobiology, 3,* 950-957.

Mohler, C.W., Goldberg, M.E., & Wurtz, R.H. (1973). Visual receptive fields of frontal eye field neurons. *Brain Research, 61,* 385-389.

Munoz, D.P. & Wurtz, R.H. (1993) Fixation cells in monkey superior colliculus I. Characteristics of cell discharge. *Journal of Neurophysiology, 70,* 559-575.

Munoz, D.P. & Wurtz, R.H. (1995). Saccade-related activity in monkey superior colliculus I. Characteristics of burst and buildup cells. *Journal of Neurophysiology, 73,* 2313-2333.

Mushiake, H., Inase, M., & Tanji, J. (1991). Neuronal activity in the primate premotor, supplementary, and precentral motor cortex during visually guided and internally determined sequential movements. *Journal of Neurophysiology, 66,* 705-718.

Nambu, A., Tokuno, H., & Takada, M. (2002) Functional significance of the the cortico-subthalamo-pallidal 'hyperdirect' pathway. *Neuroscience Research, 43,* 111-117.

Oorschot, D.E. (1996). Total number of neurones in the neostriatal, pallidal, subthalamic, and substantia nigral nuclei of the rat basal ganglia: a stereological study using the cavalieri and optical dissector methods. *Journal of Comparative Neurology, 366,* 580-599.

Otani, S., Auclair, N., Desce, J.M., Roisin, M.P., & Crepel, F. (1999). Dopamine receptors and groups I and II mGluRs cooperate for long-term depression induction in rat prefrontal cortex through converging postsynaptic activation of MAP kinases. *Journal of Neuroscience, 19,* 9788-9802.

Ottes, F.P., Van Gisbergen, J.A., & Eggermont, J.J. (1984). Metrics of saccade responses to visual double stimuli: Two different modes. *Vision Research, 24,* 1169-1179.

Parent, A. & Hazrati, L.N. (1995). Functional anatomy of the basal ganglia. II. The place of the subthalamic nucleus and external pallidum in basal ganglia circuitry. *Brain Research Reviews, 20,* 128-154.

Parthasarathy, H.B., Schall, J.D., & Graybiel, A.M. (1992). Distributed but convergent ordering of corticostriatal projections: analysis of the frontal eye field and the supplementary eye field in the macaque monkey. *Journal of Neuroscience, 12,* 4468-4488.

Passingham, R. (1993). *The frontal lobes and voluntary action*. Oxford: Oxford U. Press.

Pellizzer, G. & Hedges, J.H. (2003). Motor planning: effect of directional uncertainty with discrete spatial cues. *Experimental Brain Research, 150,* 276-289.

Pierrot-Deseilligny, C., Israel, I., Berthoz, A., Rivaud, S., & Gaymard, B. (1993). Role of the different frontal lobe areas in the control of the horizontal component of memory-guided saccades in man. *Experimental Brain Research, 95,* 166-171.

Platt, M.L. & Glimcher, P.W. (1999). Neural correlates of decision variables in parietal cortex. *Nature, 400,* 233-238.

Redgrave, P., Prescott, T.J., & Gurney, K. (1999). The basal ganglia: A vertebrate solution to the selection problem? *Neuroscience, 89,* 1009-1023.

Reynolds, J.N., Hyland, B.I., & Wickens, J.R. (2001). A cellular mechanism of reward-related learning. *Nature, 413,* 67-70.

Royce, G.J. & Bromley, S. (1984). Florescent double labeling studies of thalamostriatal and corticostriatal neurons. In J.S. McKenzie, R.E. Kemm & L.N. Wilcock (Eds.) *The basal ganglia* (pp. 131-146). New York: Plenum.

Sawaguchi, T. (2001). Laminar and topographic distributions of prefrontal cortical neurons related to an oculomotor delayed response task in monkeys. *Society for Neuroscience Abstracts, 27,* 852.20

Schall, J.D. (1991). Neuronal activity related to visually guided saccades in the frontal eye fields of rhesus monkeys: Comparison with supplementary eye fields. *Journal of Neurophysiology, 66,* 559-579.

Schall, J.D. & Bichot, N.P. (1998). Neural correlates of visual and motor decision processes. *Current Opinion in Neurobiology, 8,* 211-217.

Schall, J.D., Hanes, D.P., Thompson, K.G., & King, D.J. (1995b). Saccade target selection in frontal eye field of macaque. I. Visual and premovement activation. *Journal of Neuroscience, 15,* 6905-6918.

Schall, J.D., Morel, A., King, D.J., & Bullier, J. (1995a). Topography of visual cortex connections with frontal eye field in macaque: convergence and segregation of processing streams. *Journal of Neuroscience, 15,* 4464-4487.

Schiller, P.H. (1998). The neural control of visually-guided eye movements. In J. E. Richards (Ed.), *Cognitive neuroscience of attention.* Mahwah, NJ: Lawrence Erlbaum Assoc.

Schiller, P.H., True, S.D., & Conway, J.L. (1980). Deficits in eye movements following frontal eye field and superior colliculus ablations. *Journal of Neurophysiology, 44,* 1175-1189.

Schlag, J. & Schlag-Rey, M. (1987). Evidence for a supplementary eye field. *Journal of Neurophysiology, 57,* 179-200.

Schlag-Rey, M., Amador, N., Sanchez, H., & Schlag, J. (1997). Antisaccade performance predicted by neuronal activity in the supplementary eye field. *Nature. 390,* 398-401.

Schlag-Rey, M. & Schlag, J. (1984). Visuomotor functions of central thalamus in monkey. II. Unit activity related to visual events, targeting, and fixation. *Journal of Neurophysiology, 51,* 1175-1195.

Schultz, W. (1998) Predictive reward signals of dopamine neurons. *Journal of Neurophysiology, 80,* 1-27.

Segraves, M.A. & Goldberg, M.E. (1987). Functional properties of corticotectal neurons in the monkey's frontal eye field. *Journal of Neurophysiology, 58,* 1387-1419.

Shink, E., Bevan, M.D., Bolam, J.P., & Smith, Y. (1996). The subthalamic nucleus and the external pallidum: two tightly interconnected structures that control the output of the basal ganglia in the monkey. *Neuroscience, 73,* 335-357.

Sigala, N., Logothetis, N.K. (2002). Visual categorization shapes feature selectivity in the primate temporal cortex. *Nature, 415,* 318-320.

Skinner, R.D. & Garcia-Rill, E. (1990). Brainstem modulation of rhythmic functions and behaviors. In W.R. Klemm and R.P. Vertes (Eds.), *Brainstem mechanisms of behavior* (pp. 465-496). New York: Wiley.

Smith, Y. & Bolam, J.P. (1990). The output neurones and the dopaminergic neurones of the substantia nigra receive a GABA-containing input from the globus pallidus in the rat. *Journal of Comparative Neurology, 296,* 47-64.

Sommer, M.A. & Tehovnik, E.J. (1999). Reversible inactivation of macaque dorsomedial frontal cortex: effects on saccades and fixations. *Experimental Brain Research, 124,* 429-446.

Sommer, M.A. & Wurtz, R.H. (1998). Frontal eye field neurons orthodromically activated from the superior colliculus. *Journal of Neurophysiology, 80,* 3331-3333.

Sommer, M.A. & Wurtz, R.H. (2000). Composition and topographic organization of signals sent from the frontal eye field to the superior colliculus. *Journal of Neurophysiology, 83,* 1979-2001.

Steele, G.E. & Weller, R.E. (1993). Subcortical connections of subdivisions of inferior temporal cortex in squirrel monkeys. *Visual Neuroscience, 10,* 563-583.

Steiner, H. & Gerfen, C.R. (1998). Role of dynorphin and enkephalin in the regulation of striatal output pathways and behavior. *Experimental Brain Research, 123,* 60-76.

Strick, P.L., Dum, R.P., & Picard, N. (1995). Macro-organization of the circuits connecting the basal ganglia with the cortical motor areas. In J. Houk, J. Davis and D. Beiser (Eds.), *Models of information processing in the basal ganglia* (pp. 117-130). Cambridge: MIT Press.

Sung, K.W., Choi, S., & Lovinger, D.M. (2001). Activation of group I mGluRs is necessary for induction of long-term depression at striatal synapses. *Journal of Neurophysiology, 86,* 2405-2412.

Suri, R.E., Albani, C., & Glattfelder, A.H. (1997). A dynamic model of motor basal ganglia functions. *Biological Cybernetics, 76,* 451-458.

Suri, R.E., Bargas, J., Arbib, M.A. (2001). Modeling functions of striatal dopamine modulation in learning and planning. *Neuroscience, 103,* 65-85.

Sutton, R.S. & Barto, A.G. (1981). Toward a modern theory of adaptive networks: expectation and prediction. *Psychological Review, 88,* 135-170.

Sweeney, J.A., Mintun, M.A., Kwee, S., Wiseman, M.B., Brown, D.L., Rosenberg, D.R., & Carl, J.R. (1996). Positron emission tomography study of voluntary saccadic eye movements and spatial working memory. *Journal of Neurophysiology, 75,* 454-468.

Takikawa, Y., Kawagoe, R., Itoh, H., Nakahara, H., & Hikosaka, O. (2002). Modulation of saccadic eye movements by predicted reward outcome. *Experimental Brain Research, 142,* 284-291.

Tanaka, K., Saito, H., Fukada, Y., & Moriya, M. (1991). Coding visual images of objects in the inferotemporal cortex of the macaque monkey. *Journal of Neurophysiology, 66,* 170-189.

Taylor, J.G. & Taylor, N.R. (2000). Analysis of recurrent cortico-basal ganglia-thalamic loops for working memory. *Biological Cybernetics, 82,* 415-432.

Thompson, K.G., Bichot, N.P., & Schall, J.D. (1997). Dissociation of visual discrimination from saccade programming in macaque frontal eye field. *Journal of Neurophysiology, 77,* 1046-1050.

Turner, R.S. & Anderson, M.E. (1997). Pallidal discharge related to the kinematics of reaching movements in two dimensions. *Journal of Neurophysiology, 77,* 1051-1074.

Turner, R.S. & DeLong, M.R. (2000). Corticostriatal activity in primary motor cortex of the macaque. *Journal of Neuroscience, 20,* 7096-7108.

Turner, R.S., Grafton, S.T., Votaw, J.R., Delong, M.R., & Hoffman, J.M. (1998). Motor subcircuits mediating the control of movement velocity: a PET study. *Journal of Neurophysiology, 80,* 2162-2176.

Vezina, P. & Kim, J.H. (1999). Metabotropic glutamate receptors and the generation of locomotor activity: interactions with midbrain dopamine. *Neuroscience and Biobehavioral Reviews, 23,* 577-589.

Weiss, P., Stelmach, G.E., & Hefter, H. (1997). Programming of a movement sequence in Parkinson's disease. *Brain, 120,* 91-102.

Wichmann, T., Bergman, H., & DeLong, M.R. (1994). The primate subthalamic nucleus. I. Functional properties in intact animals. *Journal of Neurophysiology, 72,* 494-506.

Wichmann, T., DeLong, M. (1996). Functional and pathophysiological models of the basal ganglia. *Current Opinion in Neurobiology, 6,* 751-758.

Wickens, J., Begg, A., & Arbuthnott, G. (1996). Dopamine reverses the depression of rat corticostriatal synapses which normally follows high-frequency stimulation of cortex in vitro. *Neuroscience, 70,* 1-5.

Wickens, J. (1997). Basal ganglia: Structure and computations. *Network: Computation in Neural Systems, 8,* R77-R109.

Wilson, C. (1995a). The contribution of cortical neurons to the firing pattern of striatal spiny neurons. In J. Houk, J. Davis and D. Beiser (Eds.), *Models of information processing in the basal ganglia* (pp. 29-50). Cambridge, MA: MIT Press.

Wilson, C. (1995b). Corticostriatal neurons of the medial agranular cortex of rats. In M. Kimura and A. Graybiel (Eds.), *Functions of the cortico-basal ganglia loop* (pp. 50-72). Tokyo: Springer-Verlag.

Wilson, C.J., Kita, H., & Kawaguchi, Y. (1989). GABAergic interneurons, rather than spiny cell axon

collaterals, are responsible for the IPSP responses to afferent stimulation in neostriatal spiny neurons. *Society for Neuroscience Abstracts, 15,* 907.

Wise, S.P. & Murray, E.A. (2000). Arbitrary associations between antecedents and actions. *Trends in Neurosciences, 23,* 271-276.

Wurtz, R.H., Sommer, M.A., Pare, M., & Ferraina, S. (2001). Signal transformations from cerebral cortex to superior colliculus for the generation of saccades. *Vision Research, 41,* 3399-3412.

Yeterian, E.H. & Hoesen, G.W.V. (1978). Cortico-striate projections in the rhesus monkey: The organization of certain cortico-caudate connections. *Brain Research, 139,* 43-63.

Yeterian, E.H. & Pandya, D.N. (1994). Laminar origin of striatal and thalamic projections of the prefrontal cortex in rhesus monkeys. *Experimental Brain Research, 99,* 383-398.

Young, A.B. & Penney, J.B. (2001). What we know and what we have left to learn. In K. Kultas-Ilinsky and I.A. Ilinsky (Eds.), *Basal ganglia and thalamus in health and movement disorders* (pp. 3-10). Dordrecht: Kluwer Academic.

Zheng, T. & Wilson, C.J. (2002). Corticostriatal combinatorics: The implications of cortico-striatal axonal arborizations. *Journal of Neurophysiology, 87,* 1007-1017.

Zin-Ka-Ieu, S., Roger, M., & Arnault, P. (1998). Direct contacts between fibers from the ventrolateral thalamic nucleus and frontal cortical neurons projecting to the striatum: a light-microscopy study in the rat. *Anatomy and Embryology (Berlin), 197,* 77-87.

Figure Captions

Figure 1. Oculomotor tasks of Hikosaka et al. (1989). Black bars indicate intervals of visual stimulus presentations and the trace labeled E gives the horizontal component of eye position (line of gaze). In the **fixation** task, the subject must maintain gaze on the fixation point, F, despite a brief display of a distracter target, T, at a different locus. In the **saccade** task, the subject must make a pro-saccade from the fixation point to the target, which appears at a different locus, just as the fixation point shuts off. In the **overlap** task (similar to a **GO/NOGO** task), the target and the fixation point are displayed in overlapping intervals. A pro-saccade to the target is rewarded only if generated after the fixation point shuts off. The **gap** task imposes a delay between the offset of the fixation point and the onset of the target. The gap task target appears at a consistent location across trials, and the subject learns to make an anticipatory pro-saccade to the target location during the gap between fixation light offset and target onset. The **delay** task requires the subject to remember the location of a briefly-flashed target and later foveate it. [Adapted with permission from Hikosaka et al., 1989, p. 781]. The model in Figure 2 learned and performed all these tasks.

Figure 2. A laminar model of basal ganglia interactions with the FEF (frontal eye fields) and the SC (superior colliculus). Separate gray-shaded blocks highlight the major anatomical regions whose roles in planned and reactive saccade generation are treated in the model. Major anatomical abbreviations, e.g., PPC, are defined in Table 1. Excitatory links are shown as arrowheads, inhibitory as ballheads, in this and all subsequent figures. Filled semi-circles terminate cortico-striatal and cortico-cortical pathways modeled as subject to learning, which is modulated by reinforcement-related dopaminergic signals (dashed arrows). In the FEF block, Roman numerals I-VI label cortical layers; Va and Vb, respectively, are superficial and deep layer V. Further symbols are variable names in the mathematical model specified in the on-line Appendix. Subscripts xy index retinotopic coordinates, whereas subscript i denotes an FEF zone gated by an associated BG channel (details in Figure 5). All variables for FEF activities use the symbol *F*. Processed visual inputs $I_{xyi}^{(p)}$ and $I_{xyi}^{(d)}$ emerging from visual areas including V4 and posterior IT feed into the model FEF input cells and affect activations $F^{(I)}_{xyi}$. Fibers carrying such inputs are predicted to synapse on cells in layer III (and possibly layers II and IV). Visual input also excites the PPC, P_{xy}, and anterior IT, T_j. A PFC motivational signal $I^{(M)}$ arouses PFC working memory activity C_i, which in turn provides a top-down arousal signal to model FEF layer VI cells, with activities $F^{(G)}_i$. The FEF input cell activities $F^{(I)}_{xyi}$ excite FEF planning cells $F^{(P)}_{xyi}$, which are

predicted to reside in layers III/Va (and possibly layer II). Distinct plan layer activities represent alternative potential motor responses to input signals, e.g. a saccade to an eccentric target or to a central fixation point. FEF layer VI activities $F^{(G)}_i$ excite the groups/categories of plans associated with gatable cortical zones *i* and associated thalamic zones *k*. The BG decide which plan to execute and send a disinhibitory gating signal that allows thalamic activation V_k, which excites FEF layer Vb output cell activities $F^{(O)}_{xyi}$ to execute the plan. The model distinguishes (Kemel et al., 1988) a thalamus-controlling BG pathway, whose variables are symbolized by *B*, and a colliculus-controlling pathway, whose variables are symbolized by *G*. Thus, the striatal direct (*SD*) pathway activities $B^{(SD)}_k$ and $G^{(SD)}_{xy}$, respectively, inhibit GPi activities $B^{(GPi)}_k$ and SNr activities $G^{(SNr)}_{xy}$, which, respectively, inhibit thalamic activities V_k and collicular activities S_{xy}. As detailed in Figure 3, if the FEF saccade plan matches the most salient sensory input to the PPC, then the basal ganglia disinhibit the SC to open the gate and generate the saccade. However, if there is conflict between the bottom-up input to PPC and the top-down planned saccade from FEF, then the BG-SC gate is held shut by feedforward striatal inhibition (note BG blocks labeled GABA) until the cortical competition resolves. When a plan is chosen, the resulting saccade-related FEF output signal $F^{(O)}_{xyi}$ activates PPC, the STN and the SC (S_{xy}). The SC excites FEF post-saccadic cell activities $F^{(X)}_{xy}$, which delete the executed FEF plan activity. The STN activation helps prevent premature interruption of plan execution by a subsequent plan or by stimuli engendered by the early part of movement.

Figure 3. Cortical and striatal processes in location-specific gating of the SC by the BG. (A) When multiple stimuli exist as potential saccade goals, the corresponding PPC representations specifically excite striatal spiny projection neurons (SPNs; shown in the rectangle within the BG rectangle) and non-specifically (convergently) excite feedforward inhibitory interneurons (labeled with a capital sigma), via corticostriatal projections. If more than one saccade plan is active, then striatal feedforward inhibition from all active plans prevents any one plan from activating its corresponding striatal SPNs to open the BG gate. This is because the pooled inhibitory input to each SPN can overwhelm the specific excitatory input. Therefore the SC is not released from inhibition from the SNr, and movement is prevented while the conflicting cortical plan activity remains unresolved. **(B)** Targets compete in PPC via inhibitory interactions. When competition resolves so that the movement plan is unambiguous, the PPC's excitatory input to striatal SPNs eventually exceeds striatal feedforward inhibition, which wanes as competing plans lose activation and stop convergent excitation of striatal inhibitory interneurons. The winning SPN's discharge inhibits SNr (opens the normally-closed BG gate), which disinhibits part of the SC map. **(C**) If the FEF plans a saccade goal that differs from the location of a strong visual stimulus, the competing frontal and parietal activities collectively drive striatal feedforward inhibition to keep the BG gate shut until the conflict resolves. **(D)** As the frontal cortex imposes its saccade goal on the parietal cortex, the competition between saccade goals resolves, and the BG gate opens to generate the unambiguous saccade. Note: The absence of an icon for FEF activity in **(B)** indicates not that FEF would be inactive in case **(B)**, but only that FEF contains no plan contrary to PPC in case **(B)**.

Figure 4. Direct and indirect pathways in the BG circuit model. The BG direct pathway projects from the striatum to the GPi or SNr. Because it disinhibits thalamo-cortical excitation, activation of the direct pathway normally generates a "GO signal" that enables action plans to be executed. Activation of the indirect pathway, which projects from the striatum to the GPe to the GPi or SNr, inhibits PNR-THAL and can thus STOP planned actions, even if there is activation in the direct pathway that would otherwise suffice to generate a GO signal. The feedback from thalamus to striatum helps solve a credit assignment problem inherent in learning stimulus control of STOP signals (see text for details). Weights on cortico-striatal afferents of SPNs are subject to learning that depends partly on dopaminergic (DA) signals. In the indirect pathway, a phasic DA dip disinhibits D2 receptors and permits LTP. In the direct pathway, a DA burst rather than a dip permits LTP by activating D1 receptors. Model cortico-striatal synapses on SPNs also exhibit LTD, consistent with Calabresi et al. (2000).

Figure 5. **Grid of gatable zones and laminar organization. (A)** Maps of retinotopic inputs and motor error outputs at cortical and collicular levels are represented by two-dimensional grids. For convenience, the cells are indexed by a Cartesian coordinate system, which could be replaced by a space-variant

representation. **(B)** The model FEF contains three distinct gatable cortical zones (GCZs), each possessing input, plan, and output layers, as well as some distinctive cortical afferents. These three GCZs are indexed by *i*, whereas *k* (see Figure 2) indexes the corresponding three BG-thalamic channels that control them.

Figure 6. Modeled afferent signals, and mathematical symbols for physiological variables, associated with model cell types. As implied by Figure 2, the model includes a large number of cell types distinguishable by their afferent and efferent connections. See text and on-line Appendix for details. **(A)** Cell types of the cortical model. **(B)** Cell types of the subcortical model.

Figure 7. Model of a canonical plan-execute episode. (A) Top-down arousal from higher or more anterior cortical areas excites layer VI, which in turn primes action plan representations in layer III/Va. (Layer VI-to-III projections are pre-set in the present model but could be learned.) The combination of priming and sensory input supraliminally activates layer III/Va plan cells. **(B)** Layer III/Va activity persists after the offset of sensory input and excites specific movement-related cells in layer Vb, though not sufficiently to supraliminally activate layer Vb cells. **(C)** Layer III/Va plan cells excite the direct pathway of the BG, which removes the tonic inhibition of the thalamus. This disinhibition allows the existing layer VI signals to thalamus to supraliminally activate disinhibited thalamic cells. **(D)** These thalamic cells excite layer Vb cells. The combination of layer III/Va and thalamic inputs drives localized layer Vb activity above the threshold needed to generate output to the SC and STN. **(E)** Buildup of activity in direction-tuned cells of the SC sends feedback to FEF that initially excites plan cells tuned to the same direction. Once the buildup becomes large enough to initiate movement, the stronger feedback to FEF transiently activates postsaccadic cells, which are modeled as inhibitory interneurons that shut off the movement-related activity in layers III/Va and Vb. This prevents perseveration of already executed plans.

Figure 8. Activation dynamics of 22 simulated cell types during performance of the overlap task. From left to right in each column of plots, the three vertical lines respectively mark target onset time, fixation light offset time, and saccade onset time. **(A)** Two FEF input layer cells (governed by equation 12; details in on-line Appendix) whose retinotopic receptive fields cover the target position. Only one shows a second burst due to delayed input (from ITp) conditional upon target's position *and* features. **(B)** FEF layer VI cell (eqn. 13). (**C**) GPi/SNr cell (eqn. 35) associated with the Fixation-feature GCZ. (**D**) GPi/SNr cell (eqn. 35) associated with the Target-feature GCZ. **(E)** Striatal SPN in the direct pathway (eqn. 27) associated with SC saccade-related cells. **(F)** SNr saccade-related cell (eqn. 32) that receives inhibition from the cell in **(E)**. **(G)** SNr cell (eqn. 32) associated with SC fixation cells. **(H)** Fixation cell (eqn. 11) of the SC. **(I)** Saccade-related cell (eqn. 11) of the SC. **(J)** FEF post-saccadic cell (eqn. 26). **(K)** Thalamic cell (eqn. 38) associated with the Target GCZ. The late (post movement) discharge of this cell is associated with postsaccadic fixation of the Target object. There is little pre-movement thalamic activity, because the movement to the still visible target is generated by the reactive, PPC-SC, pathway (not via FEF) once Fixation stimulus offset removes the indirect channel's STOP signal. **(L)** FEF fixation plan cell (eqn. 14) of layer III/Va. Dotted line shows associated trace ($\overline{F}$) variable (eqn. 45). **(M)** Winning FEF saccade plan cell (eqn. 14) of layer III/Va, showing discharge of the sustained sensory-movement type. **(N)** Losing FEF saccade plan cell (eqn. 14) showing discharge of the transient sensory-movement type. **(O)** Striatal direct path SPN (eqn. 33) associated with FEF fixation cells. **(P)** Striatal direct path SPN (eqn. 33) associated with FEF saccade-related cells. **(Q)** PPC fixation-related cell (eqn. 6). **(R)** PPC saccade-related cell (eqn 6). **(S)** FEF layer Vb fixation cell (eqn. 21). **(T)** Striatal SPN of the indirect pathway (eqn. 34) that inhibits the FEF Target-feature module. This cell receives strong input from the FEF fixation cell in (L). **(U)** GPe cell (eqn. 36) in the pathway that inhibits the FEF Target-feature module. This cell receives strong inhibition from the cell in (T).

Figure 9. Comparison of dynamics of real and simulated FEF cells. Data appear above model fits in all panels except **(G)**. Figure 9A simulation and data are from the delay task, 9B from the discrimination task, and 9C, D, E, F, and G from the overlap task. **(A)** Discharge of FEF visual cells and activation level of model FEF input layer cells. [Data adapted with permission from Schall et al., 1995a.] **(B)** FEF

visuomovement cells and model FEF plan layer cells. In the simulation plot, the solid trace is from the winning plan and the dashed trace from a losing plan. [Data adapted with permission from Schall & Bichot, 1998.] **(C)** FEF transient sensory-movement cells and model FEF *losing* plan layer cells [Data adapted with permission from Schall, 1991.] **(D)** FEF presaccadic movement cells and model FEF layer Vb (output) layer cells. **(E)** FEF postsaccadic cells and model FEF inhibitory feedback cells [**(D)** and **(E)** data plots adapted with permission from Schall, 1991.] **(F)** FEF sustained sensory-movement cells and model FEF plan layer cells that represent planned but not yet executed saccades. [Data adapted with permission from Hanes et al., 1998.] **(G)** FEF preparatory set cells (left) and model FEF fixation cells (right). Vertical line on right denotes saccade onset. [Data adapted with permission from Schall et al., 1995b.]

Figure 10. Comparison of dynamics of simulated and real BG and PNR-THAL cells for the delay task. (A) On left, real GPe cells increase their firing rate prior to movement onset whereas GPi cells pause. On the right are corresponding model GPe and GPi cells. In the model, GPi pausing permits movement execution. Model STN cell activity beginning at movement initiation transiently increases both the GPi and GPe activities. [Data adapted with permission from Turner & Anderson, 1997.] **(B)** Above, real thalamic cells show a transient burst just prior to movement initiation. Below, the model thalamic burst reflects excitation from layer 6 and transient disinhibition (gating) by the GPi. [Data adapted with permission from Schlag-Rey & Schlag, 1984.] **(C)** Above, real STN cells show a transient increase in activity immediately following movement onset. Below, the model STN burst reflects a transient corollary discharge from FEF output layer cells. [Data adapted with permission from Wichmann et al., 1994.]

Figure 11. Comparison of dynamics of simulated and real PPC, SC, and SC-related BG cells for the overlap task. Data appear above simulation in each panel. **(A)** Real SNr cell pauses during saccades near its preferred direction. Model SNr cell pauses to allow model SC to generate a saccade near the cell's preferred direction. [Data adapted with permission from Hikosaka & Wurtz, 1989, Fig. 10b.] **(B)** Real SC burst cell activity during the overlap task compared with model SC burst cell. [Data adapted with permission from Munoz & Wurtz, 1995.] **(C)** Real PPC activity during a task similar to the overlap task compared with model PPC activity during the overlap task. [Data adapted with permission from the reaching study of Kalaska & Crammond, 1995.] **(D)** Real fixation-cell activity in the rostral SC, where fixation cells pause briefly during a saccade, compared to a model SC fixation cell. [Data adapted with permission from Munoz & Wurtz, 1993.]

Tables

TABLE 1. Anatomical abbreviations

BG	basal ganglia, including striatum, GPi, GPe, STN, SNc, SNr
FEF	the frontal eye fields
GABA-SI	GABA-ergic striatal interneurons
GPe	the external (lateral) segment of the globus pallidus
GPi	the internal (medial) segment of the globus pallidus
ITa	anterior infero-temporal cortex
ITp	posterior infero-temporal cortex
LP/PUL	lateral posterior/pulvinar nuclear complex of the dorsal thalamus
OT	optic tectum (called the superior colliculus in primates)
PFC	prefrontal cortex
PNR-THAL	a pallidal- (GPi) or a nigral- (SNr) receiving zone of the thalamus, e.g., mediodorsal, ventral anterior, and ventral lateral pars oralis nuclei
PPC	posterior parietal cortex
SNc	the substantia nigra pars compacta
SNr	the substantia nigra pars reticulata
SPN	spiny projection neuron of the dorsal striatum (caudate or putamen)
STN	the subthalamic nucleus
VTA	ventral tegmental area

TABLE 2. Selected Anatomical Studies

From	To	Species	References
Layer VI	Layer III, V	cat	Kang & Kayuno, 1994
Distant cortex	Layer II, III	cat	Iriki et al., 1991
Layer III	Layer V	cat	Kimura et al., 1994
Layer III, V	Striatum	rhesus monkey, rat	Jones et al., 1977; Yeterian & Pandya, 1994; Levesque et al., 1996
Layer VI	VA, MD nuclei of thalamus	rhesus monkey, rat	Yeterian & Pandya, 1994; Levesque et al., 1996
VL (Thalamus)	Layer V, III	rat	Zin-Ka-Ieu et al., 1998
Layer V	STN	rat	Canteras et al., 1990; Gerfen, 1992
GPe	GPi	squirrel monkey, rhesus monkey	Hazrati et al., 1990; Parent & Hazrati, 1993; 1995
GPe	SNr	rat	Smith & Bolam, 1990
STN	GPe, GPi	squirrel monkey	Parent & Hazrati, 1993; Shink et al., 1996
SC, intermediate layers	FEF (via thalamus)	Cebus monkey	Lynch et al. (1994); Sommer & Wurtz (1998)
ITa	FEF zone 45B	monkey	Bullier et al. 1996
ITp	FEF zone 45A	monkey	Bullier et al. 1996

TABLE 3. Simulated Saccadic Reaction Times for Tasks

Task	**Saccade**	**Overlap**	**Gap**	**Delay**	**Choice**
Reaction Time (ms)	79	55	163	233	210

TABLE 4. Electrophysiological Cell Types

Area	Cell Type Names	Simulation-Data Comparison Figure	References
FEF	1. Visual	Figure 2A	Schall et al., 1995a; Schall, 1991
	2. Visual with second burst	Figure 2A	
FEF	3. Visuomovement	Figure 2B	Schall & Bichot, 1998
	4. Discriminating visuomovement	Figure 2B	
FEF	5. Transient Sensory-Movement	Figure 2C	Schall, 1991; Segraves & Goldberg, 1987
FEF	6. Presaccadic	Figure 2D	Schall, 1991; Bruce et al., 1985; Segraves & Goldberg, 1987
FEF	7. Postsaccadic	Figure 2E	Schall, 1991; Bruce & Goldberg, 1985; Bruce et al., 1985
FEF	8. Sustained Sensory-Movement	Figure 2F	Hanes et al. 1998; Schall, 1991
FEF	9. Preparatory Set/Fixation	Figure 2G	Schall et al., 1995b; Schall, 1991
GPe	10. Burster	Figure 3A	Turner & Anderson, 1997
GPi	11. Pause-burster	Figure 3A	Turner & Anderson, 1997
Motor Thalamus	12. Burster	Figure 3B	Schlag-Rey & Schlag, 1984; Turner & Anderson, 1997
STN	13. Burster	Figure 3C	Wichmann et al., 1994
SNr	14. Pauser	Figure 4A	Hikosaka & Wurtz, 1989
PPC	15. Movement-related	Figure 4C	Kalaska & Crammond, 1995
SC	16. Saccade-related	Figure 4B	Munoz & Wurtz, 1995
SC	17. Fixation-related	Figure 4D	Munoz & Wurtz, 1993

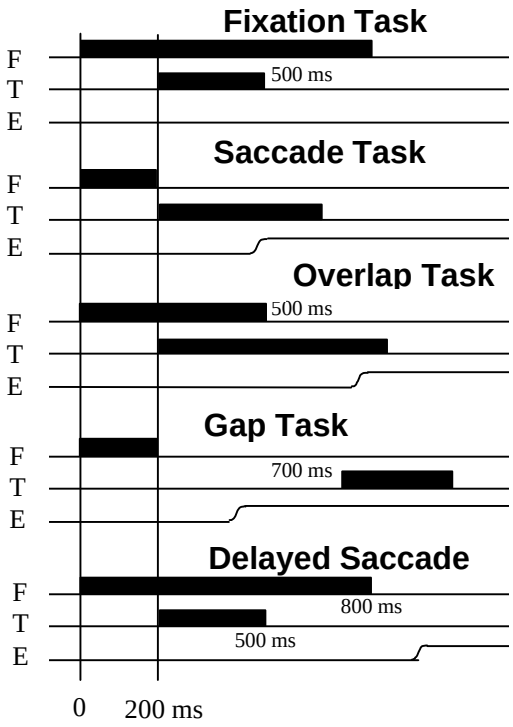
Fixation Task
F
T
E
500 ms
Saccade Task
F
T
E
Overlap Task
500 ms
F
T
E
Gap Task
F
T
E
700 ms
Delayed Saccade
F
T
E
800 ms
500 ms
0
200 ms

Figure 1

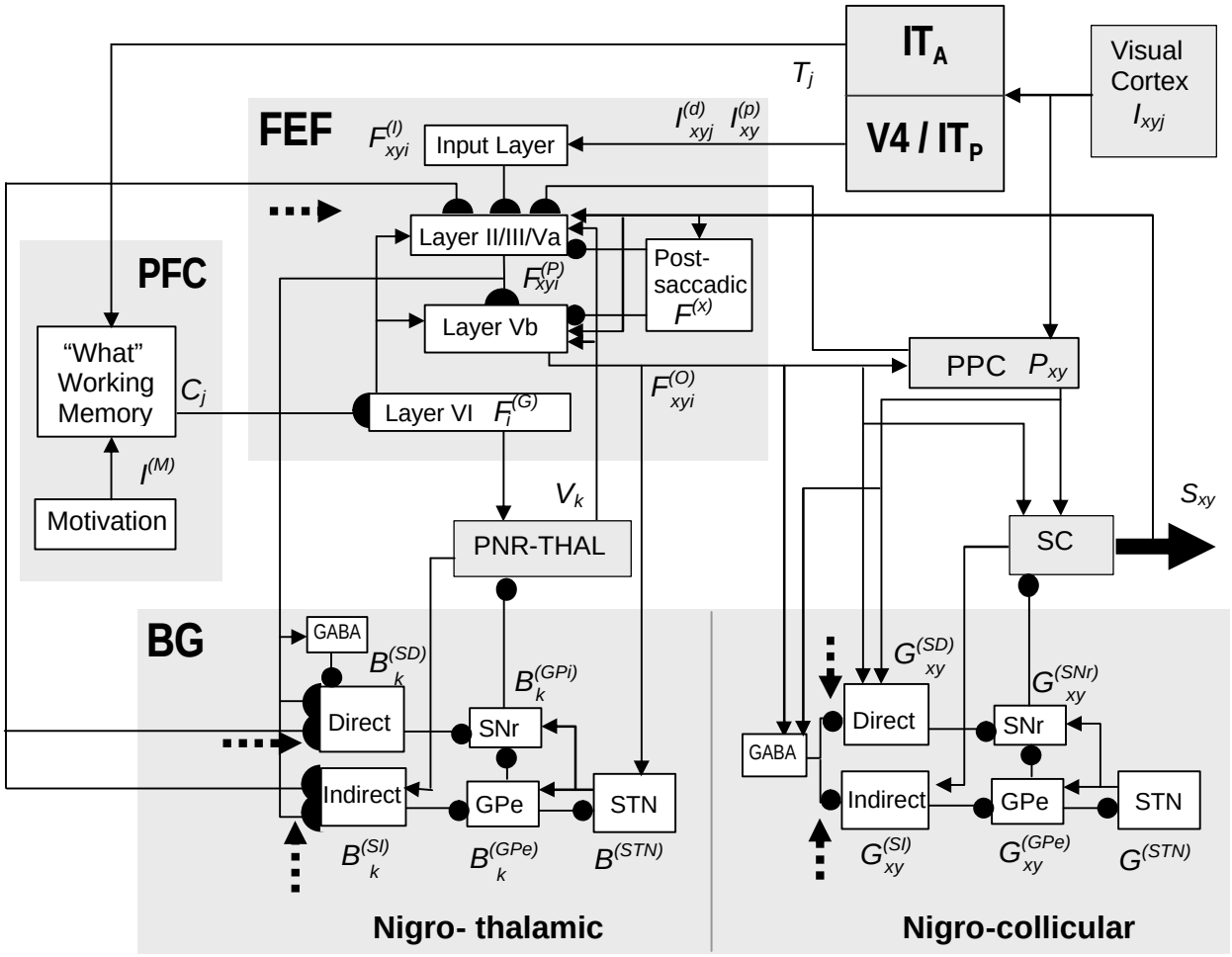
IT_A
V4 / IT_P
Visual Cortex
I_xyj
T_j
FEF
F(I)xyi
Input Layer
I(d)xyj I(p)xy
Layer II/III/Va
Post-saccadic F(x)
F(P)xyi
Layer Vb
PPC Pxy
F(O)xyi
PFC
"What" Working Memory
Cj
Layer VI F(G)i
I(M)
Motivation
Vk
Sxy
PNR-THAL
SC
BG
GABA
B(SD)k
B(GPi)k
Direct
SNr
Indirect
GPe
STN
B(SI)k
B(GPe)k
B(STN)
G(SD)xy
G(SNr)xy
G(SI)xy
G(GPe)xy
G(STN)
Nigro- thalamic
Nigro-collicular

Figure 2

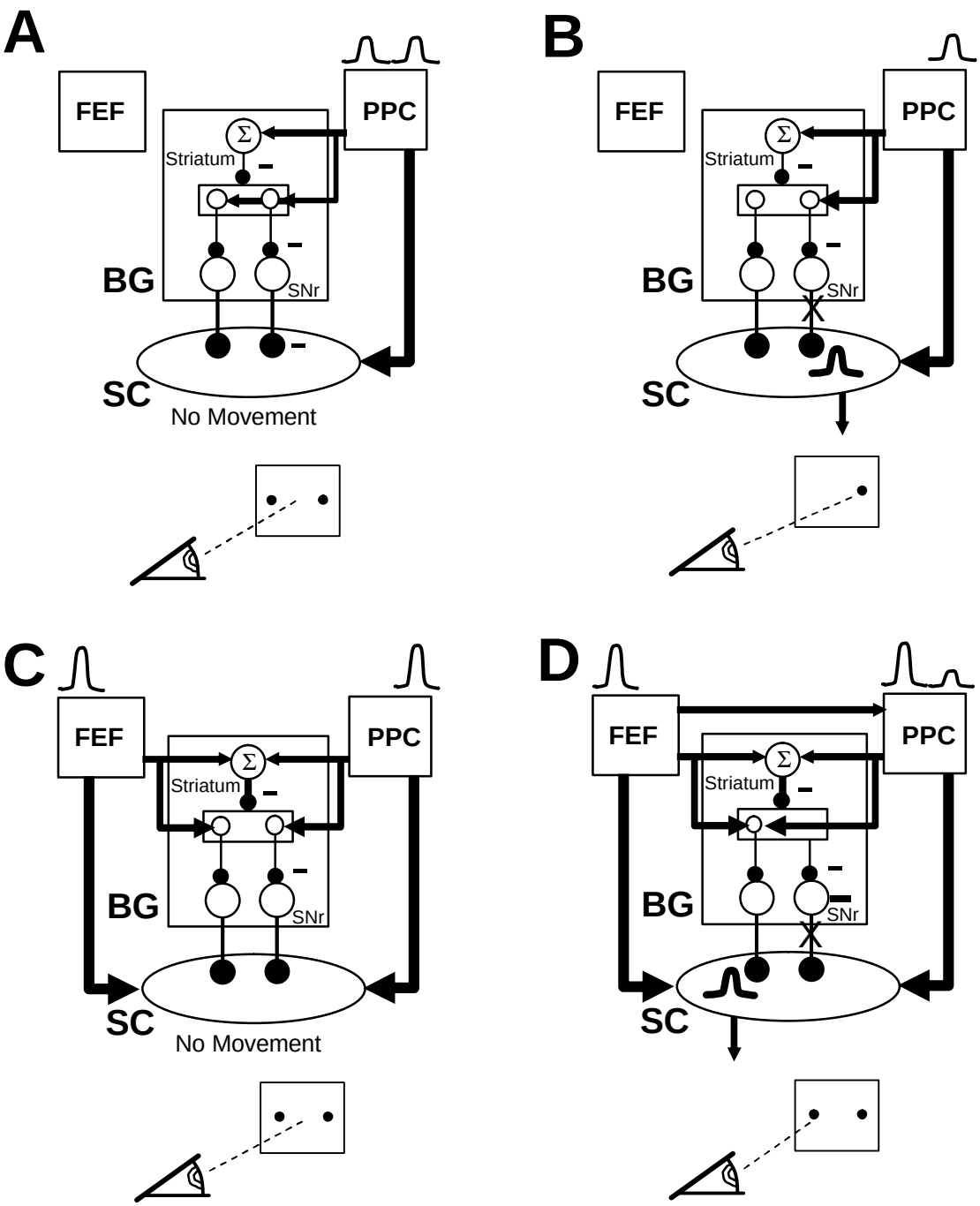
A
FEF
PPC
Striatum
BG
SNr
SC
No Movement
B
FEF
PPC
Striatum
BG
SNr
SC
C
FEF
PPC
Striatum
BG
SNr
SC
No Movement
D
FEF
PPC
Striatum
BG
SNr
SC

Figure 3

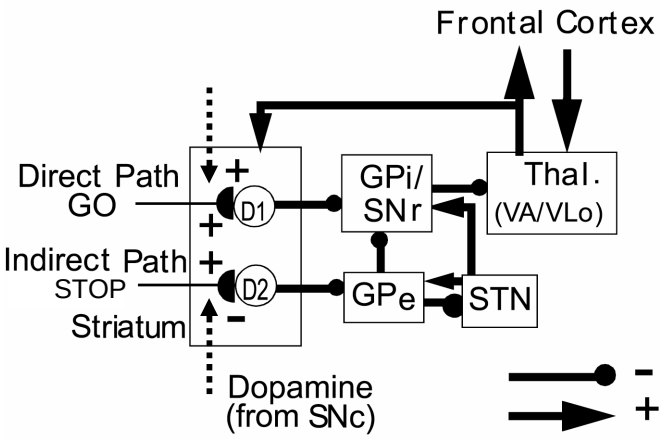
Frontal Cortex
Direct Path
GO
D1
GPi/
SNr
Thal.
(VA/VLo)
Indirect Path
STOP
D2
GPe
STN
Striatum
Dopamine
(from SNc)

Figure 4

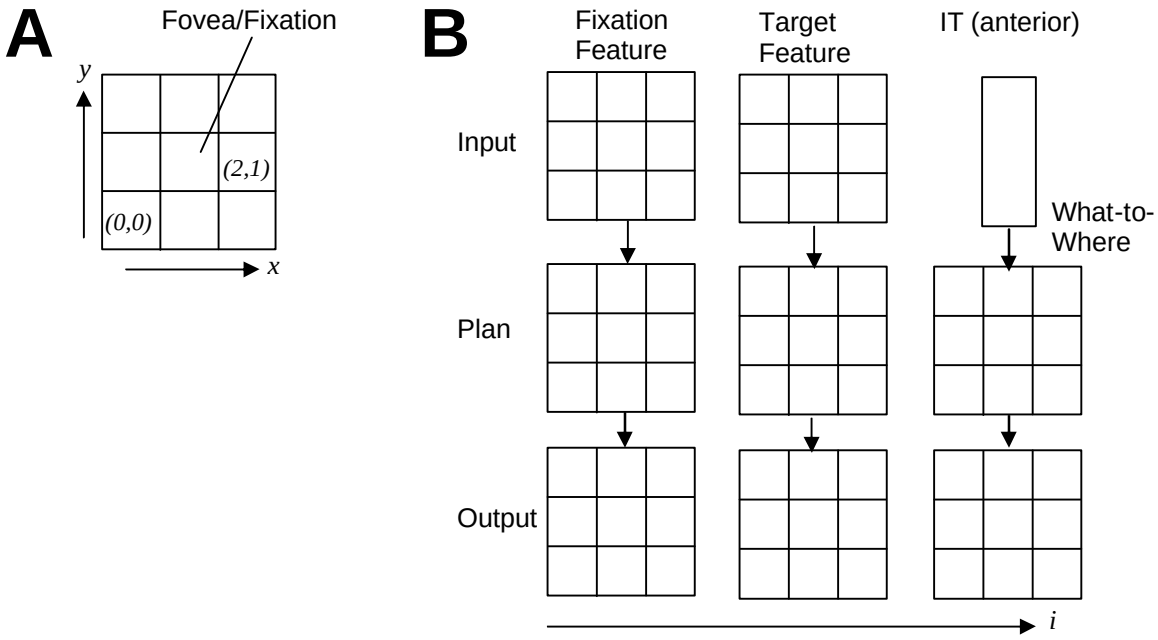
A
Fovea/Fixation
y
(2,1)
(0,0)
x
B
Fixation Feature
Target Feature
IT (anterior)
Input
What-to-Where
Plan
Output
i

Figure 5

Cortical Cell Types Modeled

FEF Plan Cells (Layers II/III/Va): $F^{(P)}$, $\overline{F}^{(P)}$, $\overline{F}^{(PA)}$, $\overline{T}$

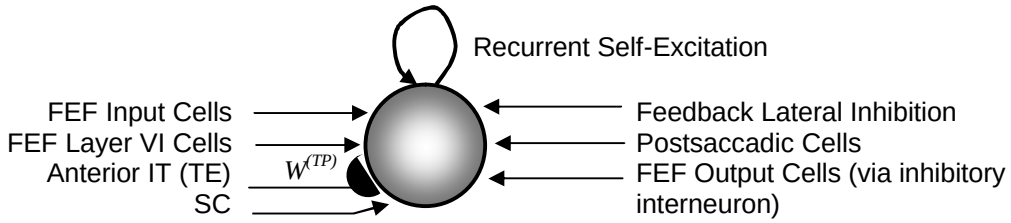

FEF Output Layer Cells (Layer Vb): $F^{(O)}$

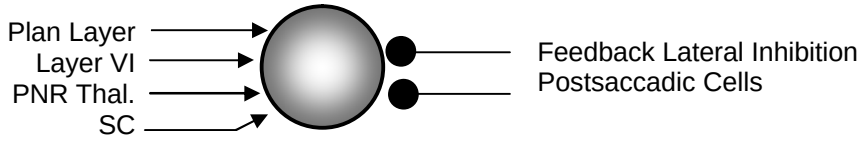

Visual/Input Cells: $F^{(I)}$

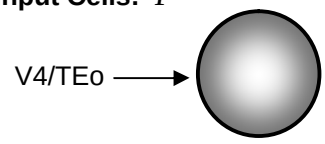

FEF Postsaccadic Cells: $F^{(X)}$

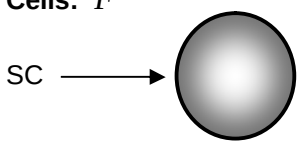

FEF Category Cells (Layer VI): $F^{(G)}$, $\overline{F}^{(G)}$

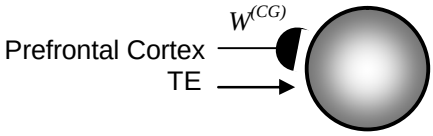

TE (Anterior IT): T, $\overline{T}$

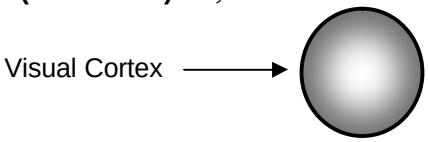

Parietal Cortex (LIP): P

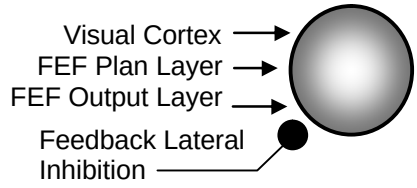

Dorsolateral Prefrontal Cortex: C

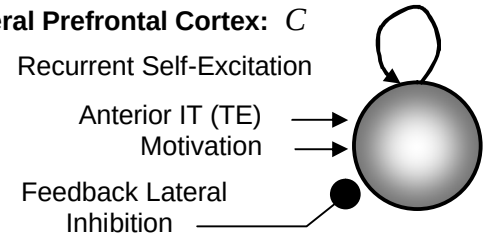

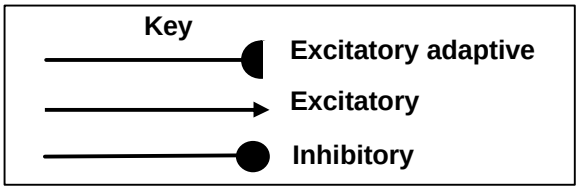

Figure 6a

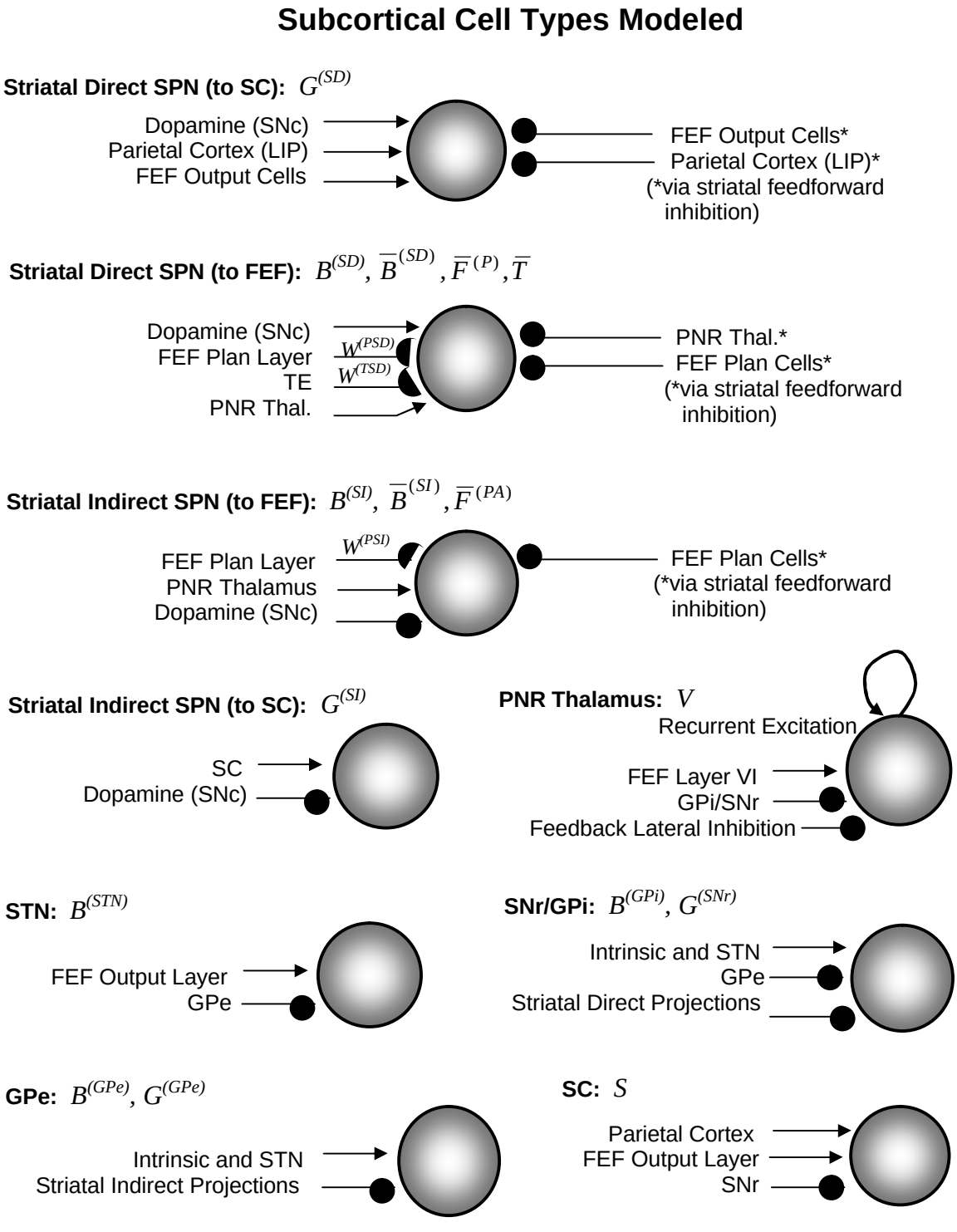
Subcortical Cell Types Modeled
Striatal Direct SPN (to SC): $G^{(SD)}$
Dopamine (SNc)
Parietal Cortex (LIP)
FEF Output Cells
FEF Output Cells*
Parietal Cortex (LIP)*
(*via striatal feedforward inhibition)
Striatal Direct SPN (to FEF): $B^{(SD)}, \overline{B}^{(SD)}, \overline{F}^{(P)}, \overline{T}$
Dopamine (SNc)
FEF Plan Layer
TE
PNR Thal.
$W^{(PSD)}$
$W^{(TSD)}$
PNR Thal.*
FEF Plan Cells*
(*via striatal feedforward inhibition)
Striatal Indirect SPN (to FEF): $B^{(SI)}, \overline{B}^{(SI)}, \overline{F}^{(PA)}$
FEF Plan Layer
PNR Thalamus
Dopamine (SNc)
$W^{(PSI)}$
FEF Plan Cells*
(*via striatal feedforward inhibition)
Striatal Indirect SPN (to SC): $G^{(SI)}$
SC
Dopamine (SNc)
PNR Thalamus: V
Recurrent Excitation
FEF Layer VI
GPi/SNr
Feedback Lateral Inhibition
STN: $B^{(STN)}$
FEF Output Layer
GPe
SNr/GPi: $B^{(GPi)}, G^{(SNr)}$
Intrinsic and STN
GPe
Striatal Direct Projections
GPe: $B^{(GPe)}, G^{(GPe)}$
Intrinsic and STN
Striatal Indirect Projections
SC: S
Parietal Cortex
FEF Output Layer
SNr

Figure 6b

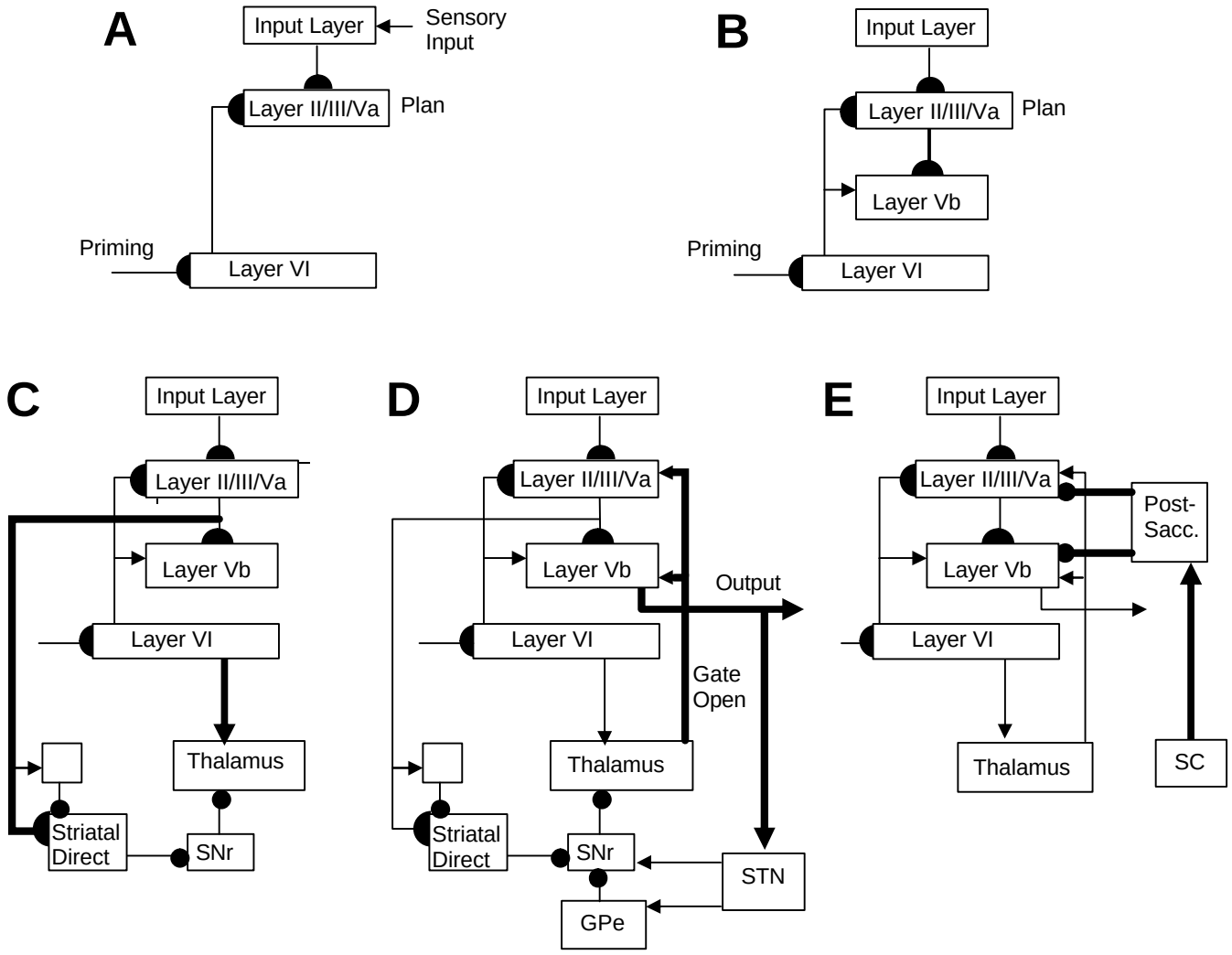
A
Input Layer
Sensory Input
Layer II/III/Va
Plan
Priming
Layer VI
B
Input Layer
Layer II/III/Va
Plan
Layer Vb
Priming
Layer VI
C
Input Layer
Layer II/III/Va
Layer Vb
Layer VI
Thalamus
Striatal Direct
SNr
D
Input Layer
Layer II/III/Va
Layer Vb
Output
Layer VI
Gate Open
Thalamus
Striatal Direct
SNr
STN
GPe
E
Input Layer
Layer II/III/Va
Post-Sacc.
Layer Vb
Layer VI
Thalamus
SC

Figure 7

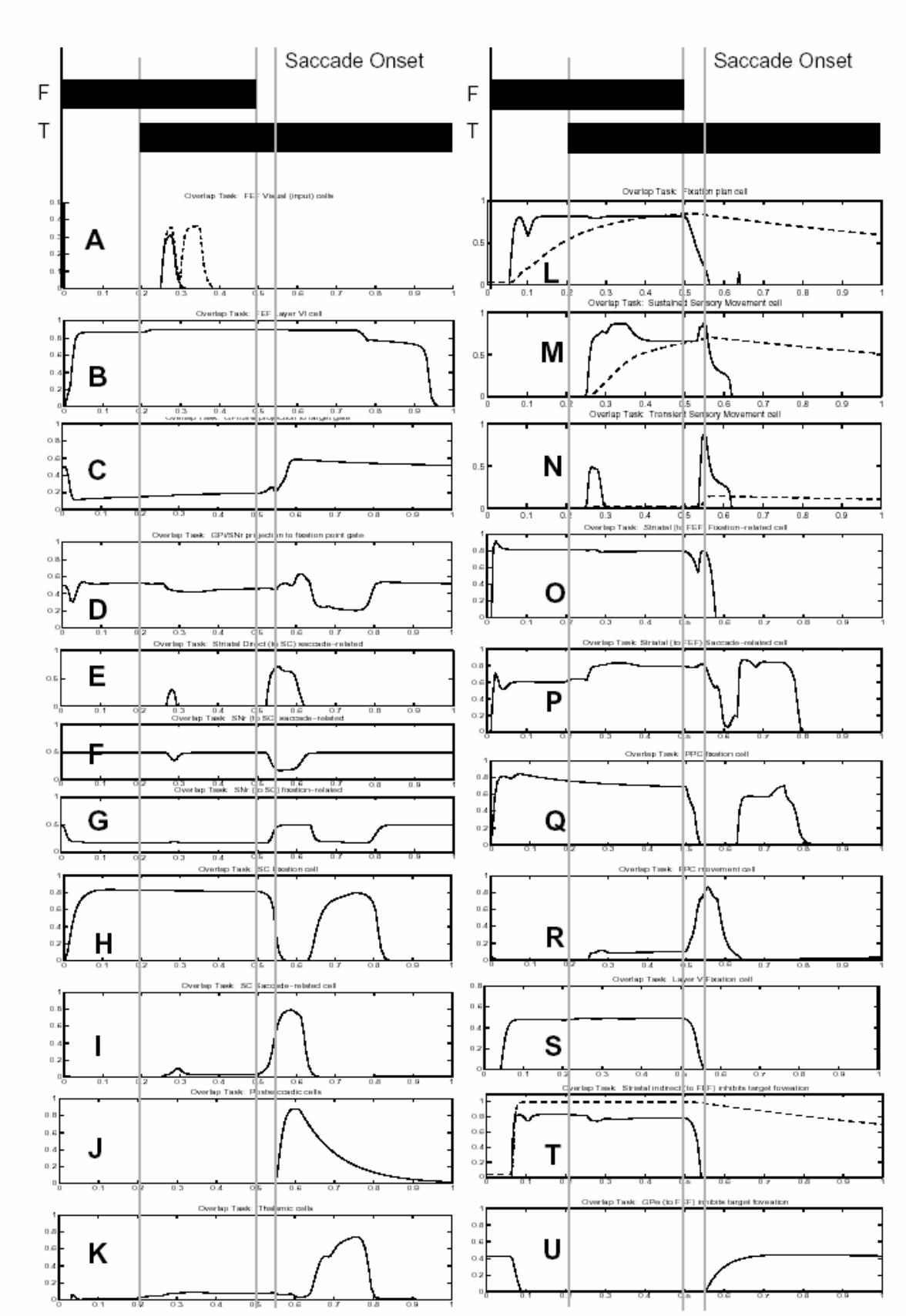

Figure 8:

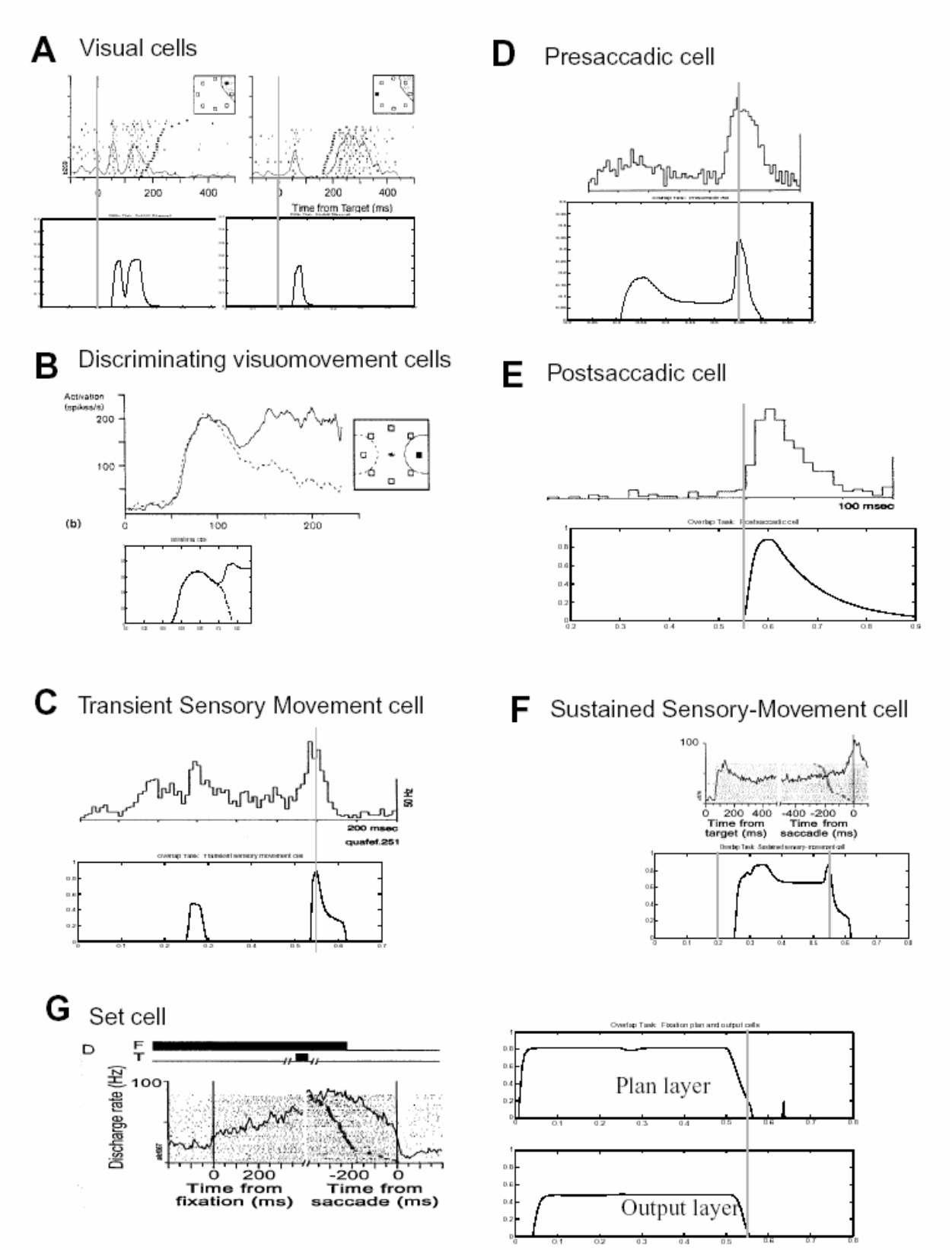
A Visual cells
200
400
Time from Target (ms)
B Discriminating visuomovement cells
Activation (spikes/s)
200
100
(b)
0
100
200
C Transient Sensory Movement cell
50 Hz
200 msec
quafef.251
D Presaccadic cell
E Postsaccadic cell
100 msec
F Sustained Sensory-Movement cell
100
0 200 400
Time from target (ms)
-400 -200 0
Time from saccade (ms)
G Set cell
D
F
T
Discharge rate (Hz)
100
0 200
Time from fixation (ms)
-200 0
Time from saccade (ms)
Plan layer
Output layer

Figure 9

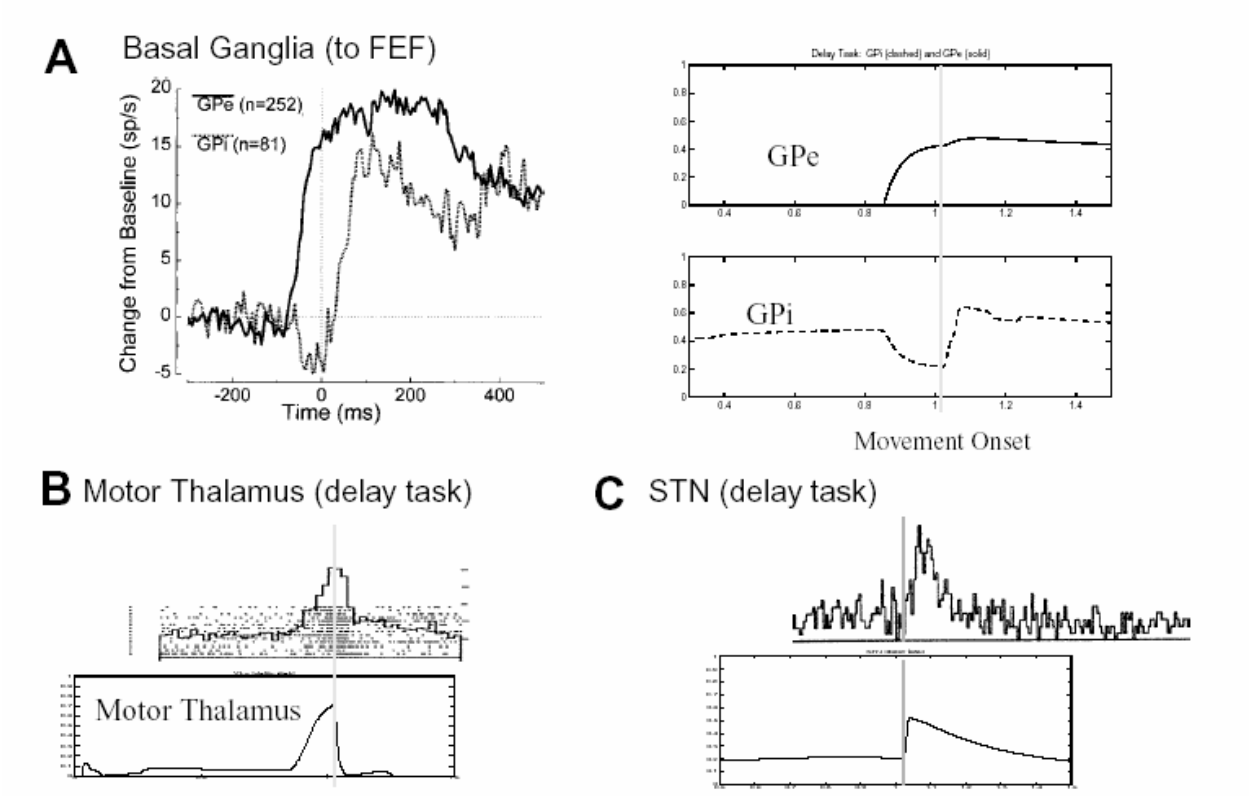
A
Basal Ganglia (to FEF)
GPe (n=252)
GPi (n=81)
Change from Baseline (sp/s)
Time (ms)
Delay Task: GPi (dashed) and GPe (solid)
GPe
GPi
Movement Onset
B Motor Thalamus (delay task)
Motor Thalamus
C STN (delay task)

Figure 10

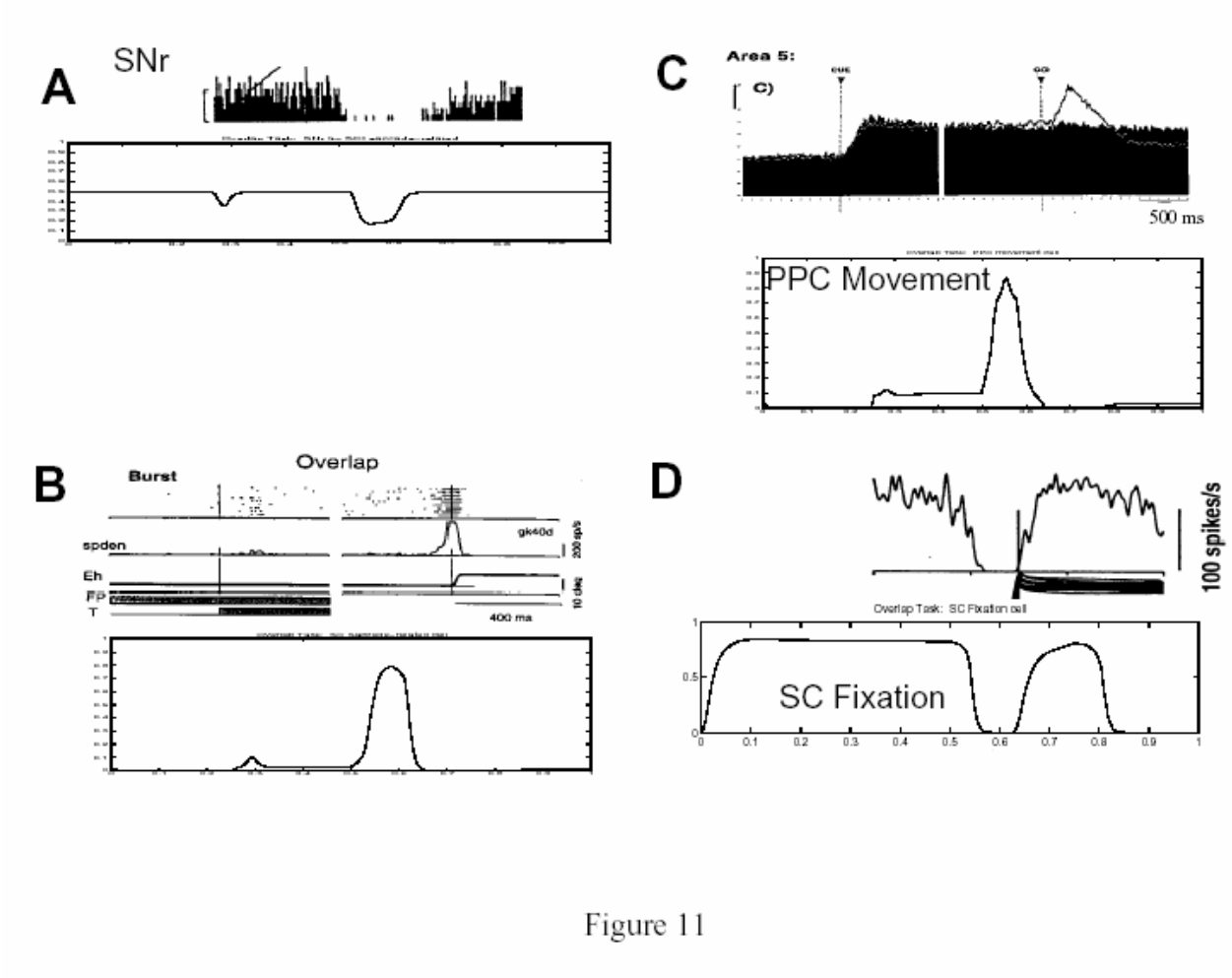
A
SNr
B
Burst
Overlap
spden
Eh
FP
T
gk40d
200 sp/s
10 deg
400 ms
C
Area 5:
C)
500 ms
PPC Movement
D
100 spikes/s
Overlap Task: SC Fixation cell
SC Fixation
0
0.5
1
0.1
0.2
0.3
0.4
0.5
0.6
0.7
0.8
0.9

Figure 11